DEPARTMENT OF THE ARMY
CORPS OF ENGINEERS

Technical Report 1663-TR

HASTY DEMOLITION OF CONCRETE STRUCTURES

Project 8F07-10-002-01

13 January 1961

U. S. Army Engineer Research and Development Laboratories

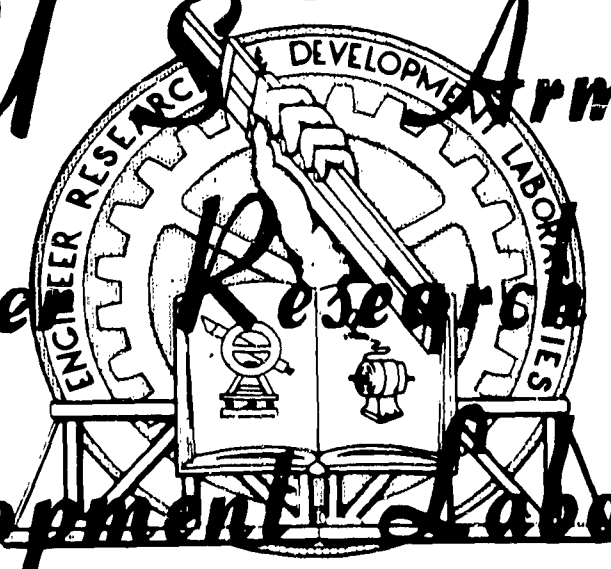

FORT BELVOIR, VIR

PAGES _____

ARE

MISSING

IN

ORIGINAL

DOCUMENT

U. S. ARMY ENGINEER RESEARCH AND DEVELOPMENT LABORATORIES
CORPS OF ENGINEERS

Technical Report 1663-TR

HASTY DEMOLITION OF CONCRETE STRUCTURES

Project 3F07-10-002-01

13 January 1961

Distributed by

The Director
U. S. Army Engineer Research and Development Laboratories
Corps of Engineers

Prepared by

Howard J. Vandersluis
Demolitions and Fortifications Branch
Military Department
U. S. Army Engineer Research and Development Laboratories
Corps of Engineers
Fort Belvoir, Virginia

CONTENTS

LIST OF TABLES

LIST OF ILLUSTRATIONS

LIST OF ILLUSTRATIONS (cont'd)

LIST OF ILLUSTRATIONS (cont'd)

LIST OF ILLUSTRATIONS (cont'd)

LIST OF ILLUSTRATIONS (cont'd)

LIST OF ILLUSTRATIONS (cont'd)

SUMMARY

This report covers a test program in which improved techniques for the use of explosives against reinforced concrete structures were developed and utilized to establish the minimum explosive necessary to breach piers 1 to 8 feet thick. A subordinate objective of the tests was to enhance understanding of the principles surrounding the destructive effect of explosives on a target, research which has been valuable not only in validating the conclusions of the tests but also in providing a framework for further studies of concrete.

The report concludes that:

a. Explosive placed at least the thickness of the pier above the base of a pier is more effective than explosive placed at the base.

b. The relationship of thickness of charge to contact area is critical; a material change from the optimum will significantly decrease destructiveness of the charge.

c. Central initiation of a charge is as effective as corner initiation or two-corner, simultaneous initiation.

d. Plastic placed between explosive and a concrete target (representing the plastic cover of the standard C-4 block) does not significantly alter destructiveness of the explosive.

e. On 1-foot-thick walls, mud confinement of the explosive (tamping) makes possible a 30-percent reduction in the weight of explosive required to achieve equivalent results (this conclusion will probably not hold true for thicker walls).

f. A square charge is more effective than a rectangular charge.

g. Optimum practicable charge sizes are as shown in Table XV.

HASTY DEMOLITION OF CONCRETE STRUCTURES

I. INTRODUCTION

1. Subject. This report covers a test program in which improved techniques for the use of explosives against reinforced concrete structures were developed and utilized to establish the minimum explosive necessary to breach piers 1 to 8 feet thick. This test program is also described in ERDL motion picture report No. 1897, "Demolition of Concrete Structures." A subordinate objective of the tests was to enhance understanding of the principles surrounding the destructive effect of explosives on a target, research which has been valuable not only in validating the conclusions of the tests but also in providing a framework for further studies of concrete.

2. Background and Previous Investigations. The U. S. Army Engineer Research and Development Laboratories (USAERDL) began a program in June 1955 to revise the Army demolition formulas. Stanford Research Institute (SRI), under a contract supervised by USAERDL, began a comprehensive examination of the demolition techniques contained in FM 5-25. In the SRI report[1] it was concluded that the formula for explosives prescribed in FM 5-25 was excessive for all concrete breaching except for 1-foot-thick concrete walls. SRI was not given time to test its conclusions, but the theoretical findings were of great value in establishing the course of USAERDL experiments. SRI concluded from the results of its tests that the explosive should be placed on the concrete wall at a distance from the ground equal to or greater than the thickness of the wall and also suggested the importance of making the charge relatively thin with respect to its cross sectional area. Two reports[2,3] provided important background material for the tests.

---

1. G. B. Huber and S. A. Moses, Fundamental Studies of Explosive Charges Vol II: Concrete Breaching and Wood Cutting Charges (Menlo Park, Calif.: SRI, 1957).

2. D. G. Kretsinger, Contact Explosions on Concrete (Confidential Report) (National Research Council, 1944).

3. Part I German Experimental Work on the Attack of Reinforced Concrete by Explosives and Projectiles (Confidential Report) (British Intelligence Objectives Sub-Committee, 1945).

II. INVESTIGATION

A. BASIC STUDIES

3. General. Basic studies laid the groundwork for tests on full-scale piers. Conducted on a reduced scale, the studies produced results which could be defined mathematically and thus provided a quantitative basis for the full-scale tests. Variously shaped explosive was detonated on an energy-measuring device, and the results were first compared with charges detonated on unreinforced concrete and then on reinforced concrete. Tests on concrete also provided data for evaluation of procedures for placing and detonating charges. Basic tests were conducted at Fort Belvoir, Virginia, and at the West Virginia Ordnance Sub-Depot near Point Pleasant, West Virginia, from 15 May 1958 through 30 June 1958.

4. Ballistic Pendulum Studies. A simple pendulum compared the explosive impact produced by various thicknesses of charges (Fig. 1). As the thickness of explosive varied, the energy transmitted to the target also varied.

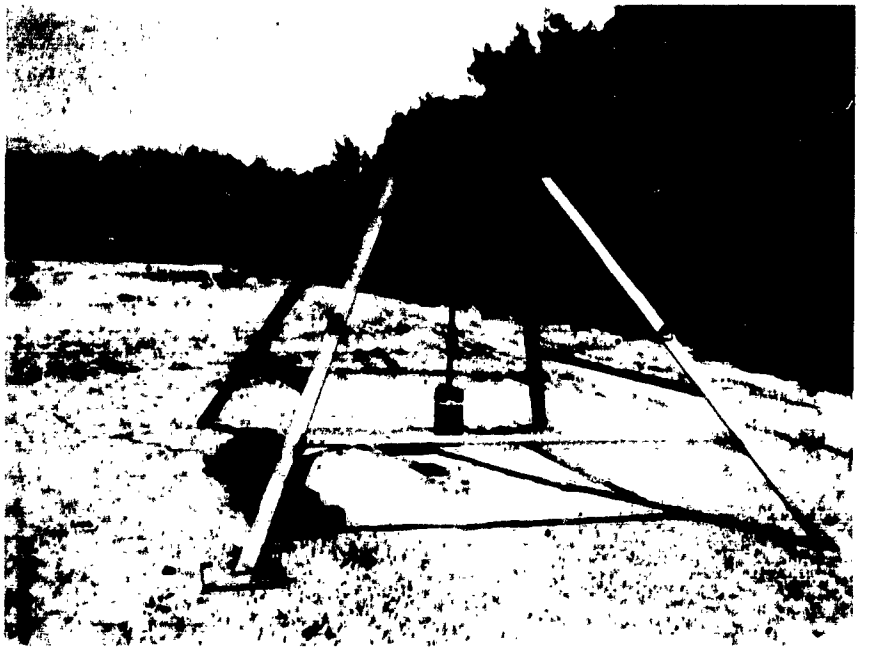

E7078

Fig. 1. Pendulum employed to compare relative effectiveness of charges having equal weights but different thicknesses.

Square 25-gram charges were tested first. Testmen molded the plastic explosive, Composition C-4, into charges 1/4, 3/8, 1/2, 5/8, and 3/4 inch thick. The charges were hand-tamped to a density

of approximately 1.6 grams per cubic centimeter. Each charge was placed on the pendulum head at the center of impact. A 10-gram booster charge formed from loosely packed Composition C-4 insured high-order detonation of the charge when initiated by a J-2 special electric cap (Fig. 2).

E7077

Fig. 2. Square 25-gram charges fastened to pendulum head with 10-gram booster charge in place.

The arc of the pendulum swing, recorded by a stylus on a scribe plate (Fig. 3), proved that the explosive effect was greatest with the thinnest charge. Since the ratio of thickness to contact area was just 1:16, the pendulum was redesigned so that smaller ratios, as shown in Table I, could be tested. As the thickness of the charge was reduced, the arc formed by the pendulum (shown in Table I in terms of its vertical component) increased.

In the next series of pendulum tests, the charge weight was increased to 218 grams with thicknesses of 1/4, 5/16, 3/8, 7/16, 1/2, 5/8, and 1-5/16 inches. Just as with the 25-gram charges, when the thickness of the 218-gram charges decreased, the work accomplished by the charges uniformly increased as shown in Table II.

A third series of pendulum tests were conducted using 300-gram charges with thicknesses of 1/4, 5/16, 3/8, 7/16, and 1/2 inch (Fig. 4). As the ratio decreased, the energy output as measured by the pendulum swing increased just as in the 25- and 218-gram charges (Table III).

E7079

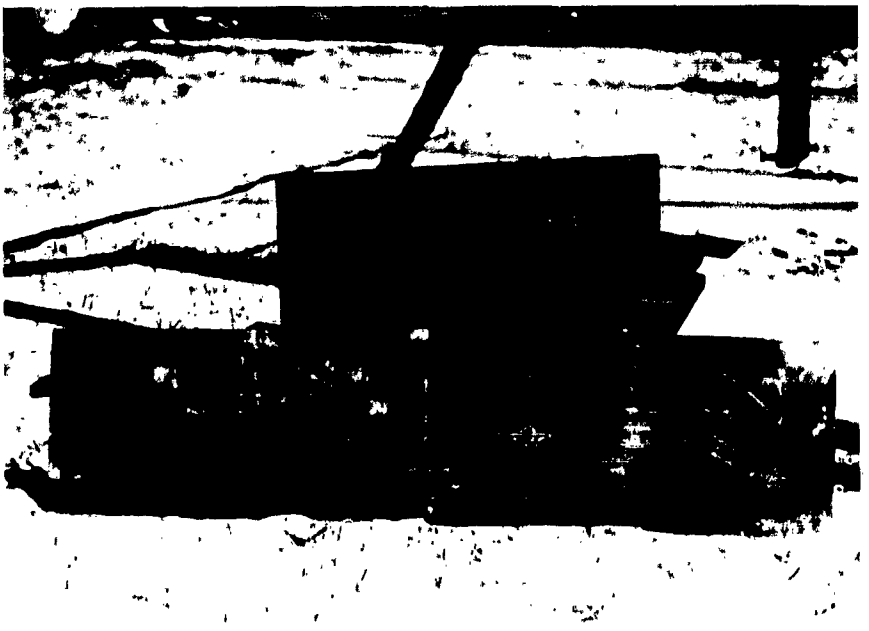

E7080

Fig. 3. Top: Stylus recording the arc of the pendulum. Bottom: Five arcs produced by five different charge thicknesses, the thinnest ($\frac{1}{11}$ inch) producing the greatest arc.

Table I. Effect of Thickness of 25-Gram Charge on Vertical Rise of Pendulum

Test No.	Dimensions of Charge (in.)	Ratio of Thickness to Contact Area	Vertical Rise (in.)
2	3/4 x 1-1/8 x 1-1/8	1:1.5	0.83
8	"	"	0.91
13	"	"	0.97
1	5/8 x 1-1/4 x 1-9/32	1:2.6	1.06
7	"	"	1.31
11	"	"	1.25
4	1/2 x 1-1/2 x 1-3/8	1:4.4	1.41
10	"	"	1.59
12	"	"	1.44
5	3/8 x 1-5/8 x 1-11/16	1:7.3	1.97
9	"	"	2.13
14	"	"	2.16
3	1/4 x 2 x 1-15/16	1:16	2.66
6	"	"	2.59
15	"	"	2.91

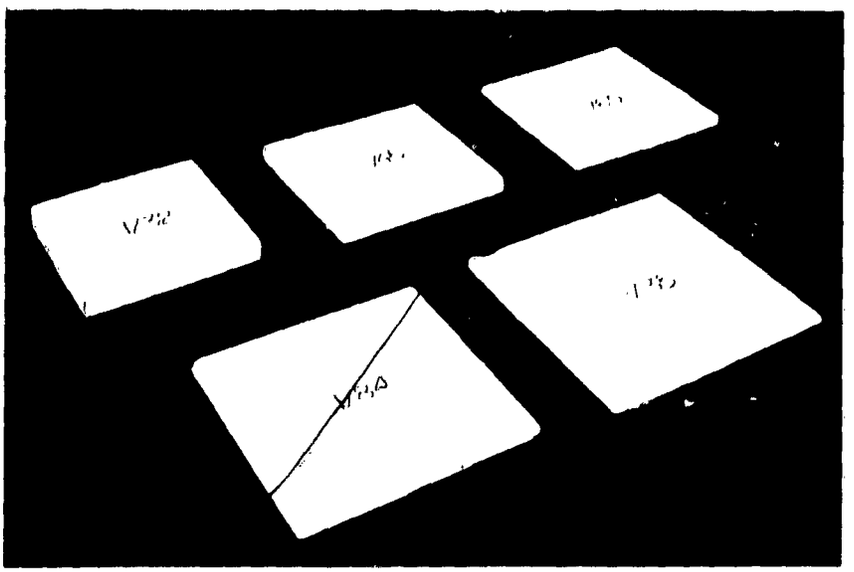

G5741

Fig. 4. 300-gram charges having thicknesses varying from $\frac{1}{4}$ to $\frac{1}{2}$ inch used for third series of pendulum tests.

Table II. Effect of Thickness of 218-Gram Charge on Vertical Rise of Pendulum

Test No.	Dimensions of Charge (in.)	Ratio of Thickness to Contact Area	Vertical Rise (in.)
12	15/16 x 3 x 3	1:10	1.7
11	"	"	1.7
9	"	"	1.9
2	"	"	1.7
16	5/8 x 3-5/8 x 3-5/8	1:20	2.4
13	"	"	2.5
10	"	"	2.5
7	"	"	2.4
14	1/2 x 4 x 4	1:30	2.5
8	"	"	2.5
5	"	"	2.7
1	"	"	2.5
15	7/16 x 4-7/16 x 4-7/16	1:45	3.2
6	"	"	2.9
4	"	"	3.1
3	"	"	3.0
28	3/8 x 4-3/4 x 4-3/4	1:60	3.2
25	"	"	3.1
23	"	"	3.1
21	"	"	3.1
27	5/16 x 5-3/16 x 5-3/16	1:85	3.4
24	"	"	3.3
18	"	"	3.3
17	"	"	3.2
26	1/4 x 5-13/16 x 5-13/16	1:135	3.5
22	"	"	3.5
20	"	"	3.4
19	"	"	3.5

Table III. Effect of Thickness of 300-Gram Charge on Vertical Rise of Pendulum

Test No.	Dimensions of Charge (in.)	Ratio of Thickness to Contact Area	Vertical Rise (in.)
2	1/2 x 4-13/16 x 4-13/16	1:45	0.84
7	"	"	0.74
14	"	"	0.80
4	7/16 x 5-1/8 x 5-1/8	1:60	1.06
9	"	"	1.05
12	"	"	1.04
1	3/8 x 5-9/16 x 5-9/16	1:85	1.24
6	"	"	1.35
11	"	"	1.23
5	5/16 x 6-1/16 x 6-1/16	1:115	1.79
10	"	"	1.85
15	"	"	1.88
3	1/4 x 6-13/16 x 6-13/16	1:185	2.55
8	"	"	2.42
13	"	"	2.58

The ratio of explosive thickness to contact area with the 25-gram charges started at 1:1.5 and decreased to 1:16; for the 218-gram charges, 1:10 to 1:135; and for the 300-gram charges, 1:45 to 1:185.

When work accomplished by each shape of charge was plotted against thickness of charge, the resulting curve sloped upward (Fig. 5, top) showing that the thinner the explosive detonated on the pendulum, the higher the swing and, thus, the more foot-pounds of work accomplished. But when the work was divided by the contact area of the explosive and then plotted against the thickness of the charge, the curve sloped downward (Fig. 5, bottom). Obviously, the thinner the explosive, the less foot-pounds of work accomplished per square inch of contact area. This was the key to a hypothesis explaining the apparent contradiction to the pendulum results which developed in similar tests conducted on concrete structures. The hypothesis is presented and discussed in paragraph 12a.

5. Model Charge Studies, Unreinforced Concrete. Initial concrete studies were conducted on low-quality, unreinforced concrete

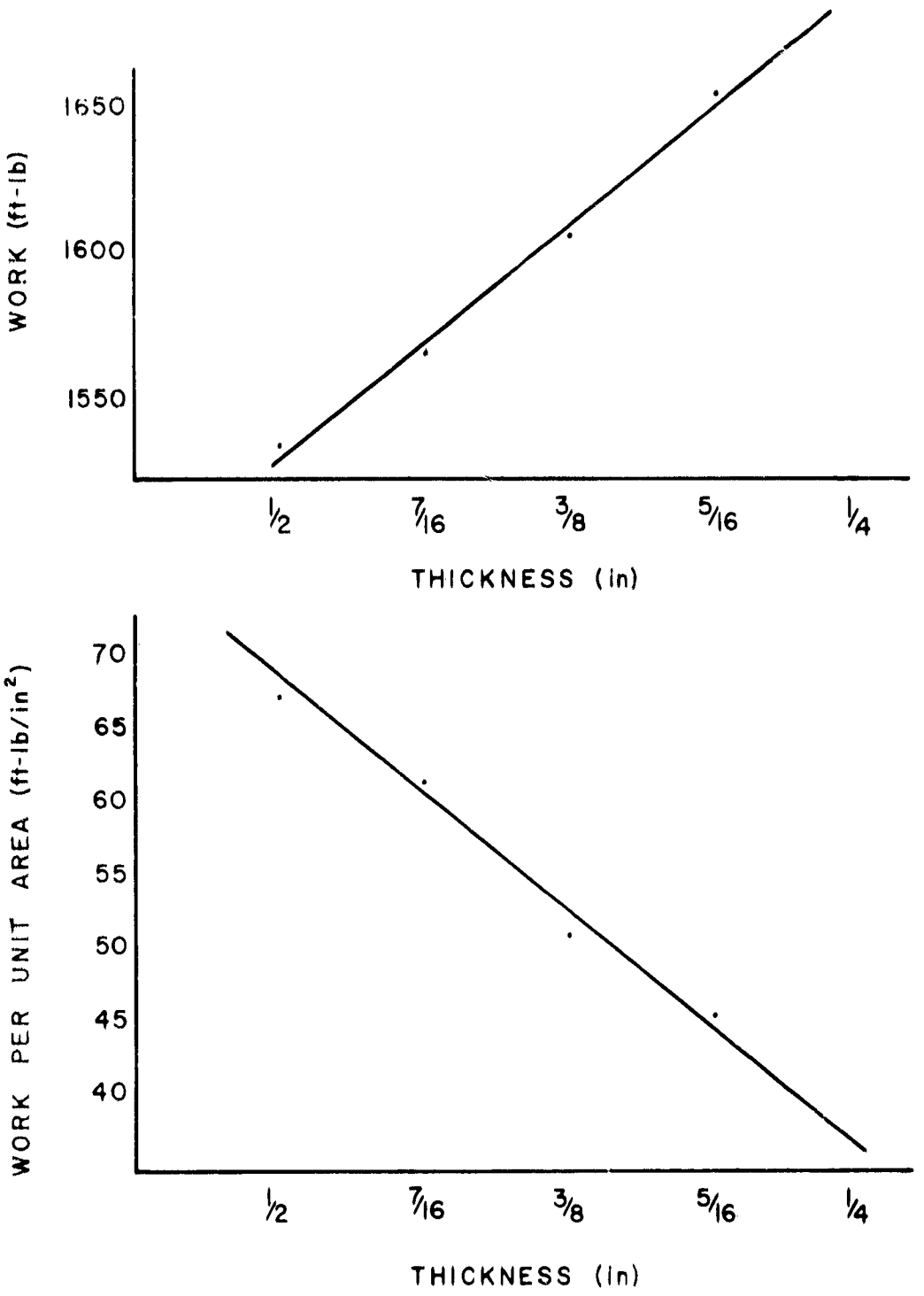

Fig. 5. Top: Foot-pounds of work versus thickness of explosive. Bottom: Foot-pounds of work per square inch of contact area versus thickness of explosive.

recovered from floor slabs of demolished buildings. A statistical design for the experiments was employed so that significance of the change of thickness of the explosives could be established mathematically. The experiment was also designed to investigate simultaneously the best position of the charge on the wall, effect of plastic cover on destructiveness of the charge, and all interactions between these variables.

Two sets of walls were cut from the floor slabs, one set approximately 4 inches thick and the other approximately 6 inches thick. One face of these walls was smooth, but the face which had been in contact with the ground was rough. Twenty-five-gram charges identical to the 25-gram charges used in the pendulum tests (1/4 inch to 3/4 inch thick) were used in all tests against the unreinforced walls. Charges were placed either at the center or at the base of the wall and were fastened either in direct contact or with a strip of plastic 6 mils thick between the charge and the wall (Fig. 6).

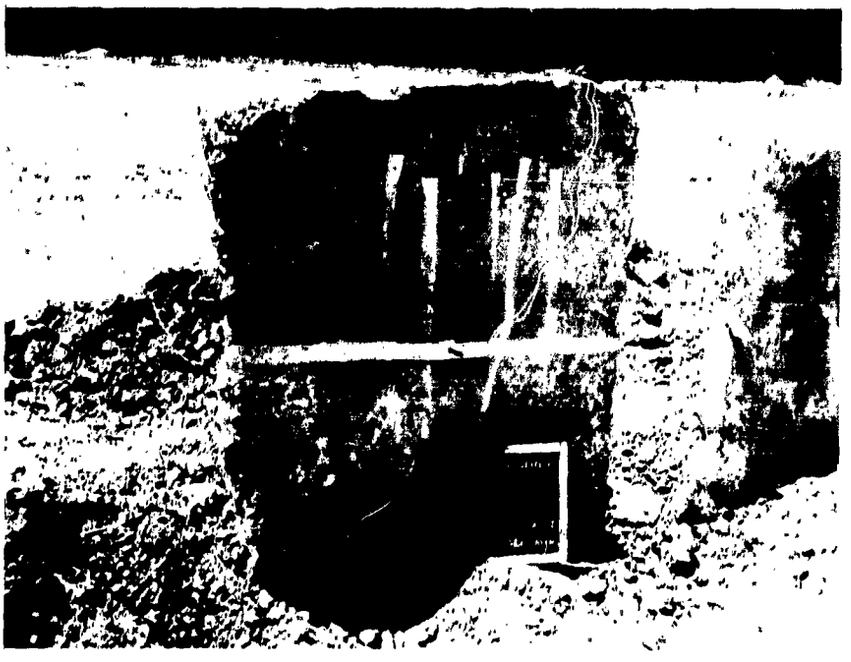

E7776

Fig. 6. A 25-gram charge, without plastic, fastened at the center of a wall.

A factorial experimental design was employed. Since there were five different ratios, two positions of the charge on the wall, and two ways (with or without the plastic layer) of mounting the explosive, there was a total of 20 (5 x 2 x 2) possible combinations of

variables. The experiment was repeated once to make a total of 40 shots in the complete design.

Tests were fired in random order. Testmen measured the volume of each crater produced by a blast by filling the crater with putty, leveling the putty off flush with the wall, removing the putty, and immersing it in a container of water. The volume of the putty and, thus, of the crater was equal to the water displaced in the container. Crater volumes were compared by analysis of variance (Appendix B), a statistical test which established the significance of the effects which the variables had on the yield of the explosive. Volumes of the craters produced by the 25-gram charges and the conditions under which each firing occurred are shown in Table IV.

Table IV. Crater Volumes Produced by 25-Gram Charges on 4-Inch-Thick Walls

Thickness to Contact Area Ratio	Crater Volume (Cu. In.)*			
	Without Plastic		With Plastic	
	Charge at Wall Bottom	Charge at Wall Center	Charge at Wall Bottom	Charge at Wall Center
1:1.5	12.9	22.7	13.9	22.5
1:2.6	15.9	23.0	15.0	24.7
1:4.4	16.9	25.3	18.7	27.1
1:7.3	15.3	26.5	17.1	21.2
1:15.5	24.6	26.5	19.4	24.2

* Average of two shots.

The thinnest charge, detonated at the center of the wall, produced the best results. Statistical tests established the degree of reliability of the results. The analysis of variance demonstrated the importance of charge thickness and also of position of the charge on the wall but found that plastic under the charge was insignificant. Another statistical test (student's "T" test) rated the thinnest charge significantly more effective than the others.

A second set of slabs, approximately 6 inches thick, was set up and tested similarly except that all charges were fired at the center of the wall, eliminating one variable. Thus, the only variables considered were thickness of the charge and presence of plastic between the explosive and the concrete. Each test was fired twice, and craters were measured in the same manner as in the first series. The results, shown in Table V, added additional evidence that the thinnest charge produced the best results and that the

plastic did not appreciably affect results. Graphs of the two tests (Fig. 7) illustrate the trend toward greater effect of smaller ratios and also proved the importance of placing the charge at the center of the wall rather than at the base. The graphs also emphasize the degree of variance between shots that plagued all tests on concrete.

Table V. Crater Volumes Produced by 25-Gram Charges on 6-Inch-Thick Walls

Thickness to Contact Area Ratio	Crater Volume (Cu. In.)*	
	Without Plastic	With Plastic
1:1.5	15.1	16.9
1:2.6	20.5	18.3
1:4.4	21.1	18.1
1:7.3	19.5	20.0
1:15.5	24.4	28.3

* Average of two shots.

6. Model Charge Studies, Reinforced Concrete (Series 1). Information obtained from unreinforced-concrete studies was applied to reinforced concrete in the next phase of testing. A TNT plant near Point Pleasant, West Virginia, had been stripped of storage tanks leaving support walls composed of reinforced, high-quality concrete. Walls (Fig. 8) 14 inches thick and approximately 8 feet wide and 8 feet high were selected for the first series of tests. Design of these tests was similar to the design of experiments for the unreinforced-concrete slabs. The charge size was increased from 25 grams to 218 grams with thicknesses of 1/4, 3/8, 1/2, and 5/8 inch. Three methods of initiating the charge and the effect of tamping (confining the charge with mud) were considered. The three methods of initiation were: center, corner, and multiple (two-corner) where the corner primers were connected by a detonating cord bridle (Fig. 9). Since importance of placing the explosive near the center of the walls and insignificance of plastic between the charge and concrete had been established, these two variables were eliminated in the reinforced-wall tests.

The three variables--thickness of charge, method of priming, and tamping--were investigated simultaneously by a factorial-type experimental design similar to that used in the first tests. There were four thicknesses of explosive, three methods of priming, and two methods of tamping (tamped and untamped) making a total of 24 possible combinations of variables (4 x 3 x 2). The entire experiment was repeated making a total of 48 shots. Testmen loaded

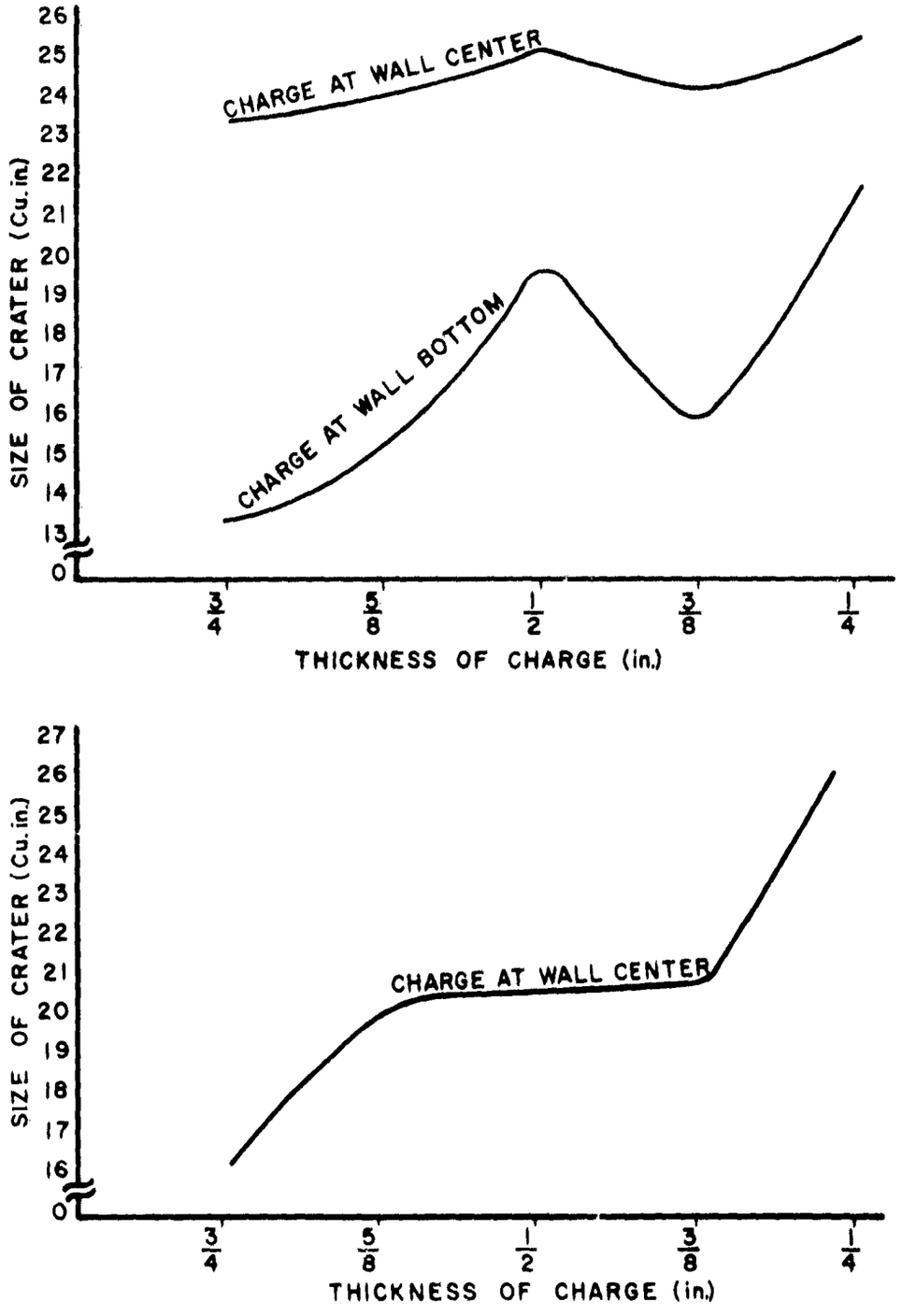

Fig. 7. Top: Tests of 25-gram charge on 4-inch unreinforced concrete walls. Bottom: Tests of 25-gram charge on 6-inch unreinforced concrete walls.

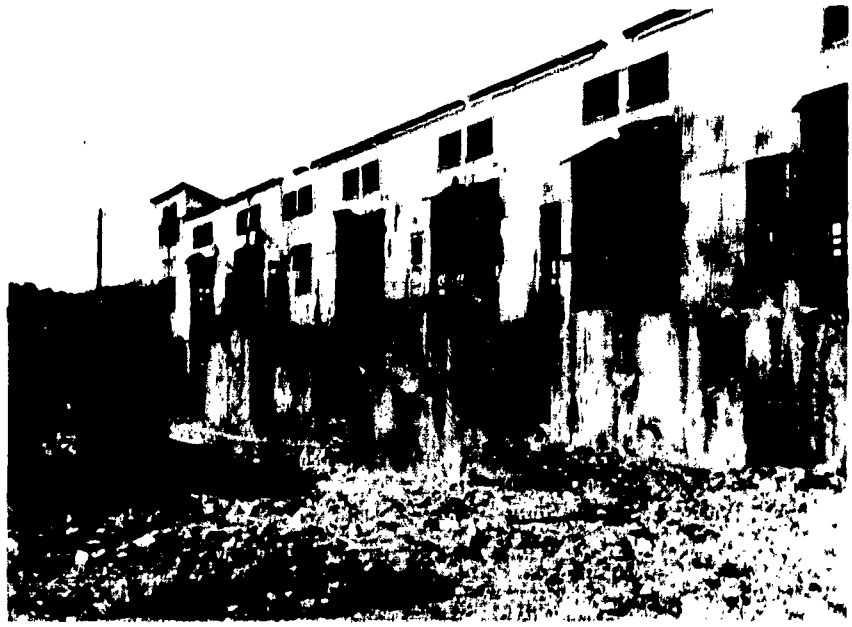

E9153

Fig. 8. Abandoned reinforced concrete walls, 14 inches thick, which were used in tests.

plastic explosive into forms made of wood in the dimensions required for each charge thickness (Fig. 10). The explosive was placed in the forms a little at a time and was compressed by pounding with wooden rods. A density of between 1.50 and 1.59 grams per cubic centimeter was obtained and the dimensions were held to the nearest 1/16 inch. Testmen taped each charge near the center of the wall making certain that the explosive was in close contact with the concrete. Charges were detonated with special electric caps (J-2) and a 10-gram booster pellet formed of loosely packed Composition C-4. For the charges primed at two corners, a 10-gram pellet was cut in half and one half used at each corner with the blasting cap. The two blasting caps and boosters were fired simultaneously by a detonating cord bridle. Wood frames placed around tamped charges enabled testmen to place equivalent amounts of mud on each charge.

Tests were fired in random order. Craters formed by the explosive on the concrete were measured by the same procedure that was used in the previous unreinforced-concrete tests (Fig. 11). In cases where concrete was spalled out of the side of the wall opposite the charge, the spall was collected and weighed. In the analysis, the volumes of the craters together with the weight of spall were the measurements of yield of the charges (Table VI). The measurements were compared by analysis of variance.

Center Priming, Untamped E8993

Center Priming, Tamped E9004

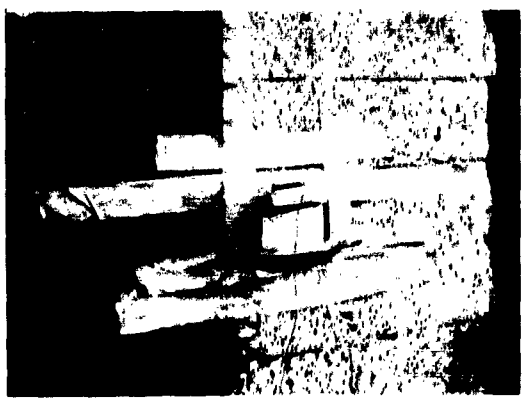

Corner Priming, Untamped E9006

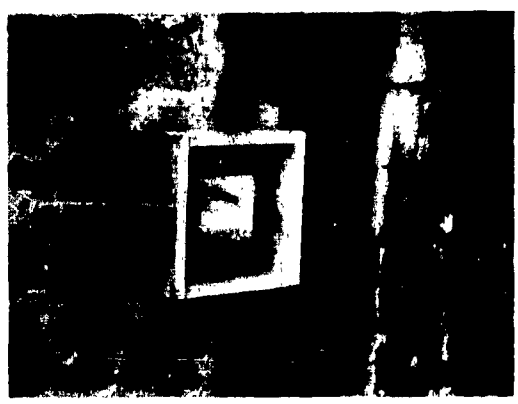

Corner Priming, Tamped E9003

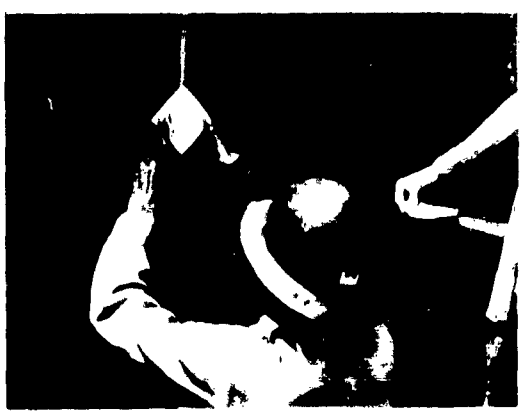

Multiple Priming, Untamped E9000

Multiple Priming, Tamped E8997

Fig. 9. Model charge tests on reinforced concrete walls (Series 1), showing the three methods of priming charge.

E9099

Fig. 10. Measuring of explosive for loading into wooden forms.

There was often a material difference in the craters produced by two charges which were presumably fired in exactly the same way. This large experimental variance prohibited attaching statistical significance to any of the effects of the variables other than tamping. However, trends developed which, in light of later tests, made possible conclusions based on qualitative data. These conclusions proved useful even though they did not meet the quantitative standards originally set. Analysis of the results shown in Table VI led to the conclusion that the optimum thickness is approximately 1/2 inch, and single priming at the center of the charge is at least as effective as the other methods of priming which were tested. With a thickness of 1/2 inch, the charge had a ratio of thickness to contact area of 1:32.

7. Full-Scale Tests on 1-Foot-Thick, Reinforced-Concrete Walls. Following the first model charge studies, a series of tests was conducted on 1-foot-thick, reinforced-concrete walls. Some of these walls were 42 inches high, and some were 55 inches high. The walls were all approximately 24 feet long (Fig. 12), and were composed of high-quality concrete, reinforced on both faces with 3/8-inch reinforcing bars, vertical and horizontal, on 12-inch centers.

a. Crater formed by charge.

b. Packing clay in crater.

c. Clay ready to be removed.

d. Removing clay.

e. Working clay to remove air pockets.

f. Immersion of clay in water to measure water displacement

Fig. 11. Method of estimating crater volumes.

Table VI. Average Crater Volumes (Cu. In.) and Spall Weights (Lb) Formed by 218-Gram Charges Tested Against 14-Inch Concrete Walls

Thickness to Contact Area Ratio	Untamped						Tamped					
	Single Cap at Center		Single Cap at Corner		2 Caps at Opp. Corners		Single Cap at Center		Single Cap at Corner		2 Caps at Opp. Corners	
	Crater	Spall	Crater	Spall	Crater	Spall	Crater	Spall	Crater	Spall	Crater	Spall
1:20	231	none	275	none	206	none	163	none	125	none	81	907
1:20	188	"	206	"	263	"	138	922	162	1140	119	none
1:32	219	"	231	"	256	"	100	none	200	1681	163	1204
1:32	175	"	244	"	200	"	181	1405	75	703	63	none
1:57	225	"	231	"	188	"	169	386	156	479	94	"
1:57	219	"	194	"	219	"	106	887	119	none	69	720
1:126	206	"	200	"	206	"	106	none	163	"	50	none
1:126	194	"	144	"	206	"	144	1331	106	1993	81	1331

E9019

Fig. 12. Walls used for testing full-scale breaching charges: (A) 12-inch-thick walls 42 inches high; (B) 12-inch-thick walls 55 inches high.

E9069

Fig. 13. Tamping a charge by pressing two mud-filled sandbags against the charge taped to the wall.

Tamped charges were tested against 1-foot walls by the same procedure as untamped charges. The charge was taped to the wall near its center, and a platform was constructed beneath the charge. Two mud-filled sandbags were placed on the platform and pressed closely around the charge (Fig. 13).

The objective of the tests on the 1-foot-thick walls was to find the minimum amount of explosive necessary to breach a 1-foot wall. A breach was defined as destruction to an extent which made the concrete no longer effective as a structural member. A hole is usually blown through the concrete, and the top of the wall is often spalled free (Fig. 14). Beginning with a 5-pound untamped charge, the test team used successively smaller charges until the minimum weight of explosive which would successfully breach a wall was established. These charges were 2 inches thick. Charges 1/2 inch to 1½ inches thick were then tested to reduce the amount of explosive necessary to obtain the same results as were obtained with the 2-inch-thick charges. The standard C-4 block was sliced with a knife to the thickness needed for each test. Test engineers compared the results and decided that the best breaches were obtained with 1-inch-thick charges (Table VII) with a ratio of thickness to contact area of 1:36. The optimum ratio for the model charge studies was believed to be in the neighborhood of 1:30. The minimum untamped charge required to consistently breach a 12-inch wall was a 2½-pound charge 1 inch thick. A 2¼-pound charge 2 inches thick damaged but did not eliminate the value of the wall (shown at the top of Fig. 14) as a structural member. The slab on top and other loose material were removed with a crowbar. The bottom of Fig. 14 shows the breach caused by a 2¼-pound charge 1 inch thick. A hole was blown through the wall, and the spall on top of the wall was partially blown off. No loose material was removed. The best breaches were obtained with a 1-3/4-pound charge 1 inch thick. The ratio of thickness to contact area was approximately 1:28, somewhat larger than the 1:36 ratio for untamped charges.

Table VII. Number of 12-Inch-Thick Walls Breached and Not Breached*

Wall Height (in.)	Untamped Charge						Tamped Charge			
	Weight (lb)	Thickness (in.)					Weight (lb)	Thickness (in.)		
		1/2	3/4	1	1½	2		3/4	1	1½
42	2	-	-	2 B 3 NB	-	-	1	-	1 NB	-
	2¼	3 B	-	3 B	-	4 NB	1-3/4	-	4 B	2 B 1 NB
55	2	1 NB	-	-	-	-	1½	3 NB	2 B	-
	2¼	-	1 B 2 NB	1 B	3 NB	-	-	-	-	-

* B = Breached. NB = Not breached.

E9043

E9030

Fig. 14. Top: Damage inflicted with 2½-pound charge 2 inches thick. Bottom: Wall breached with 2½-pound charge 1 inch thick.

Proximity of the charges to the top of the walls increased the destructiveness of the charge. Shock waves apparently traveled to the free surface at the top of the wall where a tensile wave developed which spalled concrete in a layer from the top. A charge detonated farther from the top would not have caused as much damage. This was illustrated by tests on walls 55 inches high. The earlier tests were conducted on walls 42 inches high, but when the height of the wall was increased by just 13 inches the resulting damage to the wall was decreased. A 2¼-pound charge fired on a 42-inch wall effectively breached it, but a 2½-pound charge was required to breach a wall 55 inches high.

8. Model Charge Studies, Reinforced-Concrete Walls (Series 2). The first series of model charge studies failed to achieve the anticipated mathematically definable results. Failure can be attributed to excessive variation in the experiments. In the second series, an attempt was made to eliminate several factors which had contributed to the variation. In the first series, the explosive had been tamped into wooden frames. In the second series, the explosive was cut from standard blocks in the hope that the more uniform density of the block would produce greater uniformity in the charges. This process sacrificed some accuracy in the charge dimensions. The earlier tests involved 218-gram charges, but, in the second series, 625-gram charges were used in an attempt to insure that every charge would spall the opposite side of the wall.

E9125

Fig. 15. Rectangular charge with a length three times its height and a ratio of thickness to contact area of 1:125.

There seemed to be a tendency in previous tests for the crater to increase in size in cases where no spalling occurred. Instead of three methods of priming, only one was used in these tests since the earlier tests indicated lack of significance of priming procedures. Tamping had been considered in the first model tests, but this was not included in the later tests; however, one additional variable was included--the ratio of length to height of the charge. Half the charges were square; the others were rectangular with a length to height ratio of 3:1 (Fig. 15). The four ratios of thickness to contact area chosen for the tests were 1:25, 1:50, 1:75, and 1:125.

A factorial-type design of experiment which was set up for the second series of model tests required eight tests for one complete series (4 x 2), and the series was fired three times for a total of 24 shots. Sizes of the craters formed are shown in Table VIII.

Table VIII. Sizes of Craters Formed by 625-Gram Charges

Thickness to Contact Area Ratio	Size of Craters (cu. in.)	
	1:1 Length/Height	3:1 Length/Height
1:25	637.5	481.3
	625.0	587.5
	512.5	600.0
1:50	581.3	556.3
	618.8	481.3
	637.5	462.5
1:75	575.0	656.3
	512.5	543.8
	393.8	600.0
1:125	600.0	493.8
	431.3	425.0
	468.8	475.0

Photographs shown in Fig. 16 illustrate the tremendous variation in results between the three tests fired in exactly the same way. Each line contains photographs of three identical tests. The odd lines are results of tests of charges with a length to height ratio of 3:1, and the even lines are tests of square charges which were otherwise the same as the preceding line. An analysis of the results and a study of a graph of crater sizes (Fig. 17) led to the conclusion that

Fig. 16. Photographs of craters and spalls formed by 625-gram charges in the second model charge series illustrating variation in results between three tests fired in exactly the same way.

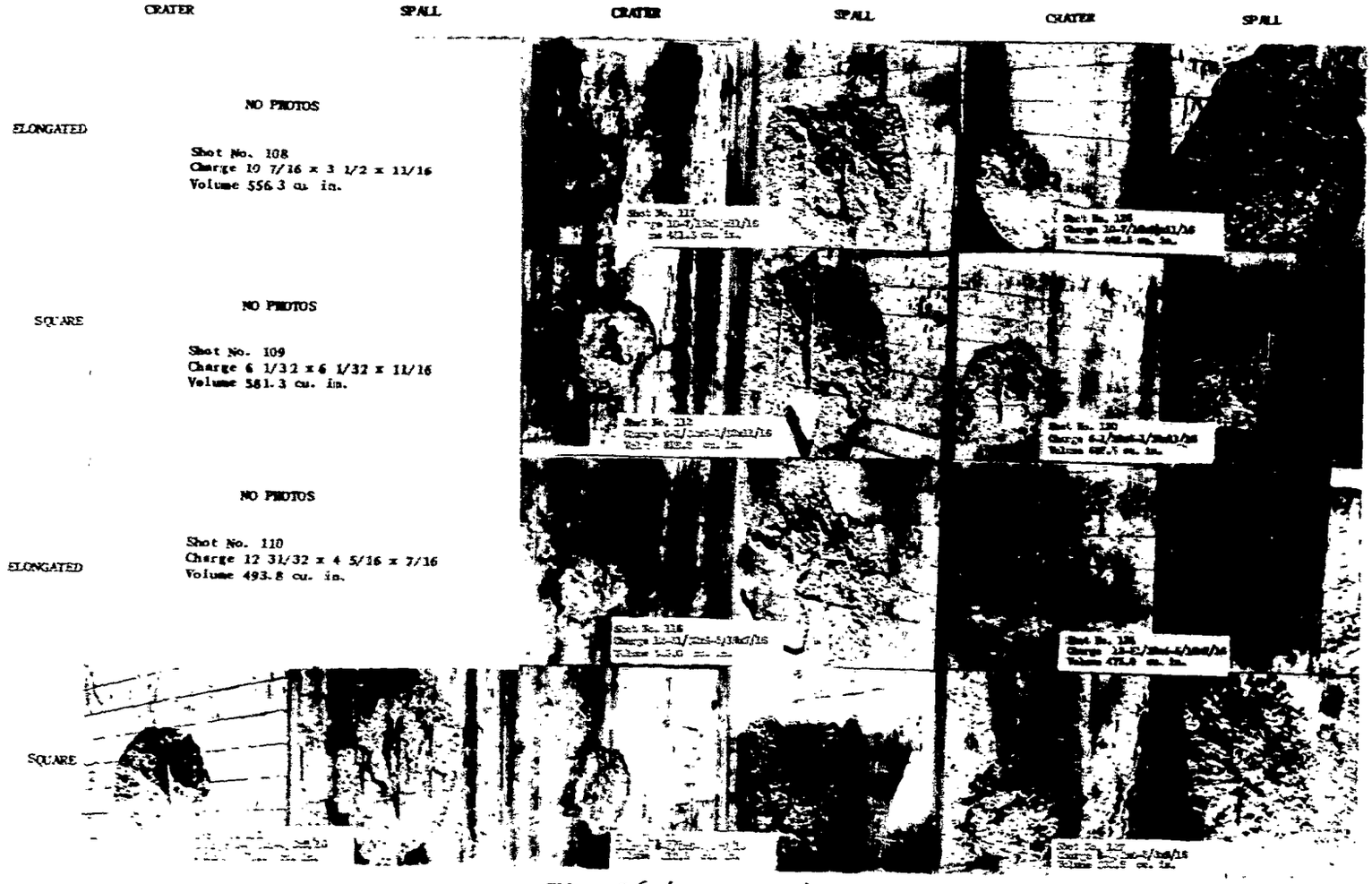

Fig. 16 (continued)

E9353

the best ratio between thickness and contact area was between 1:25 and 1:50 and that the ratio of charge height to length of 1:1 may be slightly better than 1:3.

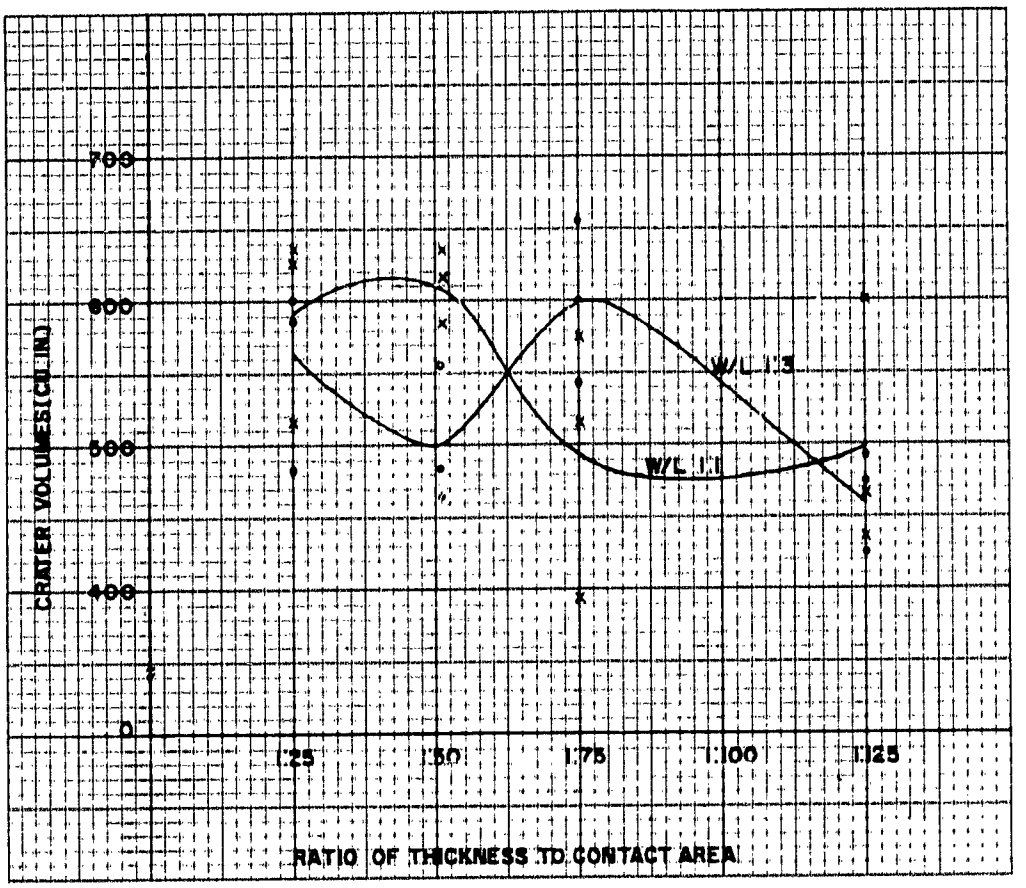

Fig. 17. Volumes of the craters formed by square and elongated 625-gram charges with thickness to contact area ratios of 1:25 to 1:125.

B. FULL-SCALE STUDIES

9. General Test Procedures. Tests against 2-, 3-, 5-, and 7-foot-thick piers were called full-scale tests. These piers were stoutly built to represent the best quality standard bridge piers. Conclusions drawn from the basic tests were applied as a basis for selecting shapes, sizes, and locations of the charges, and for developing measurement and recording procedures.

The test structures were designed as a compromise between the type of structures needed to conduct statistically sound tests and the funds available. There were 40 test structures: 10 were

2 feet thick, 6 feet wide, and 6 feet high; 10 were 3 feet thick, 6 feet wide, and 6 feet high; 10 were 5 feet thick, 8 feet wide and 11 feet high; and 10 were 7 feet thick, 10 feet wide, and 13 feet high. The compressive strength of the concrete ranged from 5,000 to 7,000 psi (Appendix C). These piers were all reinforced with steel placed near the front and rear faces (Fig. 18).

Fig. 18. Forty concrete structures built to represent bridge piers 2, 3, 5, and 7 feet thick.

Application of the knowledge gained from the basic studies reduced the number of shots necessary to obtain significant results in the full-scale studies. All charges were attached to the piers at a point several feet above the base of the wall since the basic studies proved that shots fired at the base of the wall were less effective than those fired at the center. All charges were initiated by placing the blasting caps 3/4 inch into the explosive at the midpoint of the charge. The explosive was cut to size from standard C-4 blocks, disturbing the explosive density as little as possible. Test engineers attempted to predict the explosive necessary to breach the piers.

Demolition testmen carefully fastened the charges in close contact with the concrete. They attached a wooden shelf to the concrete to support the charge and then stretched masking tape across the charge at two or three points, as necessary, to hold the charge tightly against the concrete. The center point of the charge was always midway between reinforcing bars.

F4190

Fig. 19. Tower with Fastax camera used to make nigh-angle, close-in shots.

Extensive photography recorded the results of the test. Fastax cameras were employed on most of the tests at framing speeds of from 3,000 to 9,000 frames per second. A tower (Fig. 19) made high-angle, close-in shots possible. The photographic section employed a Courtney-Pratt lenticular camera for three of the shots fired on the 5-foot-thick walls. Polaroid photographs provided an immediate record of the results of each blast and facilitated the progressive analysis. Conventional still and motion picture cameras as well as stereocameras furnished detailed records of the test procedures and the resulting damage to the concrete.

The engineers estimated the amount of explosive which would be required to breach each size pier using the Stanford Research Institute conclusions, modified by the results of the basic studies, as a guide. These estimates were graphed (Fig. 20), and the first charge to be tested on 2-foot piers was selected from the graph. When changes were made in amounts of explosive used in successive shots, the changes were usually in 20-percent increments of the first charge. These large changes made possible efficient bracketing of the optimum breaching charge. Before the next size piers were tested, the estimated curve was adjusted to reflect the new values obtained for the breaching charge for the previous size piers. This procedure helped the engineers make effective use of the small number of test structures.

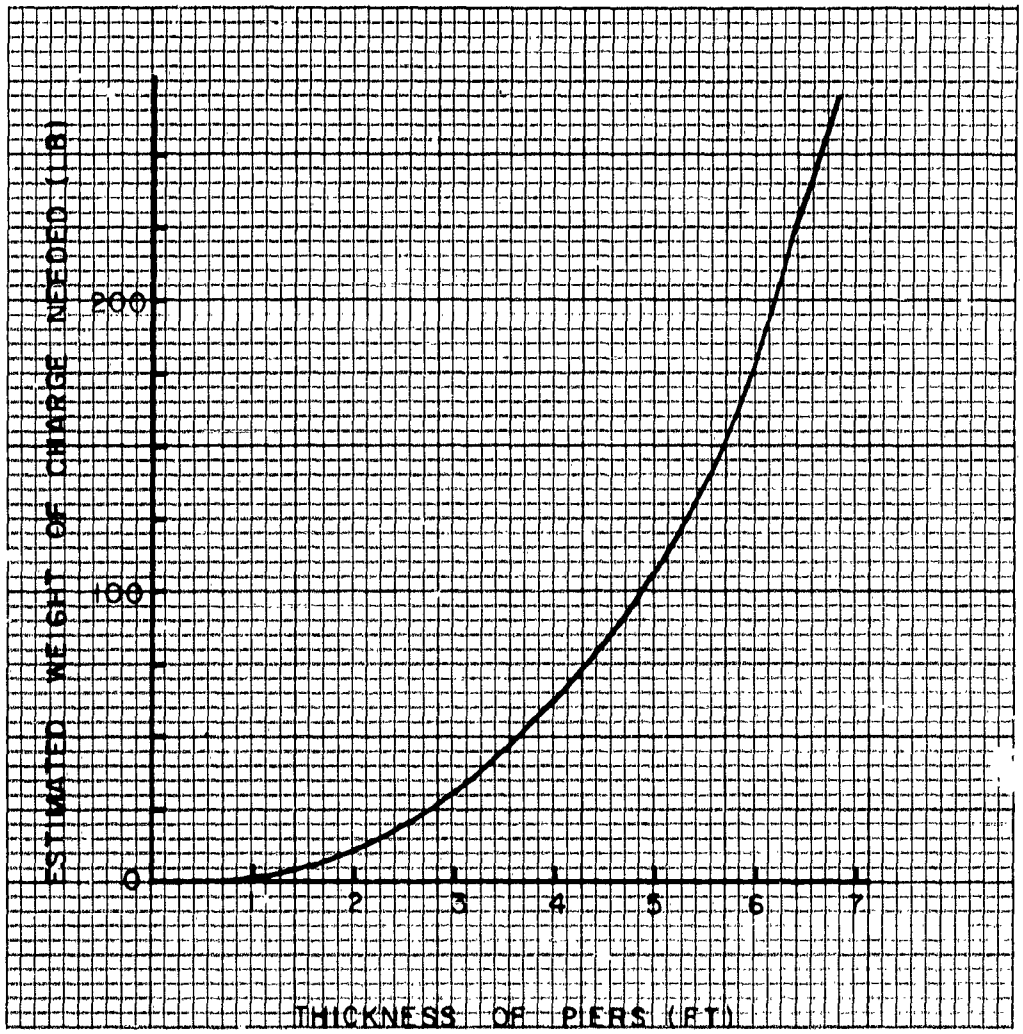

Fig. 20. Estimated amount of explosive required to breach piers 2, 3, 5, and 7 feet thick.

10. Demolition Tests and Test Results. Demolition tests against 2-, 3-, 5-, and 7-foot-thick piers and the test results are described in the following paragraphs.

a. Piers 2 Feet Thick. The 2- by 6- by 6-foot piers had an additional 3 feet of concrete (the foundation and footing) underground. The 6-foot length was estimated to be one-fourth the average length of a bridge pier. Soil was piled at both ends of the piers to increase their effective length by transmitting shock waves induced by the explosion away from the ends of the piers. This soil reduced spall from the ends and permitted them to act more like the much longer standard bridge pier. The curve depicting estimated

pounds of explosive per thickness of wall was the basis for selecting the first charge to be tested. A weight of 10.4 pounds, 80 percent of the amount which was predicted, was selected. The best ratio of thickness to contact area of explosive in the basic tests appeared to be approximately 1:40, and this ratio was used as the initial ratio in tests against 2-foot-thick piers. With a ratio of 1:40, the thickness of the charge was 2-1/8 inches and the side of the square contact area was $9\frac{1}{4}$ inches (Fig. 21).

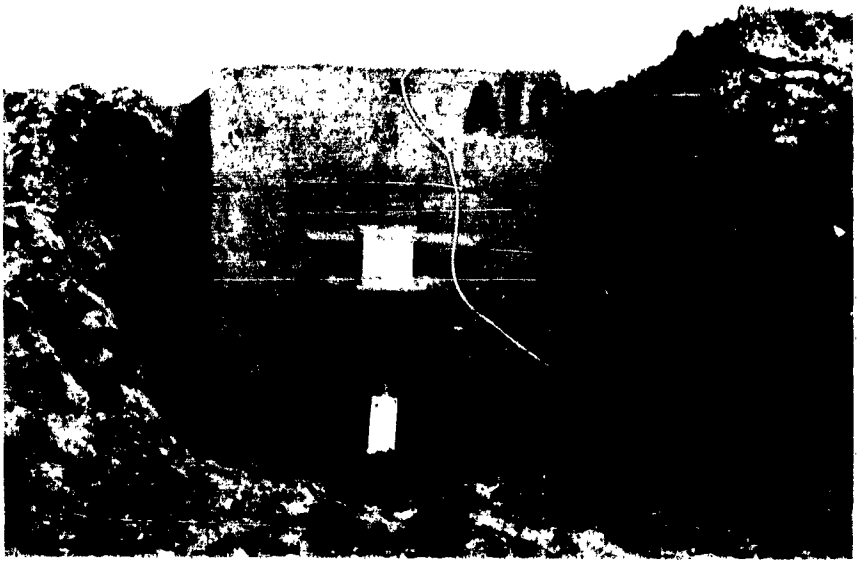

F41152

Fig. 21. A 10.4-pound charge in place on 2-foot-thick pier. Note supporting table.

The 10.4-pound charge destroyed a 2-foot pier down to 1 foot from the base. Destruction was more extensive than necessary; therefore, the next charge was reduced to 60 percent of the predicted value, or 7.8 pounds, with a ratio of 1:40. When this charge failed to breach the pier, the charge size was repeated but this time with a ratio of 1:60 (Fig. 22). At a ratio of 1:40, the thickness of the charge was 1-7/8 inches, but at a ratio of 1:60, the thickness was $1\frac{1}{2}$ inches. Although damage was somewhat greater on the latter charge, the pier was not breached. Weight of the next charge was, therefore, increased to 9.1 pounds, 70 percent of the predicted weight, with a ratio of thickness to contact area of 1:40. When the 9.1-pound charge achieved adequate destruction of the pier, two more 9.1-pound charges were fired with ratios of 1:60 (Fig. 23) and 1:80. The three 9.1-pound charges were repeated, and all shots successfully breached the piers. (It is important to note that the second series of three shots, fired under conditions nearly identical

F9220

Fig. 22. A 2-foot pier unbreached by a 7.8-pound charge having a ratio of thickness to contact area of 1:60.

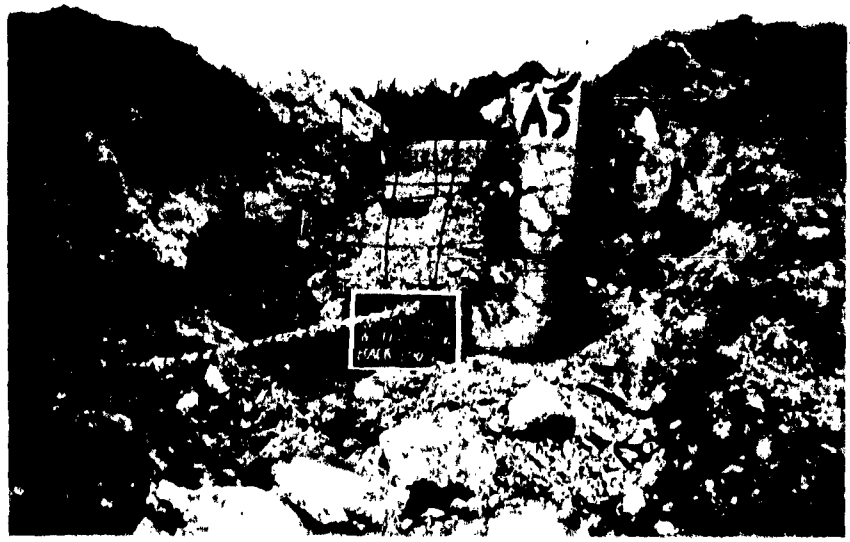

F4140

Fig. 23. A 2-foot pier breached by a 9.1-pound charge with a ratio of thickness to contact area of 1:60.

to the first series, were noticeably less effective. Since the explosive was not randomized, there is no way of knowing whether the explosive used in the second tests was defective. The six 9.1-pound shots provided a comparison between the ratios of 1:40, 1:60, and 1:80. Another 7.8-pound shot was fired at a ratio of 1:80 to complete three shots at the different ratios with 7.8-pound charges. Figure 24 shows the sequence in which each shot was fired and whether or not the shot breached the pier.

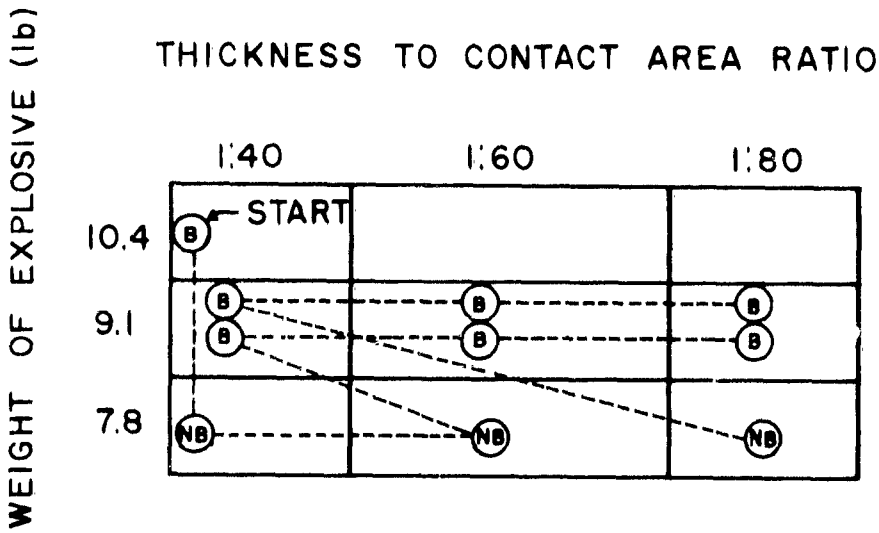

Fig. 24. Sequence and results of shots on 2-foot-thick piers: B represents a pier considered adequately breached; NB, not breached.

Fastax films taken of the demolition of the 2-foot-thick piers helped to clarify the mechanics of the breakup of the concrete (Fig. 25). That portion of the concrete directly opposite the charge mushroomed out of the pier. Cracks developed in the concrete in a radial pattern. Since shock waves travel faster through steel than through concrete, it had seemed reasonable to suppose that cracks would form along the steel reinforcing bars, but there was no indication from the photographic studies that such a rectangular breakup pattern had occurred.

The test crew attempted to obtain a quantitative measure of the effect of each charge by measuring the volume of the craters and spalls. Attempts were frustrated by many problems such as the following that were difficult to resolve. How much of the damaged material still remaining in place in the pier should be considered in the measurement, and how much should be removed and not considered? Should large chunks of concrete held to the pier by

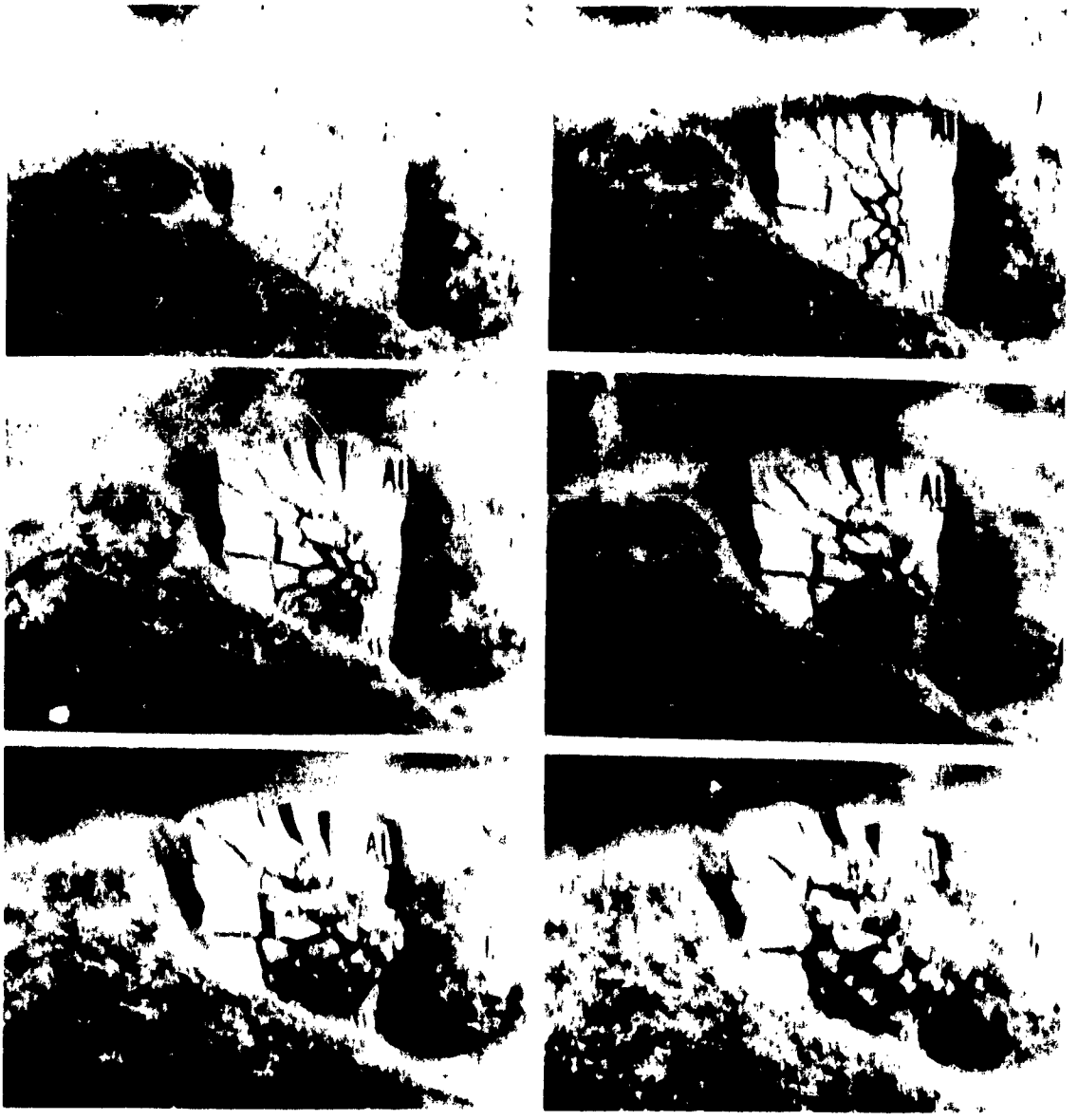

F6890

Fig. 25. Photographs printed from high-speed camera sequence illustrating mushroom breakup pattern on side of pier opposite explosion.

steel only be considered in the measurement or should they be broken loose from the steel and removed? How should heavy cracks in the material be considered? Criteria for making measurements were established and measurements taken but these were abandoned because it was soon obvious from the irrational values that they did not provide a true measure of damage. However, the diameter of each crater and spall was recorded (Table IX) for use in estimating the distance between charges on piers of normal length.

Table IX. Dimensions of the Craters and Spalls Blasted in 2-Foot-Thick Piers

Pier No.	Weight of Charge (lb)	Thickness to Contact Area Ratio	Crater Diameter (in.)	Spall Diameter (in.)	Breached or Not Breached
A-1	10.4	1:40	52	*	Breached
A-2	9.1	1:60	46	*	Breached
A-3	7.8	1:60	44	57	Not breached
A-4	7.8	1:40	36	54	Not breached
A-5	9.1	1:60	41	53	Breached
A-6	9.1	1:40	45	*	Breached
A-7	9.1	1:80	*	*	Breached
A-8	9.1	1:80	40	66	Breached
A-9	9.1	1:40	42	45	Breached
A-10	7.8	1:80	40	47	Not breached

* Pier so badly damaged that measurements were impracticable.

The 10 shots fired on 2-foot-thick piers established the minimum weight for breaching the concrete as 9.1 pounds provided that the explosive is placed on the concrete in the same manner as in the tests. The tests did not establish the optimum ratio as precisely as they did the minimum weight, but the ratio of 1:60 was estimated to have produced the best results.

b. Piers 3 Feet Thick. Dimensions, except thickness, for the 3-foot piers were the same as for the 2-foot piers (6 feet wide and 6 feet high with 3 feet of foundation and footing below ground level). The graph representing the predicted weight of the charge for the pier thickness, originally developed for the 2-foot-thick piers, was redrawn to reflect the conclusions from the experiments on 2-foot piers. According to the predicted curve, a 20-pound charge should breach a 3-foot pier. Eighteen pounds of explosive (90 percent of the predicted figure) was selected for the first test. This shot completely destroyed the upper two-thirds of the pier. After studying the high-speed film taken of the shot, test engineers

were concerned over the possibility that destruction was exaggerated by the nearness of the charge to the top of the pier. To test this theory, a wooden crib was constructed on top of a second pier and filled with mud to a height of 3½ feet above the top of the concrete (Fig. 26) to, in effect, increase the height of the pier. An 18-pound charge similar to the first charge was detonated on this pier and the results compared. The second charge created even greater destruction than the first.

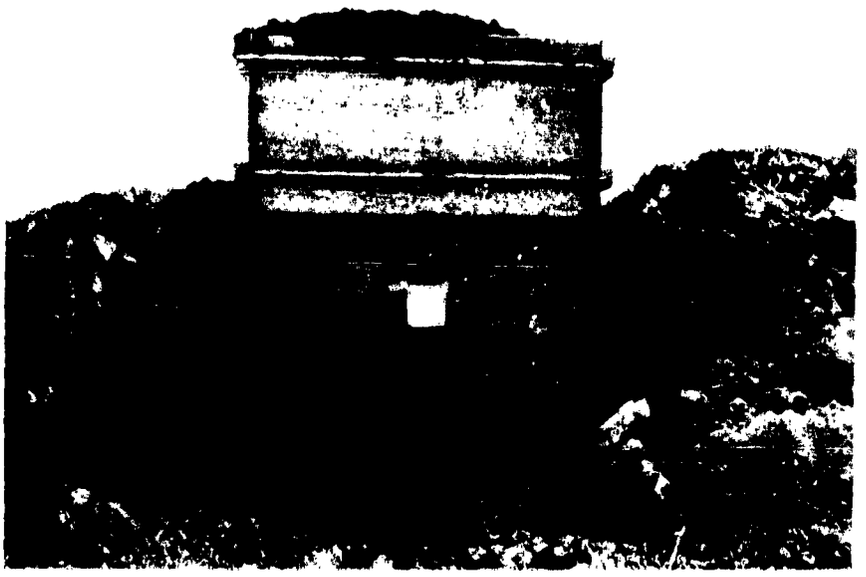

F4185

Fig. 26. Wooden crib filled with mud to a height of 3½ feet on top of a pier 3 feet thick.

The next three charges tested, each weighing 12 pounds, were made with ratios of thickness to contact area of 1:40, 1:60, and 1:80. All three charges failed to breach their piers but the ratios of 1:60 and 1:80 appeared more effective than the 1:40. Two charges weighing 15 pounds each with ratios of 1:60 and 1:80 effectively breached their piers (Fig. 27). These two shots were repeated, this time with 3½ feet of mud placed on top of the piers. Under the new conditions, the ratio of 1:60 was more effective than the previous 1:60 shot, but the ratio of 1:80 was considerably less effective than the previous 1:80 shot. A fourth 12-pound shot, with a ratio of 1:60, was fired on a pier covered with 3½ feet of mud. This shot failed to breach the pier but destruction was greater than that achieved by the previous 12-pound shot which was tested similarly but without the mud-filled crib (Fig. 28).

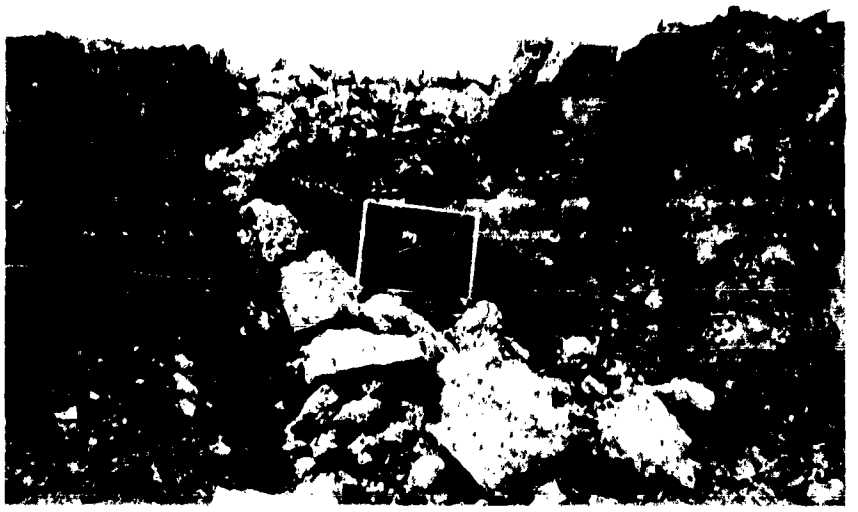

F4164

Fig. 27. 3-foot pier breached by 15-pound charge with a ratio of thickness to contact area of 1:60.

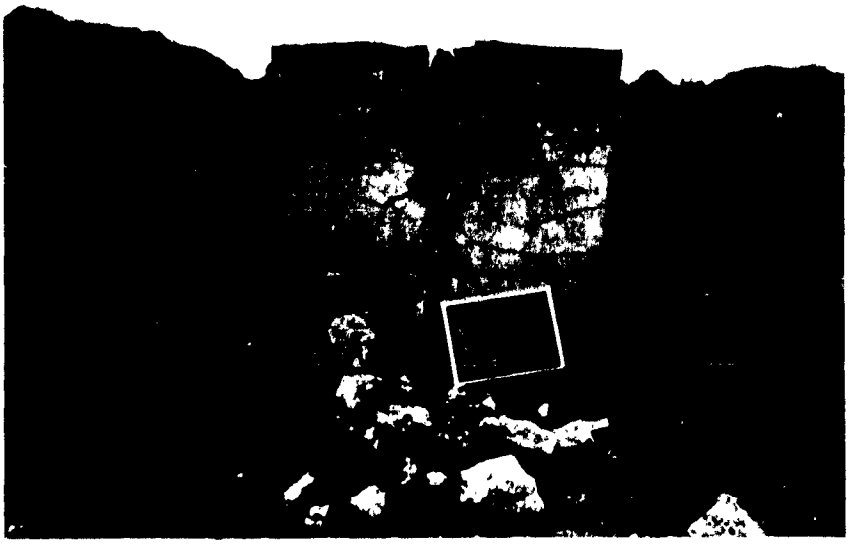

F4161

Fig. 28. 12-pound charge with a ratio of thickness to contact area of 1:80 failed to breach this 3-foot-thick pier.

The 3-foot-thick pier tests established 15 pounds as the minimum charge necessary to achieve adequate breaching. The tests did not establish an optimum ratio, but 1:80 appeared to be effective. Dimensions of the 15-pound charge with a ratio of thickness to contact area of 1:80 were 1.8 by 12.1 by 12.1 inches. The 1:60 ratio appeared to be just as effective as the 1:80 ratio. Dimensions of the 1:60 charge were 2.1 by 11.2 by 11.2 inches, virtually the same dimensions as would be obtained by using the standard C-4 block. Figure 29 shows the sequence in which each shot was fired and whether or not the shot breached the pier.

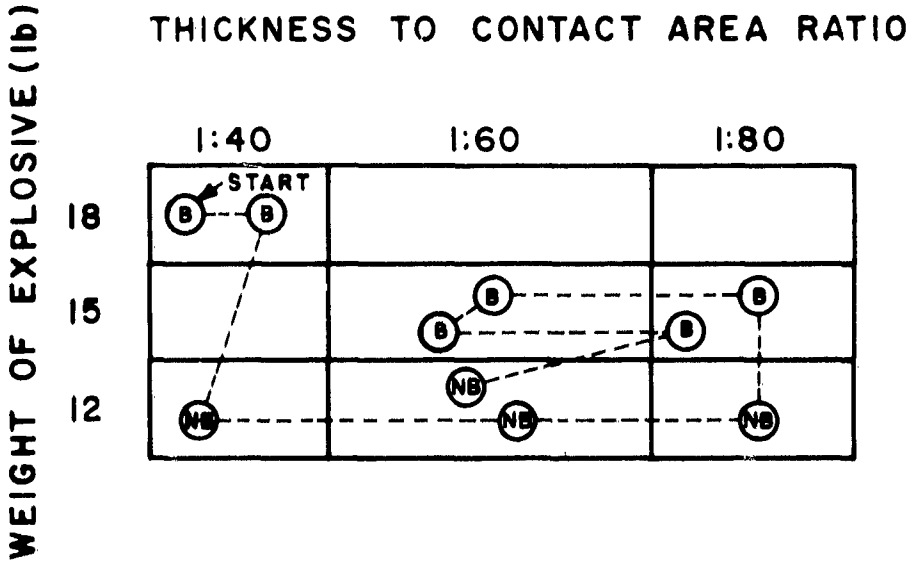

Fig. 29. Sequence and results of shots on 3-foot-thick piers: B indicates a pier considered adequately breached; NB, not breached.

Volumes were obtained of craters and, where possible, of spalls, just as in the 2-foot piers, but these measurements were also abandoned as they proved to be even less significant than the measurements obtained from the 2-foot piers. The diameter of each crater was measured and the diameter of the spalls estimated as accurately as possible (Table X). The effect of the explosive on 3-foot piers was similar to that on 2-foot piers. The crater pattern on the explosive side of the pier was clearly discernible although not as distinct as in tests on the 2-foot piers. The principal difference between the effect of explosive on the 3-foot piers and on the 2-foot piers was in the spall. Where the explosive was inadequate on the 3-foot piers, the spall did not completely detach itself from the pier except at a point opposite the charge where a small section of concrete was blown free. The spall was characterized by the same radial crackup pattern as in the 2-foot piers and,

where the spall did not completely detach itself, the outline of the spall crater could be established by cracks appearing near the top of the wall. The 3-foot piers had a tendency to crack outward to the right and to the left of the center of the charge.

Table X. Dimensions of Craters and Spalls Blasted in 3-Foot-Thick Piers

Wall No.	Weight of Charge (lb)	Thickness to Contact Area Ratio	Crater Diameter (in.)	Spall Diameter (in.)	Breached or Not Breached
B-1	18	1:40	55	*	Breached
B-2	12	1:80	53	12	Not breached
B-3	15	1:60	50	*	Breached
B-4	15	1:80	55	*	Breached
B-5	12	1:60	49	11	Not breached
B-6	15	1:60	54	*	Breached
B-7	18	1:40	53	*	Breached
B-8	15	1:80	51	38	Breached
B-9	12	1:40	45	11	Not breached
B-10	12	1:60	44	0	Not breached

* Pier so badly damaged that measurements were impracticable.

c. Piers 5 Feet Thick. Tests on 5-foot piers provided striking experimental verification of the theory that the ratio between explosive thickness and contact area is of critical importance. Statistical tests applied in the model charge studies proved that the ratio is significant, but in tests on the 2- and 3-foot walls, changing the ratio did not appear especially fruitful (probably because the spread of ratios was too small). Sub-optimum ratios on 5-foot piers, however, required as much as 40 percent more explosive to achieve the same breach as did the optimum ratio.

The first charge tested on a 5-foot pier weighed 85 pounds and had a ratio of 1:60 which gave the charge a thickness of 5 inches and dimensions of 17-5/16 inches square. The center of the charge was 54 inches from the base of the pier and was centered from right to left so that the top of the explosive was approximately 57 inches from the top of the pier. When this charge failed to effectively breach the pier, the charge for the next test was increased to 102 pounds but still at a ratio of 1:60. Even with this 20 percent increase in weight of explosive, only a marginal breach was obtained. When, on the third shot, the explosive was increased to 119 pounds at a ratio of 1:60, the wall was completely demolished. In the fourth shot, an explosive weight of 102 pounds was tested again,

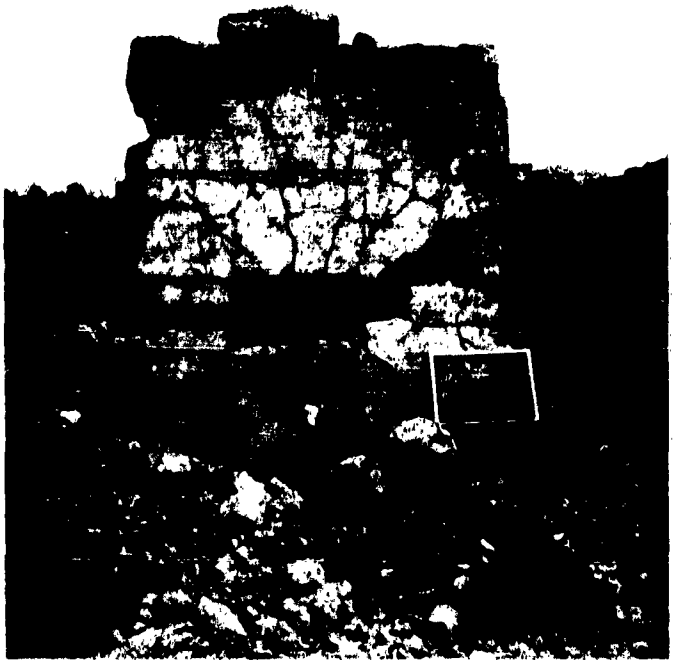

F5571

F6781

Fig. 30. Top: A 5-foot pier not effectively breached by a 76.5-pound charge at a ratio of 1:180. Bottom: Damage inflicted by a charge of the same weight but at a 1:140 ratio.

but this time the ratio was changed from 1:60 to 1:100 and an effective breach was obtained. A repeat of the 85-pound charge, this time with a ratio of 1:100, did not effectively breach the pier, but an 85-pound charge with a ratio of 1:140 produced a very effective breach. An 85-pound charge with a ratio of 1:180 did not produce as effective a breach as the ratio of 1:140; the 1:140 ratio was, therefore, tentatively established as the optimum. Two tests employing 76.5 pounds of explosive, one with a ratio of 1:140 and the other with a ratio of 1:180, added support for the selection of the 1:140 ratio. The charge fired at a ratio of 1:180 did not effectively breach the pier, but the one with a ratio of 1:140 achieved a marginal breach (Fig. 30). Figure 31 shows the sequence in which each shot was fired in the 5-foot-thick pier tests and whether or not the shot breached the pier.

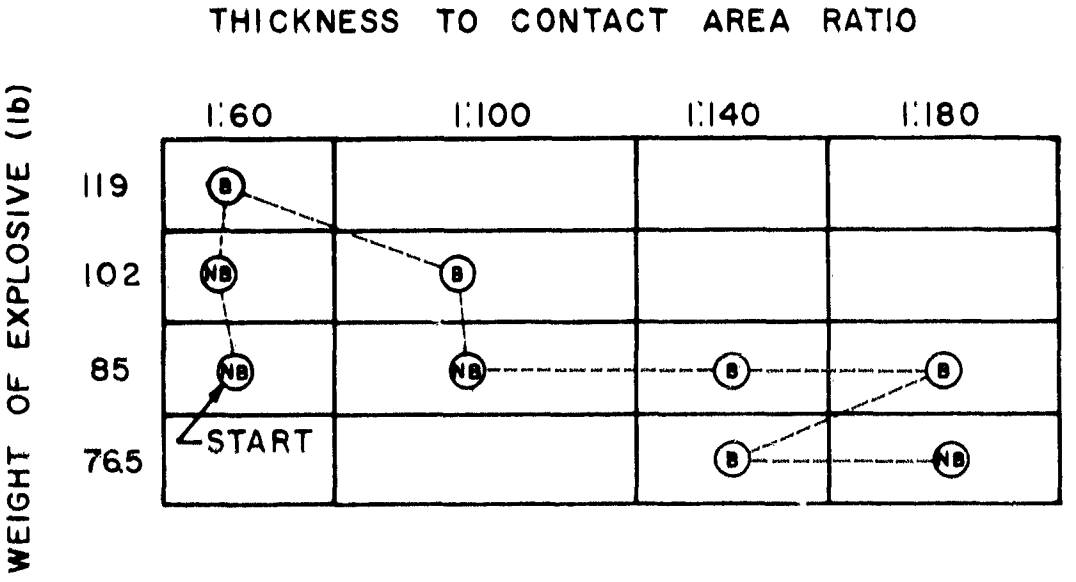

Fig. 31. Sequence and results of shots on 5-foot-thick piers: B indicates a pier considered adequately breached; NB, not breached.

The test crew conducted one experiment on a 5-foot pier using a 100-pound charge composed of five M-37 kits (20 pounds of Composition C-4 each). The purpose of this experiment was to compare the effectiveness of a charge inclosed in a canvas haversack to that of a bare charge. (Troops in combat cannot be expected to remove explosives from a case; neither was the technique used by the test crew in fabricating the experimental charges practical in combat.) The five kits were positioned in a square one kit deep (approximately 4 inches) with a ratio of about 1:110 (Fig. 32). Weight of this charge was almost 20 percent greater than the minimum

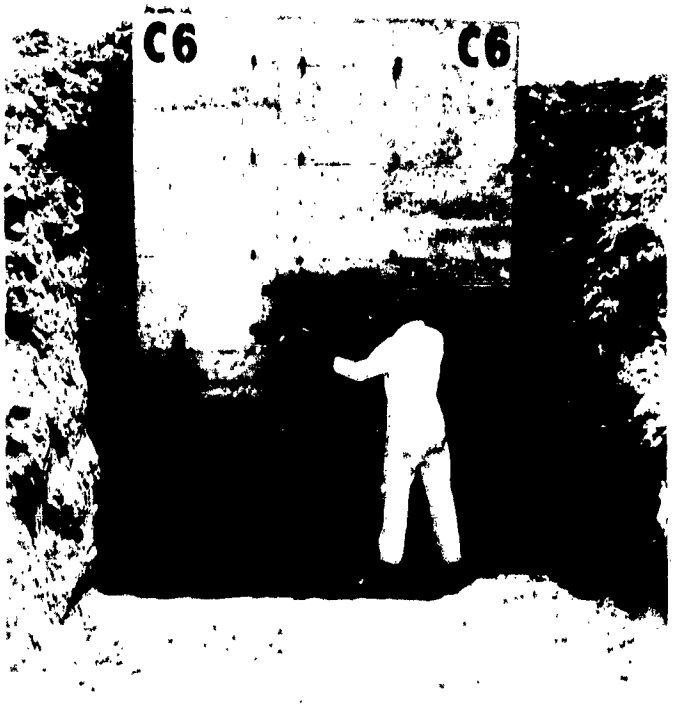

F5511

Fig. 32. Five M-37 kits fastened to a 5-foot-thick pier.

bare charge of 85 pounds previously used to allow for expected loss in explosive effectiveness. Studs from the standard explosive stud driver held the canvas haversack to the concrete, and wire was stretched across the kits and anchored to studs to keep the kits in close contact with the concrete. The five M-37 kits effectively breached the pier (Fig. 33).

Crater and spall diameters were difficult to measure because of the extensive damage to the piers. Reasonable estimates could be made, however, by noting the curvature of the craters on the explosive side and the extent of scabbling from the spall sides of the pier. Measurements made of the soil on either end of the pier indicated that there was little if any influence on wall break-up caused by variations in soil density and moisture content (Appendix D).

Craters and spalls of the 5-foot piers were similar to craters and spalls of the 2- and 3-foot piers but the 5-foot piers evidenced multiple spalls as compared to the single spalls of the smaller piers. Craters did not have the distinct shape of a segment of a sphere which was apparent on the 3-foot piers, but

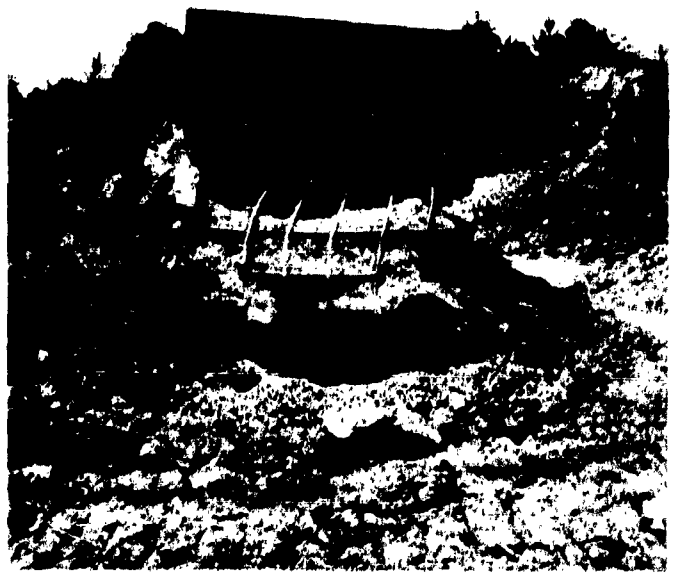

F5570

Fig. 33. Pier effectively destroyed by five M-37 kits.

careful examination gave indications that the craters would have formed into some sort of a spherical pattern had the piers been longer. In general, cracks on the spall sides were radial, centered at a point just opposite the location of the charge. In two instances, however, one straight horizontal crack appeared near the center of the pier. Plugs were blown out of the concrete in much the same way as with 3-foot piers. The top 2 or 3 feet of the pier and a section of the base about 2 by 2 feet were generally left intact (Fig. 34).

Three of the 5-foot pier explosions were photographed with a Courtney-Pratt lenticular camera at 100,000 frames per second. The photographs revealed a pulsing action in the explosion with peaks of pulses between 300 and 400 microseconds apart. As many as four pulses were counted although others may have been concealed by overplay in the camera.

Dimensions of craters and spalls were measured or estimated as closely as possible. These dimensions are shown in Table XI.

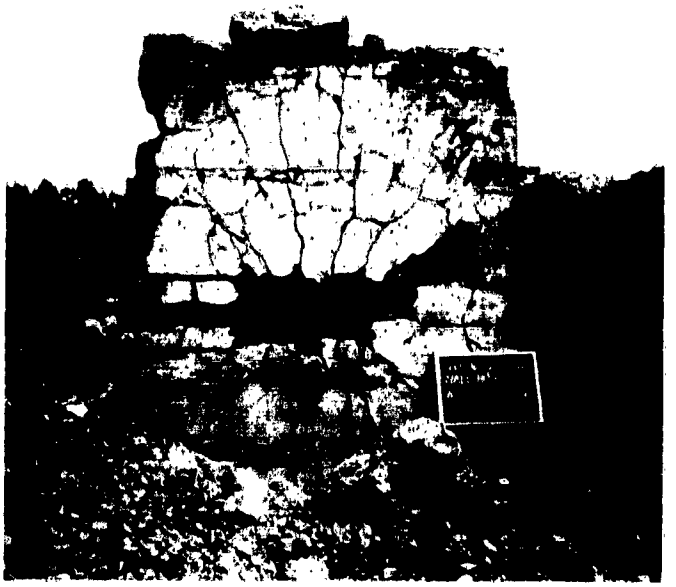

F5571

F6068

Fig. 34. Top: Radial cracks in 5-foot-thick pier. Note pronounced horizontal fissure. Bottom: General pattern of 2 to 3 feet at the top and 2- by 2-foot section at the bottom of the pier being left intact.

Table XI. Dimensions of Craters and Spalls
Blasted in 5-Foot-Thick Piers

Pier No.	Weight of Charge (lb)	Thickness to Contact Area Ratio	Crater Diameter (in.)	Spall Diameter (in.)	Breached or Not Breached
C-1	76.5	1:140	96-H[a] 80-V[b]	96	Breached
C-2	85.0	1:140	(c)	(c)	Breached
C-3	85.0	1:60	77	91	Not breached
C-4	85.0	1:180	80	136	Breached
C-5	119.0	1:60	(c)	(c)	Breached
C-6	100.0	1:110[d]	75	112	Breached
C-7	76.5	1:180	154	118	Not breached
C-8	102.0	1:100	(c)	(c)	Breached
C-9	102.0	1:60	140	(e)	Not breached
C-10	85.0	1:100	144	136	Not breached

(a) H indicates horizontal measurement.
(b) V indicates vertical measurement.
(c) Pier so badly damaged that measurements were impracticable.
(d) M-37 kits.
(e) Bulldozer, used to uncover sides of pier, backed into pier and destroyed it.

d. Piers 7 Feet Thick. Tests conducted on piers 7 feet thick proved that the 7-foot-thick piers were far less resistant to explosives than had been expected. The existing formula called for 495 pounds of explosives to breach a 7-foot pier. This was considered to be an underestimate, but initial tests with 250 pounds at a ratio of 1:180 totally demolished the pier. A 200-pound charge (a 20-percent reduction of explosive over the initial test) at a ratio of 1:180 also breached a 7-foot pier, but a 200-pound charge with a ratio of 1:300 was considerably more effective (Fig. 35). A 200-pound charge with a ratio of 1:400 appeared somewhat less effective than the charge fired at a ratio of 1:300. A 150-pound charge at a ratio of 1:300 and two 175-pound charges at ratios of 1:300 and 1:400 failed to breach their respective piers. Figure 36 shows the sequence in which each shot was fired in the 7-foot-thick pier tests and whether or not the shot breached the pier.

Three piers were reserved for testing charges made up of M-37 kits. The first charge tested consisted of 12 M-37 kits (240 pounds of Composition C-4 with a ratio of 1:330) attached to the concrete in the approximate shape of a square four kits wide and three kits high. A J-2 special electric cap placed 3/4 inch into the center of the explosive detonated the charge which completely

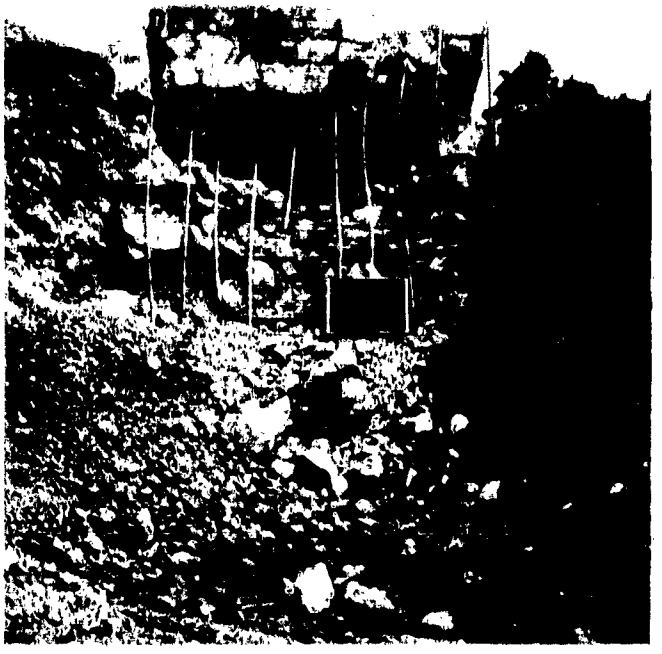

F5589

F5597

Fig. 35. Top: A 7-foot-thick pier substantially destroyed by a 200-pound charge with a ratio of thickness to contact area of 1:180. Bottom: A similar pier completely destroyed by a 200-pound charge with a ratio of 1:300.

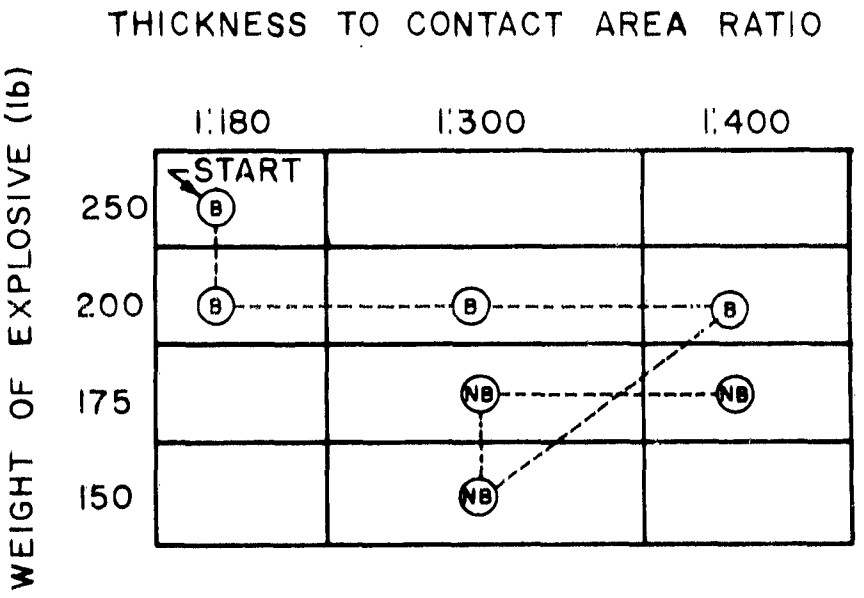

Fig. 36. Sequence and results of shots on 7-foot-thick piers: B indicates a pier considered adequately breached; NB, not breached.

demolished the pier (Fig. 37). On the next pier, 10 M-37 kits (200 pounds with a ratio of 1:220) failed to breach the pier; however, in the following test, the pier was breached with 11 kits (220 pounds).

Both craters and spalls of the 7-foot-thick piers were very similar to the craters and spalls of the 5-foot piers. The diameters of the craters were even more difficult to measure than those in the 5-foot piers. The piers were only 10 feet wide, but configuration of the craters was such that it appeared that, had the piers been longer, the diameter of the craters would have been at least 14 feet (Table XII). Spalls gave very little evidence of radial cracking but, instead, appeared to crack vertically and horizontally in a pattern that closely resembled the steel reinforcing bar pattern. The top 3 feet of the pier remained relatively undamaged after the blast just as in the 5-foot piers. Successive spalls, approximately four in number, could be seen from the ends of most of the piers which were not completely destroyed. The successive spalls were nearly parabolic in shape and were not symmetrical but increased in curvature as they approached the explosive face of the pier (Fig. 38).

F5552

F5539

Fig. 37. Top: Twelve M-37 kits (240 pounds) attached in close contact to a 7-foot-thick pier. Bottom: The pier completely destroyed by the 12 kits.

Table XII. Dimensions of Craters and Spalls Blasted in 7-Foot-Thick Piers

Wall No.	Weight of Charge (lb)	Thickness to Contact Area Ratio	Crater Diameter (in.)	Spall Diameter (in.)	Breached or Not Breached
D-1	240	1:330[a]	(b)	(b)	Breached
D-2	200	1:220[a]	102	154	Not breached
D-3	200	1:300	(b)	(b)	Breached
D-4	175	1:400	90	161	Not breached
D-5	175	1:300	101	160	Not breached
D-6	200	1:400	(b)	(b)	Breached
D-7	250	1:180	(b)	(b)	Breached
D-8	200	1:180	(b)	(b)	Breached
D-9	150	1:300	107	130	Not breached
D-10	220	(c) [a]	176	114	Breached

(a) M-37 kits.
(b) Pier so badly damaged that measurements were impracticable.
(c) The irregular shape of the charge prevented establishing a ratio.

F6074

Fig. 38. End view of 7-foot-thick pier showing successive spalls from a 175-pound charge.

III. DISCUSSION

11. Examination of Methods of Testing. Test engineers designed all experiments in accordance with established statistical models. These models provide for quantitative examination of main effects and interactions of several variables in one experiment, thus decreasing the number of samples required for experiments while increasing the information gained. Many of the conclusions were formed on a qualitative basis, however, because of excessive experimental error or inability to define an adequate measure of the explosive yield. More repetitions of each test would have increased confidence in the conclusions, but limitations on the number of test structures and on the time and money available for testing made this impracticable.

One of the least understood variables in the tests, the variability of the explosive itself, could not be evaluated. An attempt was made to reduce the explosive variability by using explosive from the same production lot for each test series. Whenever possible, the explosive within a lot was selected at random for each test to make it equally as probable for poor explosive to be in one charge as in another. It might have been advisable to assume that no significant interactions of variables existed and reduce the number of tests within each repetition. For example, if a one-half factorial design were employed, the number of repetitions of each test could have been doubled without increasing the total number of shots fired. Such a fractional design would sacrifice information on some or all of the interactions of variables in order to gain more information on the main effects. Use of the crater volume as a quantitative measure of yield was based on the hypothesis that the size of the crater is an accurate measure of the explosive effect and is proportional to the extent of breaching in concrete. This hypothesis has not been established though evidence in favor of it developed in these tests.

a. Ballistic Pendulum. In the tests conducted on the ballistic pendulum, three or four observations were taken of the work accomplished by each configuration of charge. The fair agreement of the results of successive repetitions was gratifying, especially in view of the extreme variation which occurred in later tests. This reproducibility of results furnished fairly convincing evidence that variability in the concrete-wall tests could not be ascribed solely to lack of consistency in making up the charges or nonuniform procedure in the initiation of charges. Control charges might have been employed to detect any variation in procedure on different test days; however, there was so little variance that this seemed unnecessary. Energy imparted to the pendulum by each charge was measured in foot-pounds. Friction in the pendulum was ignored since the main purpose of the test was to compare different

charges and not to make quantitative measurements of total energy output.

b. Unreinforced-Concrete Model Wall Studies. Poor quality of the concrete represented the most obvious obstacle in the concrete-slab studies. This concrete, described fully in paragraph 5, was an expedient test medium and made possible conservation of both time and funds for later tests scheduled to be completed by the end of the fiscal year. In spite of the lack of homogeneity of the concrete and the haste with which the tests were conducted, very useful information was obtained. In fact, the variance in these tests was significantly less than in the more carefully conducted experiments on the reinforced-concrete walls. The full factorial type of experimental design made possible rapid completion of the tests. In this type of design, test time can often be shortened appreciably without sacrifice of information because the analysis is made after all data is assembled rather than sequentially as in other test procedures.

c. Reinforced-Concrete Model Wall Studies (Series 1 and 2). The same statistical experimental procedure which had been used on the concrete-slab tests (par. 5) was used for the two 14-inch reinforced-concrete model wall studies. Charges were formed carefully to assure maximum possible uniformity. Utmost care was taken in setting up each test to assure detailed conformance to the test plan. The location of the reinforcing bars behind the charges was not considered, however, and it appears from the analyses that this may have been responsible for the excessive experimental variance. A mine detector or other device might have been employed advantageously to locate the steel in the concrete. This procedure probably would have reduced the variance; however, even if this precaution had been taken, it is quite possible that the reinforcing steel would still have reacted erratically under similar explosive loads.

The clay and water displacement method of measuring the volume of the craters seemed to produce reasonably accurate results as did the collection and weighing of spalled material. However, it is more difficult to justify the procedure for removing the spall. If the loose material which remained attached to the wall were not removed, then much of the effect of the charge would go unmeasured. On the other hand, if the material were removed by force, then a certain amount of additional work would be performed on the wall and the yield obtained from measuring the material would be too high. In those shots which did not produce spall, hammer blows indicated that there was a hollow space torn in the interior of the concrete. Thus, in tests where there was no spall or partial spall unmeasured work was actually performed to create this cavity. This dilemma was not resolved. The test team did not attempt to measure the spall in the second series of tests. A comparison of the spalls and craters in the first series indicated a fair degree of correlation

between the two, so it was believed that spall could be neglected especially in view of the problems of measurement.

d. Full-Scale Tests, 12-Inch, Reinforced-Concrete Walls. Full-scale tests of the 12-inch wall clearly illustrated the problems involved in evaluating the damage caused by large charges. The term "breaching" was arbitrarily defined as that degree of damage which would make concrete ineffective as a structural member. Although somewhat ambiguous, this criterion of damage was easy to apply, when damage of several experiments could be compared simultaneously.

The test engineers planned to establish the minimum weight of explosive, holding the thickness constant, to breach a 12-inch wall and then attempt to reduce the required explosive still further by varying the thickness. The photographs and drawings of each crater proved helpful in reconsidering the conclusions on completion of the tests. Even more photographs should have been made since there was not always adequate coverage to illustrate the condition of the crater before and after loose material was removed. It was intended that the minimum weight of explosive which would successfully breach a wall five successive times would be chosen as the optimum. Sufficient explosives, time, and concrete walls were not available to meet this objective, so the conclusions drawn are estimates, although some validation was gained from work done on the 14-inch walls. A few tests verified the importance of placing charges above ground level, but no attempt was made to establish a percentage by which the charge should be increased to compensate for the decrease in effectiveness when the explosive is placed close to the ground. Figure 39 shows the crater (8 inches in diameter and 3 inches deep) that was produced in a 12-inch-thick wall by a $1\frac{1}{2}$-pound tamped charge 1 inch thick when the charge was placed at the base of the wall. The same size charge detonated on a similar wall 30 inches from the base penetrated the wall. As in the 14-inch walls, it would have been better to place all charges in equivalent relationship to the reinforcing bars. An attempt should have been made to find some quantitative method of measuring the total destructive effect of each charge.

e. Full-Scale Test, 2-, 3-, 5-, and 7-Foot-Thick Piers. Full-scale tests profited materially from lessons learned in the development of the experimental procedures for the basic tests. There were only 10 structures of each size available for full-scale tests. Without the background obtained from the basic studies, the tests on full-scale structures would have been haphazard at best. The experimental techniques which evolved from the basic tests together with the experience in analysis provided a framework on which reliable data could be developed.

E9075

Fig. 39. Effect of a 1½-pound tamped charge 1 inch thick when the charge was detonated at the base of a 12-inch-thick wall.

The 2-, 3-, 5-, and 7-foot-thick test structures were similar to high-quality, reinforced-concrete, bridge piers. The 4,500- to 5,500-psi compressive strength of the concrete was above average for bridge piers; specifications usually call for strengths between 3,500 and 4,500 psi. Reinforcing steel in the concrete was similar to the typical bridge-pier steel. However, bridge piers will normally be more than 6 feet tall; data obtained from the 2- and 3-foot-thick piers must, therefore, be viewed with some concern. The four tests in which mud was piled on top of 3-foot piers achieved at least as much damage in three out of four trials as corresponding tests without the mud. The mud should simulate additional concrete by transmitting the shock pulse farther from the center of impact before the reflected tensile pulses develop. Similarity between shots with and without mud restored confidence in the tests, but higher piers would have been more satisfactory. Digging the earth away from the foundations of the piers would have been a more satisfactory solution than piling mud on top; up to 3 feet of height could have been added to the walls in this manner. Earth was excavated from the front and rear of the 5- and 7-foot-thick piers, adding 3 feet to their height. This procedure was very successful. If the 5- and 7-foot piers had been higher, the results probably would not have been altered.

Length of the 2- and 3-foot-thick piers together with the additional effective length obtained from the earth between the piers seemed adequate for simulating standard bridge piers, but the 5- and 7-foot-thick piers were not long enough. The concrete appeared to have ruptured excessively along the ends, thus contributing to the overall destructive effect; this would not have occurred in a longer pier (Fig. 40).

F6067

Fig. 40. End damage to a 5- by 8- by 11-foot pier.

In the 12-inch-thick wall studies, charges shot too close to the end of a wall produced vertical cracks near the end which greatly increased destructiveness of the charges. These vertical cracks were created by tensile reflections off the air-concrete interface on the end of the wall. These characteristic vertical and horizontal cracks did not occur in any of the full-scale structures. The only adverse effect, then, that occurred as a result of having piers that were not as long as the average bridge pier was the apparent blow-out on the end.

Experimental design for all full-scale tests followed the factorial-type design. The project engineer intended to arrive at some quantitative measure of yield so that his deductions could

be supported by the authority of mathematical statistics. All attempts at obtaining such a measure failed. In addition, there was so much variability in test results that even had quantitative measurements been obtained, no significant evaluations would have been possible. In spite of this inadequacy, the project benefitted from the logical form of the statistical procedure.

The spread between ratios in the 2-foot-thick and 3-foot-thick piers was too small. It was felt that the optimum ratio of 1:40 arrived at in the basic studies would remain constant or would decrease gradually for thickness of piers. Even if this were true, the ratio intervals probably should have been 1:40, 1:60, and 1:120. The ratio of 1:80 provided little difference in the dimensions of the charge. As a result, the bracket obtained for ratios in the 2- and 3-foot piers was not sufficient to make a good qualitative judgment. This inadequacy was corrected in the 5- and 7-foot piers.

Piling mud on the piers in the 2-foot-pier test was probably an error also. The piers were not tall enough, but the loss of repetitions of tests which occurred when four of the structures were capped with mud probably offset any benefits.

Considering the inadequate number of piers, the design of the tests on the 2-foot piers was effective. The weight of the explosive necessary to breach the pier was established clearly by six charges which breached the piers and three charges containing approximately 15 percent less explosive which did not breach the piers. The repetition of the charges which breached allowed an estimate of the variation and, thus, greatly increased confidence in the conclusions.

Four breaches at 80 percent and four no-breaches at 60 percent of the predicted weight of explosive established the weight of the minimum charges for breaching 3-foot-thick piers. Little could be said about the variability in the 3-foot piers since no tests were repeated. The piers which were intended for repetitions were utilized for tests with mud capping.

The basic experimental design for the 5-foot-thick piers was the same as that used in the previous piers. Establishing the best ratio between thickness and contact area required so many piers that repetition of experiments was impossible with only 10 structures available. The ratios of 1:60, 1:100, 1:140, and 1:180 provided a fair spread of ratios although a greater spread would have been desirable. The largest ratio probably should have been 1:80 and the smallest in the neighborhood of 1:250. It was clear from the results of the tests on the 5-foot piers that further tests should be conducted on longer piers to establish the distance

between charges on long piers. With as little as was known about demolition of 5-foot-thick piers, the selection of 85 pounds for the first charge was a remarkably good estimate. The tests which followed adequately defined the most effective ratio between thickness and cross-sectional area and established the minimum explosive necessary to breach this size pier. The one pier which was used to test the standard M-37 kit did not contribute to the rest of the experiment; therefore, just nine piers were actually available for the main tests.

Of the ten 7-foot-thick piers, three were tested with the M-37 kit leaving only seven for the main tests. The minimum charge that breached the pier was found quickly as was the optimum ratio. Charges were fired which barely breached the pier; when the explosive weight was reduced 10 percent, the charges just failed to breach the pier. The minimum weight of explosive was thus established, but the lower limit of the thickness to contact area ratio was not so clearly defined. Charges were fired with ratios of 1:300 and 1:400, but only a slight difference was observed. Fragments from the 1:300 test were smaller and were thrown farther than those from the 1:400 test. The 1:400 ratio probably should have been 1:550 to obtain clearer definition of the limits of the ratio.

The test crew conducted the tests with as much uniformity and care as conditions would permit. They did not pick explosive for the 2- and 3-foot-thick piers by random selection because of administrative problems; this proved to be detrimental in the evaluation of the experimental variance. It was possible, though, by correction of earlier difficulties, to randomize explosives employed in the 5- and 7-foot-thick piers. The testmen found that uniformity in charges was very difficult to maintain when the explosive was cut to the required dimensions by hand; by exercising great care, however, they were able to achieve acceptable dimensional tolerances. The weight of the charges was maintained to the nearest gram. In view of the limited time and facilities and the necessity for a sequential design of experiments, making up charges in the field was the only practicable solution (Fig. 41). It was not possible to fabricate forms for molding explosives or to have the explosive charges molded in advance.

The criteria for locating the charge on the wall were that the center of the charge should be between reinforcing bars and that the charge should be placed near the center of the face of the pier but at least the thickness of the pier from the top. This turned out to be an extremely effective location for the charge. The test engineers estimated that the tallest bridge piers can be breached just as effectively as the shortest piers if the charges are placed the distance from the base of the pier used in the experiments. This estimate should be verified on actual bridges.

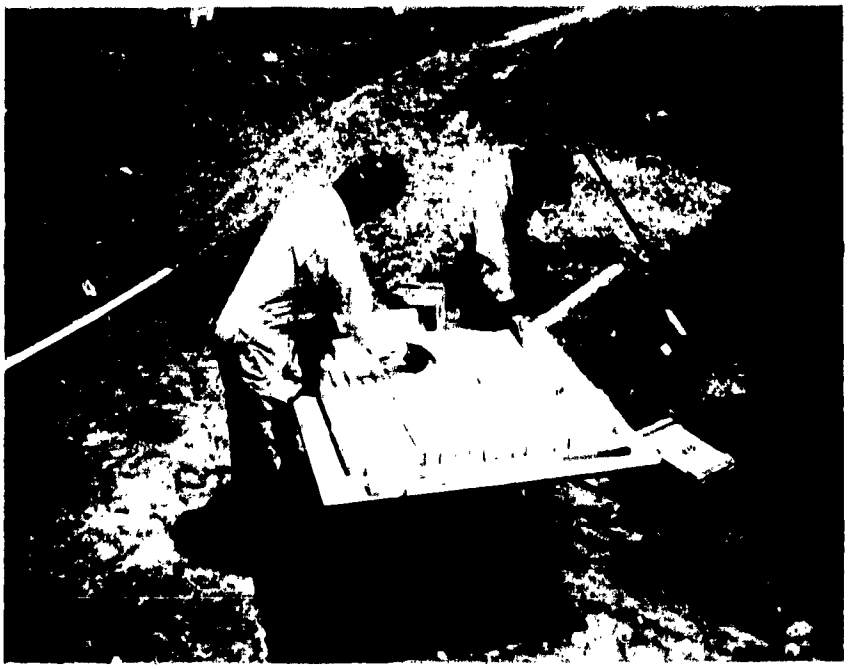

F5135

F6777

Fig. 41. Top: Cutting and piecing blocks together to form a charge to the required weight and dimensions. Bottom: Completed 200-pound charge placed on 7-foot-thick pier. Ratio of charge thickness to contact area is 1:300.

Throughout the experiments, the blasting cap was placed 3/4 inch into the explosive at the center of the charge. Experience has indicated that this is an effective technique and there was no reason to believe from the outcome of the tests that any other procedures, such as multiple priming or corner priming, would be more effective.

Difficulty experienced in finding a means to measure results of the explosions has already been mentioned. The stereophoto technique (Fig. 42) was probably the best solution devised, but for these tests it was impracticable because the procedure was time consuming and required use of complex equipment and experienced operators. The technique does have a potential for more deliberate tests of this type, however. There is equipment available for photogrammetric studies which is far simpler to operate than the equipment used in these tests. This equipment is less accurate but is adequate in consideration of the degree of variance which always seems to be present in explosive tests.

In addition to the photo theodolite plates, 35-mm stereopairs were taken. These were of great assistance in qualitative examination of the results of the explosion. All the Fastax

F5551

Fig. 42. Wild photo theodolite furnished extremely accurate stereopairs for quantitative measurements on a mapping stereocomparagraph.

photography was analyzed, and measurements were taken with the aid of the Vanguard Motion Analyzer. These measurements gave insight into the explosive phenomena and will make the knowledge gained much more applicable to other types of structures.

12. Analysis of Test Results. Test engineers, with the help of the Statistical Services Section, made a detailed analysis of all phases of the concrete tests. We felt that time spent in detailed studies of the concrete breaching phenomena would pay great dividends when the basic work was extended to include the many other types of concrete structures which might require demolition.

a. Pendulum Studies. The ballistic pendulum measured explosive energy imparted to the pendulum head. This energy increased at a uniform rate as a charge of a given weight was made thinner, but it became apparent in later tests that the work accomplished by the explosive on the concrete did not increase indefinitely as the charge was made thinner. Other factors entered into the picture, decreasing the advantages gained by making the explosive thinner until a point was reached at which the disadvantages prevailed and the optimum thickness was reached.

The reason for the increase in energy as the explosive becomes thinner seems clear. The explosive disperses energy all along its surface. As the explosive is made thinner, its surface area in contact with the target becomes greater so that the energy imparted to the target is greater. This trend, of course, ends when the explosive becomes too thin to reach full detonation. Energy imparted to the target can also be increased by holding the contact area of the explosive constant and increasing thickness (and thus weight) of the explosive. Increasing thickness increases the explosive effect in three ways: first, by adding the force of additional high-pressure detonation products to the force of the explosive in immediate contact with the target; second, by compressing the explosive in immediate contact, thereby increasing its density and increasing the rate of detonation; and third, by lengthening the duration of the shock pulse. Increasing thickness of the explosive is inefficient, however, because the force of the detonation products decreases approximately in inverse proportion to the cube of the distance from the target; an increment of explosive becomes rapidly less effective, therefore, as it is removed from the vicinity of the target. Also, the additional compression of the explosive probably adds very little to the explosive force.

b. Model Charge Studies, Unreinforced Concrete. The importance of placing the charge a distance above ground level of at least the thickness of the concrete had been demonstrated by Stanford Research Institute;[4] the model charge studies provided

4. Huber and Moses, op. cit.

verification of this by producing quantitative data which could be analyzed statistically. The crater formed by the explosive on the faces of the concrete slabs was assumed to be proportional to the total destructive effect of the explosive. Several of the conclusions based on this hypothesis were supported by results of later empirical studies. Analysis of the destructive mechanism (which will be discussed later) also lent support to the hypothesis, so it appears to be reasonably well founded.

Statistical analysis of variance proved that the location of the charge on the wall significantly changed its destructive effect. The probability that the differences in crater size when the height of placement was changed could have occurred by chance was less than 1 percent. In all but four cases, craters at the center of the wall were more effective than craters located at the base, so center placement was clearly the most favorable.

The various charge thicknesses were tested in the same way. Again, thickness was found to produce a significant effect on destructiveness. The five thicknesses were tested by another statistical test, Student's "T" test. In this test, the thicknesses were considered two at a time and their craters analyzed to determine which thickness was best. The $\frac{1}{4}$-inch charge (the thinnest) was found to be most effective.

Analysis of variance conducted on the craters formed by charges placed flush with the concrete and on craters separated from the concrete by plastic did not provide sufficient evidence that the plastic affected destructiveness of the charge. In nearly half the tests, charges with plastic actually produced better results than charges without plastic.

Use of statistical tests in an experimental program such as this was viewed as an experiment in itself. The statistical tests are all based on the normal probability law. There is actually little reason to suppose that the probability distribution for explosives detonated on concrete is normal. If the distribution approaches normal, the tests are still valid; but the large experimental variation calculated for later tests places the distribution under suspicion. The data was analyzed graphically and reanalyzed in light of each new set of data as it became available. As a result, the final analysis is considered reliable.

Studies on the second set of unreinforced walls helped to verify conclusions made on the first set concerning the optimum ratio and the effect of the plastic. The $\frac{1}{4}$-inch thickness was clearly the best, and the plastic had little effect.

c. Model Charge Studies, Reinforced Concrete. We considered the effects of charge confinement (tamping) for the first time in the reinforced-concrete wall tests. Three methods of priming were also considered for the first time. These tests also compared four ratios of thickness to contact area. For testing the effects of charge confinement, a wooden frame was placed around the charge and filled with mud covering the charge to a depth of about 2 inches and surrounding it in a 12- by 12-inch square. Mud tends to restrain the gases from detonation giving them increased time to act on the concrete. Water in the mud carries the shock pulse from the explosion out to the edges of the mud square increasing the effective area of contact of the explosive.[5]

The mud may have another effect which could account for some of the discrepancy in crater volumes. (Volumes of the craters produced by tamped charges were usually smaller than volumes by untamped charges, even though the tamped charges produced much more spall.) The acoustic impedance between air and the highly compressed explosive gases is very high. As a result, the shock pulse is not as readily dissipated to air as it is to a material such as mud which has a lower acoustic impedance with explosive. The pulse is also more readily dissipated from mud to air than from explosive to air. Mud, then, permits energy to be released from the detonation process faster than from a bare charge, reducing the width of the detonation head, that is, decreasing the time interval at which the amplitude of the shock wave is at its peak. The mud has restrained the gases, however, increasing duration of the total pulse. The total energy in the mud-confined explosive pulse is, therefore, greater than in the unconfined explosive pulse, even though the time interval at maximum amplitude is less. Thus, duration of the portion of the shock pulse which is strong enough to overcome the compressive strength of concrete is shorter in the confined charge than in the unconfined charge so the crater formed is smaller. (The crater is formed, for the most part, by compressive failure of the concrete under explosive loading.) The energy remaining in the shock pulse after the initial concrete is pulverized is greater for the confined charge because of the longer duration of the pulse. Figure 43 is a comparison of theoretical wave shapes of shock pulses formed by an unconfined and a confined charge. As time (T) increases, pressure (P) increases rapidly to a head, levels off, then decreases. The area under the curve above the dashed line represents energy capable of cratering concrete.

Some of the difference in crater size between tamped and untamped charges may also be accounted for in another way. The explosive shock wave in the concrete produces compressive forces parallel to the face of the wall in the vicinity of the charge.

---

5. Ibid.

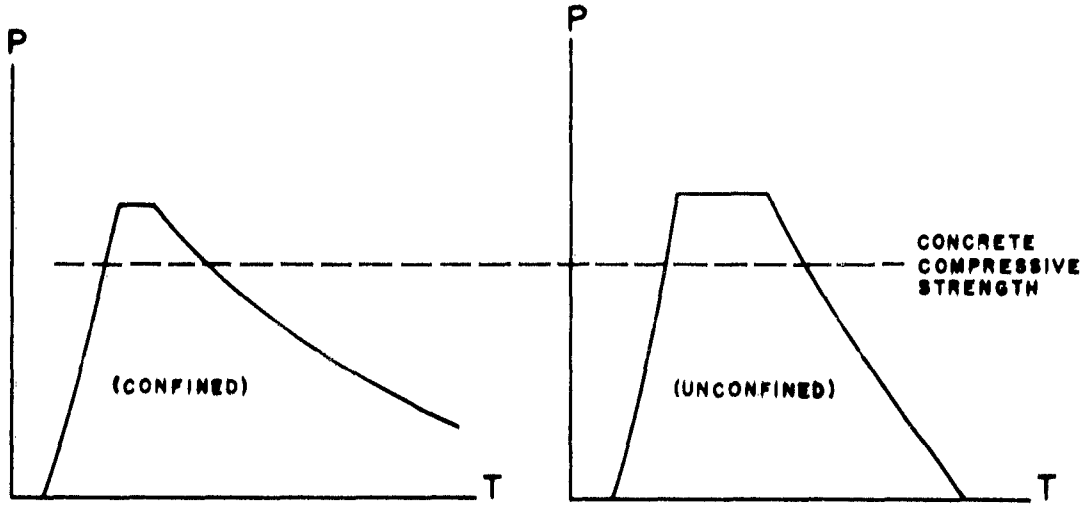

Fig. 43. Comparison of theoretical wave shapes of shock pulses formed by a confined charge (left) and an unconfined charge (right).

These compressive waves reach the concrete-air interface after the blast pressure has been relieved and generate tensile pulses back into the concrete. The tensile pulses are strong enough to overcome the tensile strength of the concrete and produce spalling which increases volume of the crater. On the other hand, when mud is placed on the charge and on the concrete surrounding the charge, the compressive waves generate tensile waves at the air-mud interface rather than at the concrete-mud interface. These tensile waves spall mud and not concrete if the mud is thick enough to absorb all the tensile wave energy above the tensile failure point of the concrete. Observations supporting this theory are discussed in paragraph 12d.

A study of explosive energy as it passes from the crater into the remainder of the concrete wall provides an explanation of the existence of an optimum charge thickness. The pendulum study revealed that explosive energy directed toward a target is increased as a charge of a given weight is made thinner, but the concrete wall tests proved that other factors offset this increase in energy so that some intermediate thickness produces the largest crater. As the charge is made thinner, its contact area increases. The explosive pulse continues to pulverize concrete until the pulse loses enough energy to reduce its amplitude below the level necessary to overcome compressive strength of the concrete. The point at which this level is reached is therefore marked by the inner surface of the crater. As the contact area of the explosive increases, energy available per square inch decreases even though total energy

is greater; therefore, less energy per unit area is available in excess of the compressive strength of the concrete. The amount of energy available which is capable of causing the concrete to fail in compression decreases faster than the total energy delivered increases as a result of making the charge thinner; thus, at some thickness this energy loss overtakes the energy gained and the crater reaches a maximum.

The three methods of priming tested did not significantly affect crater volumes. Changes in location of the primer should modify the form of the shock wave. Multiple priming produces interactions of shock waves within the explosive and the target which could assist the concrete breakup. However, if there are any real benefits to be derived from corner or multiple priming as compared to center priming, they were not apparent in the 48 tests conducted on 14-inch walls in the first series. Single priming at the center of the charge is certainly the most practicable method in military operations; unless later tests prove that results can be materially improved by a more complex priming procedure, center priming will be recommended. This, of course, does not preclude double priming to insure detonation.

d. Full-Scale Tests on 1-Foot-Thick, Reinforced-Concrete Walls. The 1-foot walls were difficult to analyze because of the many variables that entered into the tests as a result of inadequate h 'ght of the walls, nonuniform location of the steel with respect to charges, and lack of complete uniformity in the charges themselves. Damage produced by each of the 40 charges was compared to that produced by previous charges. Each result was classified as a breach or as no breach immediately after the test. Top spall contributed heavily to the total destruction effect, but the test engineers believe that they selected a breach level which would be effective on 1-foot-thick walls regardless of their height.

The long spall at the top of the wall was produced independently from the craters at the front and rear of the wall (Fig. 44). This spall seemed to have been caused by a tensile shock wave generated by the compressive wave from the explosion as the wave was reflected from the free surface at the top of the wall. This failure occurred between 6 and 8 inches from the top of the wall. Failure generally occurred along the top horizontal reinforcing bars but this was believed to be coincidental.

In several trails conducted prior to the beginning of the one-foot-thick-wall tests, the explosive was placed too close to the end of the walls. As a result, a slab of concrete spalled off the end of the wall similar to that produced at the top. This end effect was characterized by a vertical crack running parallel to the end of the wall.

E9048

Fig. 44. Long (74-inch) top spall produced in a 12-inch-thick wall with a 2½-pound charge 2 inches thick. Explosive side of the wall is shown in the foreground; reverse side of another wall fired with a similar charge is shown in the background (loose material has been removed).

The mechanism in formation of the crater in 12-inch walls was similar to the model charge studies discussed previously. Concrete in the immediate vicinity of the charge failed as a result of the strong compressive force from the explosive. This compressive failure could be detected by noting the finely pulverized area in the vicinity of the charge which generally appeared white as compared to the darker shade of the area of the concrete which failed in tension or shear (Fig. 45).

Tensile failures appeared in the area along the edges of the tamping material. These splotches of tensile failure probably occurred at points which were not covered with the tamping material (Fig. 46). The splotches of tensile failure add support to the theory (par. 12c) that the smaller crater size for the untamped charges occurred because the mud prevented the spall. When the mud was not in close contact, spalled areas appeared. This is illustrated even more convincingly in Fig. 47.

Concrete which spalled off the side of the wall opposite the explosive failed in tension. Fragments from the back of

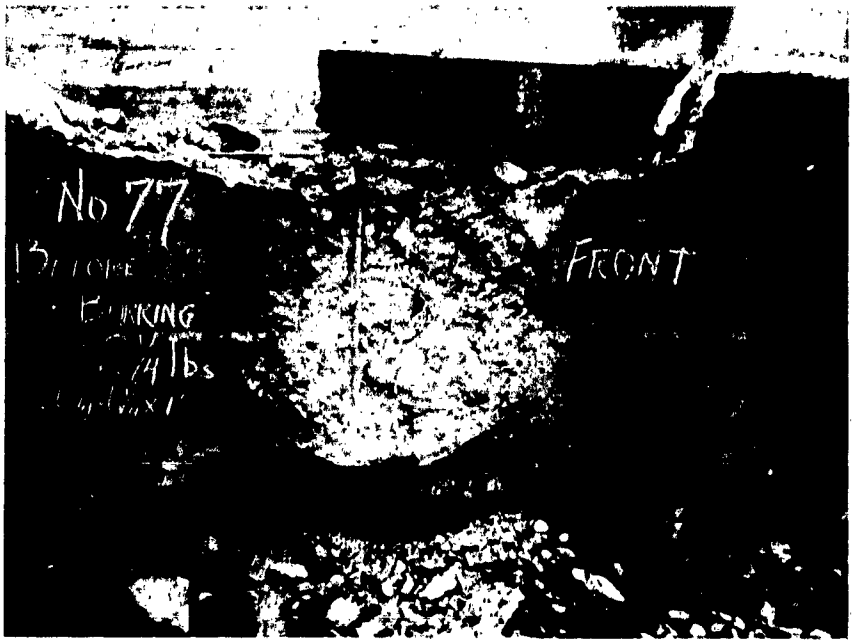

E9055

Fig. 45. Area of crater formed by compressive failure of the concrete appeared lighter and smoother than surrounding area which failed in tension.

E9072

Fig. 46. Craters formed by tamped charges appeared smaller and with steeper sides than craters formed by untamped charges. Note splotches of tensile failure around crater.

E9074

E9075

Fig. 47. Top: Charge placed at base of wall and tamped with mud-filled bag. Bottom: Line of spall occurred just above mud-filled bag/concrete contact area.

the wall were generally not pulverized but were in the form of broken chunks of still solid concrete. From examination of the spall fragments, it could be seen that failure occurred under the surface of the concrete (Fig. 48).

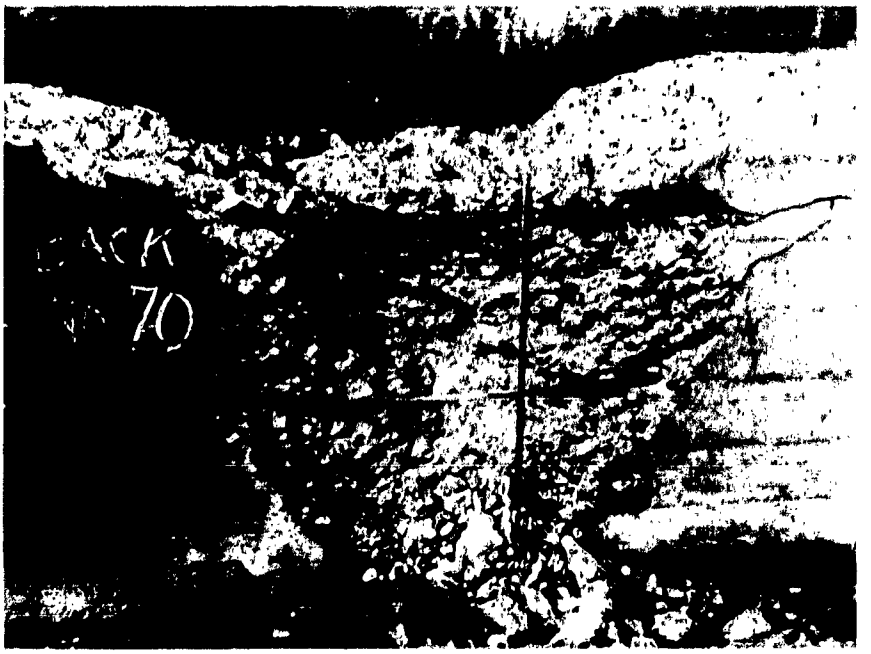

E9036

Fig. 48. Tension failure in concrete beneath wall surface on side of wall opposite 2½-pound charge.

The classic explanation for spalling of a material seems applicable to the 1-foot wall. A strong compressive wave created by the explosion passes through the concrete wall. As the compressive wave reaches the free face of the concrete, the wave is released into the comparative vacuum of the atmosphere; the wave is released, a tensile wave is generated which moves back into the concrete toward the explosive face. The force of the tensile wave is initially weakened by that portion of the original compressive wave which still remains in the wall. As the tensile wave moves back into the wall, the compressive wave moves out, reducing force of the tensile wave by less and less until the tensile wave is finally strong enough to overcome the tensile strength of the concrete. At this point within the wall, tensile failure of the concrete occurs (Fig. 49).

e. Full-Scale Studies, 2-, 3-, 5-, and 7-Foot Piers. The cratering and spalling of the 2-, 3-, 5-, and 7-foot piers were similar to the 1-foot walls except that multiple spalls were apparent

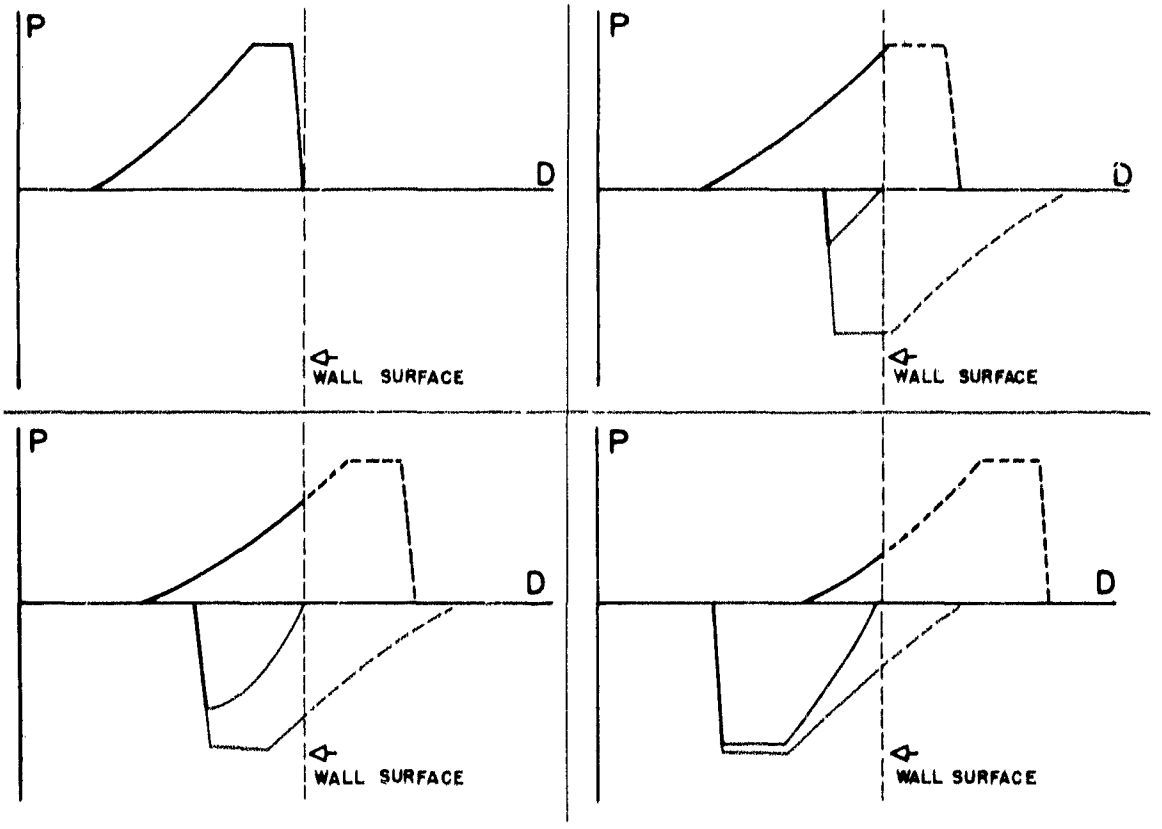

Fig. 49. The generation of a tensile pulse by a compressive pulse as it leaves the concrete. The tensile pulse is counteracted by the portion of the compressive pulse still in the pier and does not produce failure until the resultant pulse reaches the tensile failure point of the concrete.

in those 5 and 7 feet thick. Elimination of the top spall on the 5- and 7-foot piers helped to simplify the analysis, although inadequate length of the piers added end effects which tended to confuse the shock-pattern study. Information was obtained on the shock pattern within the concrete by a study of the cracks in the ends of the piers, so the inadequate length provided more help than hindrance in the analysis.

A study of the multiple spall pattern observed in the 5- and 7-foot piers supported by the high-speed Courtney-Pratt photographs of several of the explosions led to the hypothesis that an explosion produces multiple shocks and that these successive shocks are responsible for the multiple spalls observed in the thicker piers. In photographs taken with the Courtney-Pratt camera, successive flashes produced by the explosive were clearly discernible.

The first pulse (according to hypothesis) acts in the manner described for the 1-foot-thick wall. As the shock front reaches the opposite face of the pier, a tensile wave is generated which spalls off a layer of concrete. The spall occurs at the depth at which the tensile wave overcomes the counteracting influence of the portion of the compressive wave still remaining in the pier. The second explosive pulse increases the depth of the crater on the explosive side of the pier. The first crater is relatively flat because the shock pulse travels slower in concrete than in explosive along the face of the concrete which flattens the curvature of the shock wave (Fig. 50). The second pulse operates against the slight curvature created by the first pulse pulverizing more concrete and transmitting a pulse with greater curvature through the pier. This pulse strikes the new, free surface formed by the spalling action of the first pulse and generates a tensile pulse back into the concrete which produces a second spall. A third pulse from the explosive follows and creates a third spall. This process continues until the shocks become too weak to produce spall (Fig. 51).

Prior theories explain multiple spalling by a single pulse. The pulse generates a tensile wave in the concrete as it reaches the concrete-air interface on the opposite side of the pier. This tensile wave moves through the pier until the tail of the compressive wave has decreased in strength to a point at which the resultant tensile wave is capable of overcoming the tensile strength of the concrete. (The theory up to this point is identical with the new hypothesis.) The tail of the compressive wave, which is still passing out of the concrete, then produces a second tensile pulse at the new interface. This pulse moves back into the concrete until it, in turn, overcomes the strength of the remaining compressive tail and produces a second spall. This process continues until the energy in the tail of the compressive wave decays below an

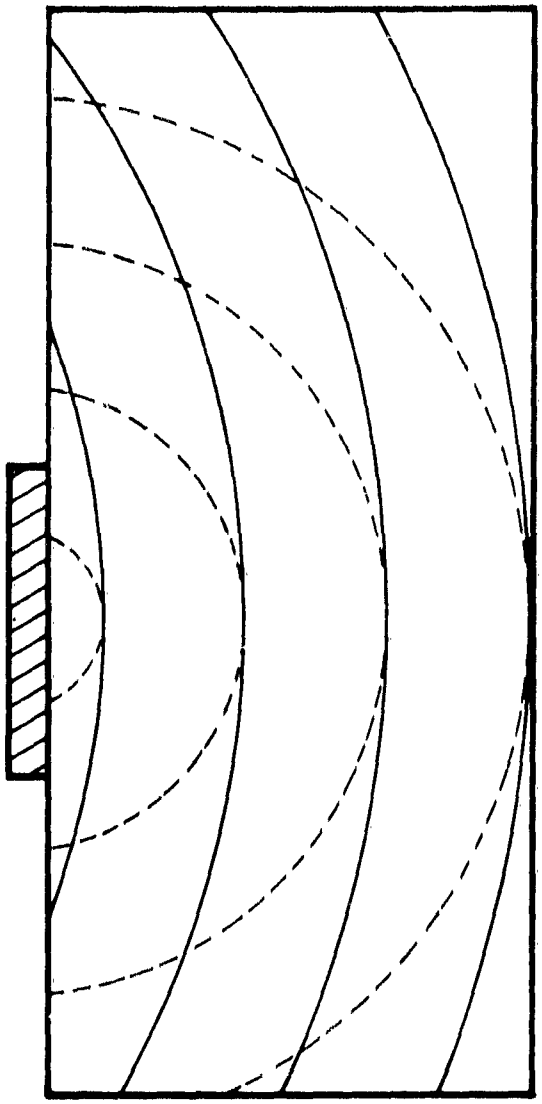

Fig. 50. Curvature of shock wave in concrete. Dotted lines show what the curvature would have been without the flattening effect of the concrete.

effective level. Figure 52 illustrates the spalls created by a single shock wave as the generated tensile pulse travels into the wall.

For the single pulse theory to be correct, the compressive wave must have a length greater than 4 feet for charges fired on the 7-foot piers. (The last spall on some of the 7-foot piers is as much as 4 feet from the rear face of the pier.) The spalls should also be arcs of concentric circles, although this may be modified by the rapid decay of the pulse along the periphery so as to take on a configuration similar to the solid lines in Fig. 52.

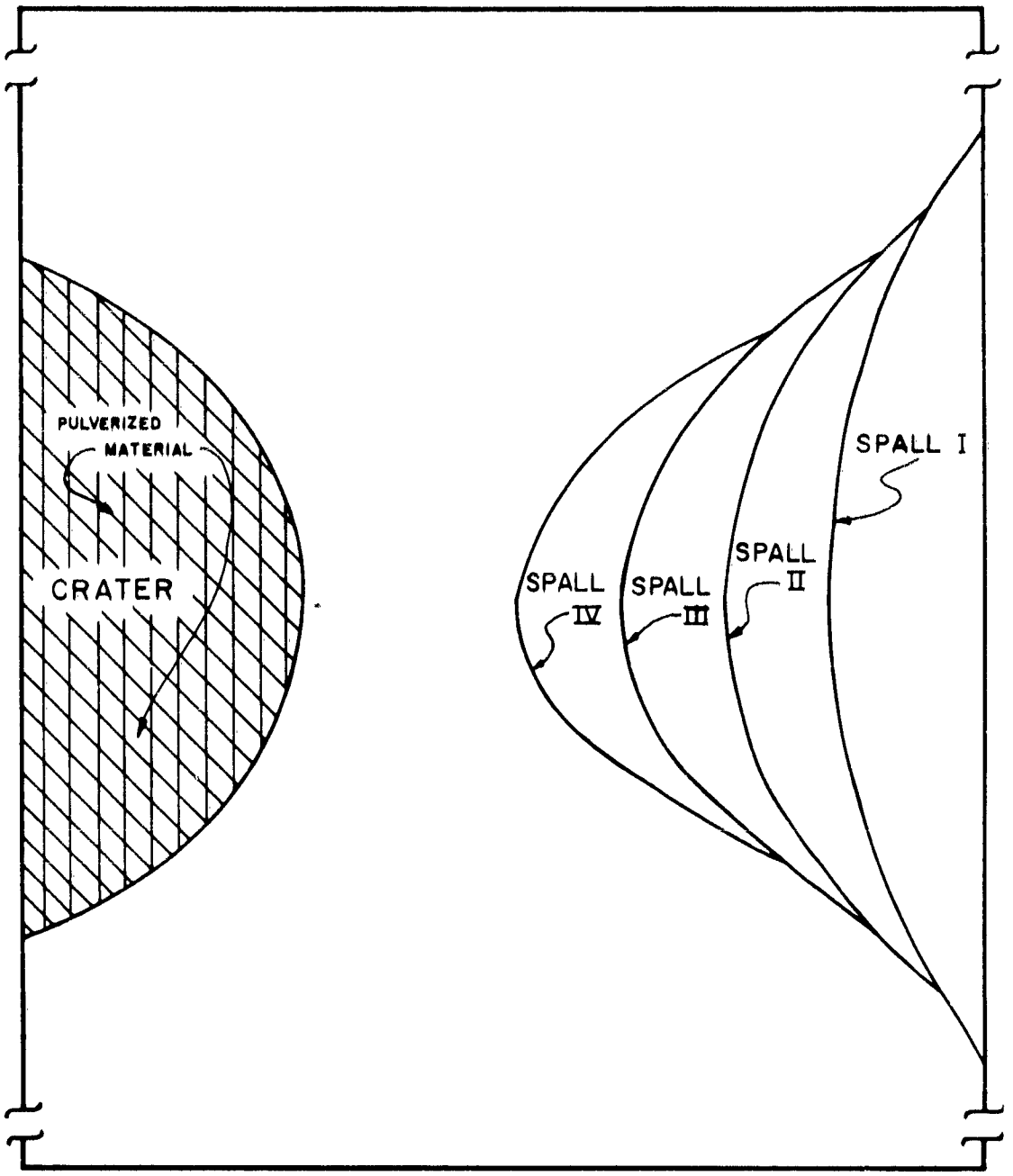

Fig. 51. Spalls created by successive shock waves emanating from the explosion.

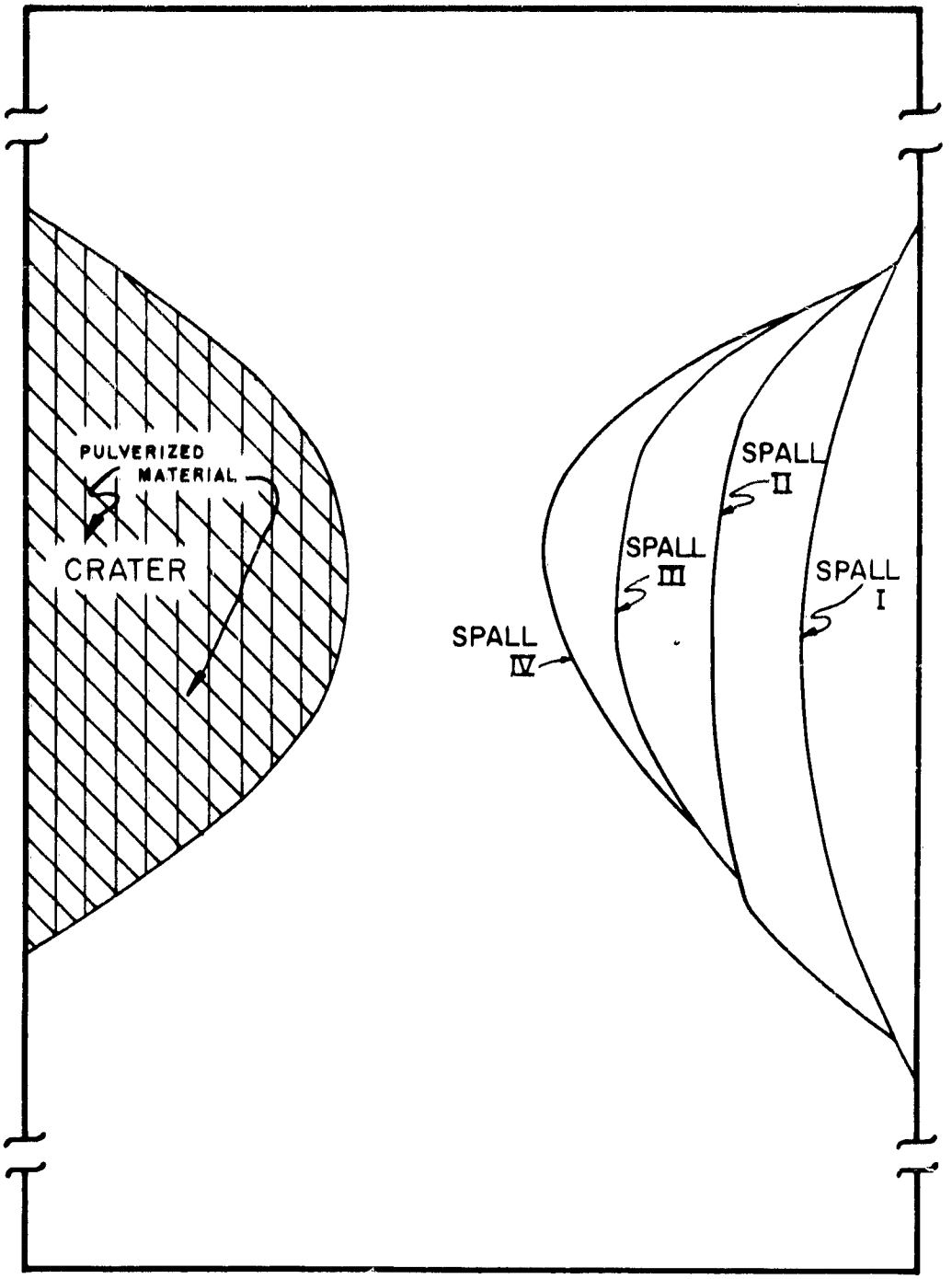

SIDE VIEW

Fig. 52. Spalls created by a single shock wave.

F6082

F6099

F6059

F6111

Fig. 53. Cracks formed in ends of 5-foot piers (top) and 7-foot piers (bottom).

Ends of the 5- and 7-foot piers showed cracks (Fig. 53) which generally conformed to the multiple-pulse hypothesis. The tops and bottoms of the 5- and 7-foot piers also behaved in good agreement with the multiple-pulse theory. The parabolic shape of the waves which are formed by the interaction of the pulses with the spalled surfaces should leave the peculiarly shaped undamaged sections of concrete which were observed (Fig. 54).

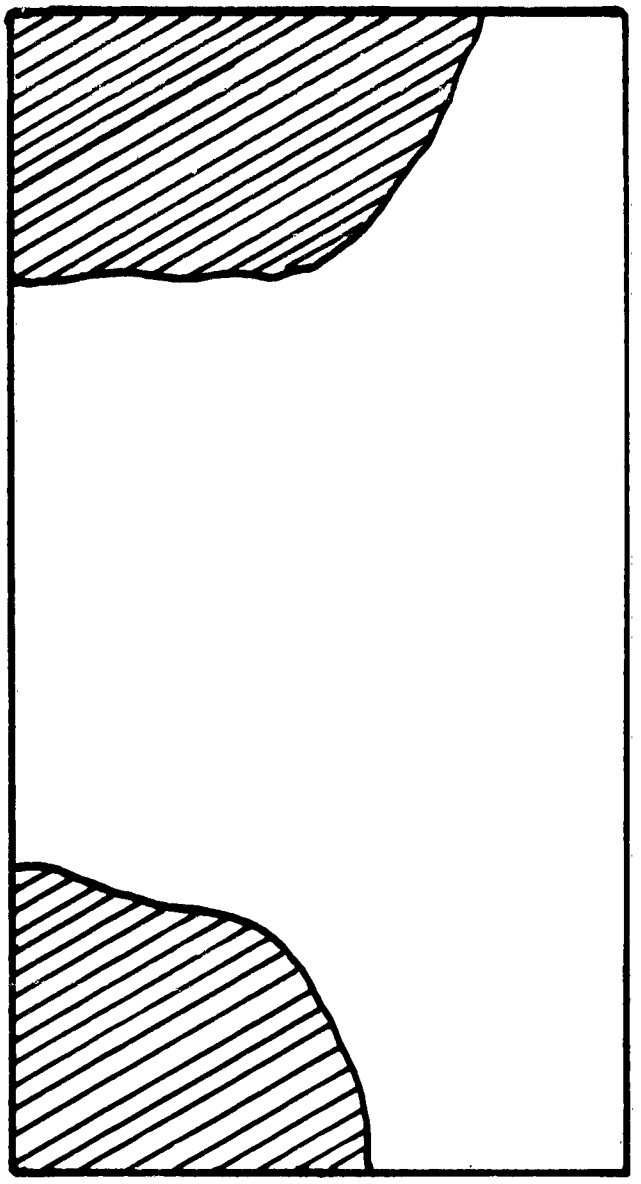

Fig. 54. Most of the tests left heavy sections of undamaged concrete in the top and bottom of the 5- and 7-foot piers which had a configuration similar to the shaded area in this sketch.

A multiple pulse in the explosion could be created as a result of the acoustic impedance between explosive and air. Shock waves attempting to pass from the highly compressed explosive gases into the air slow down very rapidly, creating pulses traveling back into the center of the explosive. The pulses collide and rebound in a second pulse. This process continues until the explosive energy is finally absorbed.

No evidence of multiple spalling was discovered in the 1-, 2-, and 3-foot piers. The charges used on these piers were small so their detonations were short in duration and relatively low in energy. The first pulse was probably the only one strong enough to produce a spall. Diameters of the craters and spalls were considerably smaller in relation to the widths of the piers than in the 5- and 7-foot piers so that even if successive spalling existed, it would not show up on the sides of the piers and evidence of such spalling in the interior would be lost in the jumble of pulverized concrete.

Tests on 5- and 7-foot piers supported the theory that the ratio between thickness and contact area of the explosive significantly affects destructiveness of the charge. It may be contended that the number of tests was inadequate to establish significance and that observed optimum effects might have been the result of chance failures in the concrete. The test engineers believe, however, that the data obtained in all of the previous tests supports the conclusions from the 5- and 7-foot tests and that the results obtained in the larger piers were clear-cut enough in themselves to be reasonably reliable. A graph of the ratios also seems to confirm the theory (Fig. 55). A rate-of-change graph of this curve (semi-log) plots as a straight line indicating uniform rate of change of curvature (Fig. 56).

The charge weights which were chosen as minimum breaching weights for each pier thickness appear reliable in spite of the statistically inadequate number of tests. A summary of minimum weight charges which will breach 1-, 2-, 3-, 5-, and 7-foot piers provided that the optimum thickness to contact area ratio is employed is shown in Table XIII.

Effectiveness of the charges on 1-, 2-, and 3-foot piers may have been influenced by the inadequate height of the piers, but the charges are nevertheless considered adequate. The charges recommended for field use will be larger, however, and the space between charges on longer piers will be reduced to insure destruction.

The weights of charges selected as minimum breaching charges for the 5- and 7-foot piers are not marginal. They may have been influenced by inadequate length of the piers but the damage

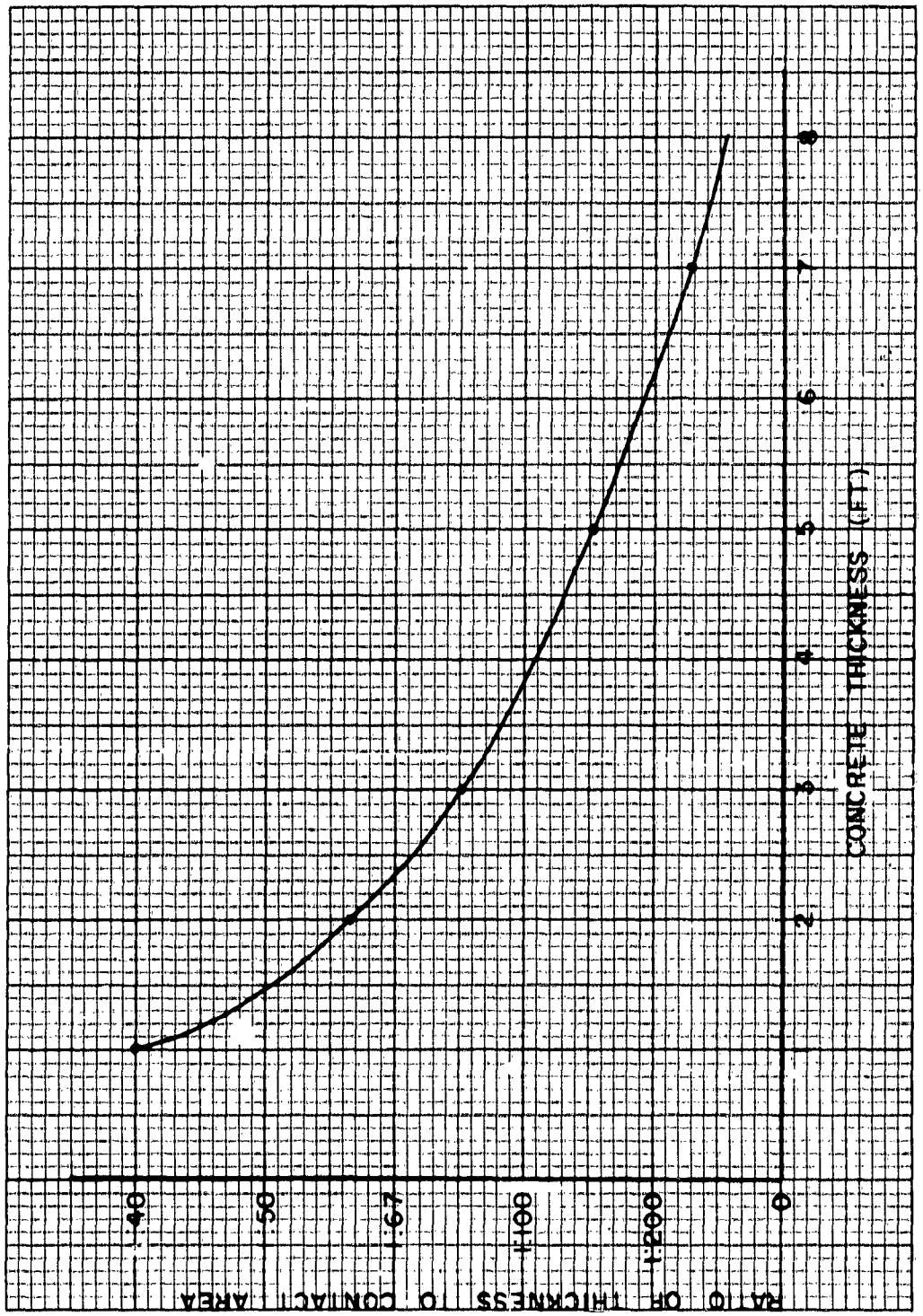

Fig. 55. Change in ratio of thickness to contact area as piers become thicker.

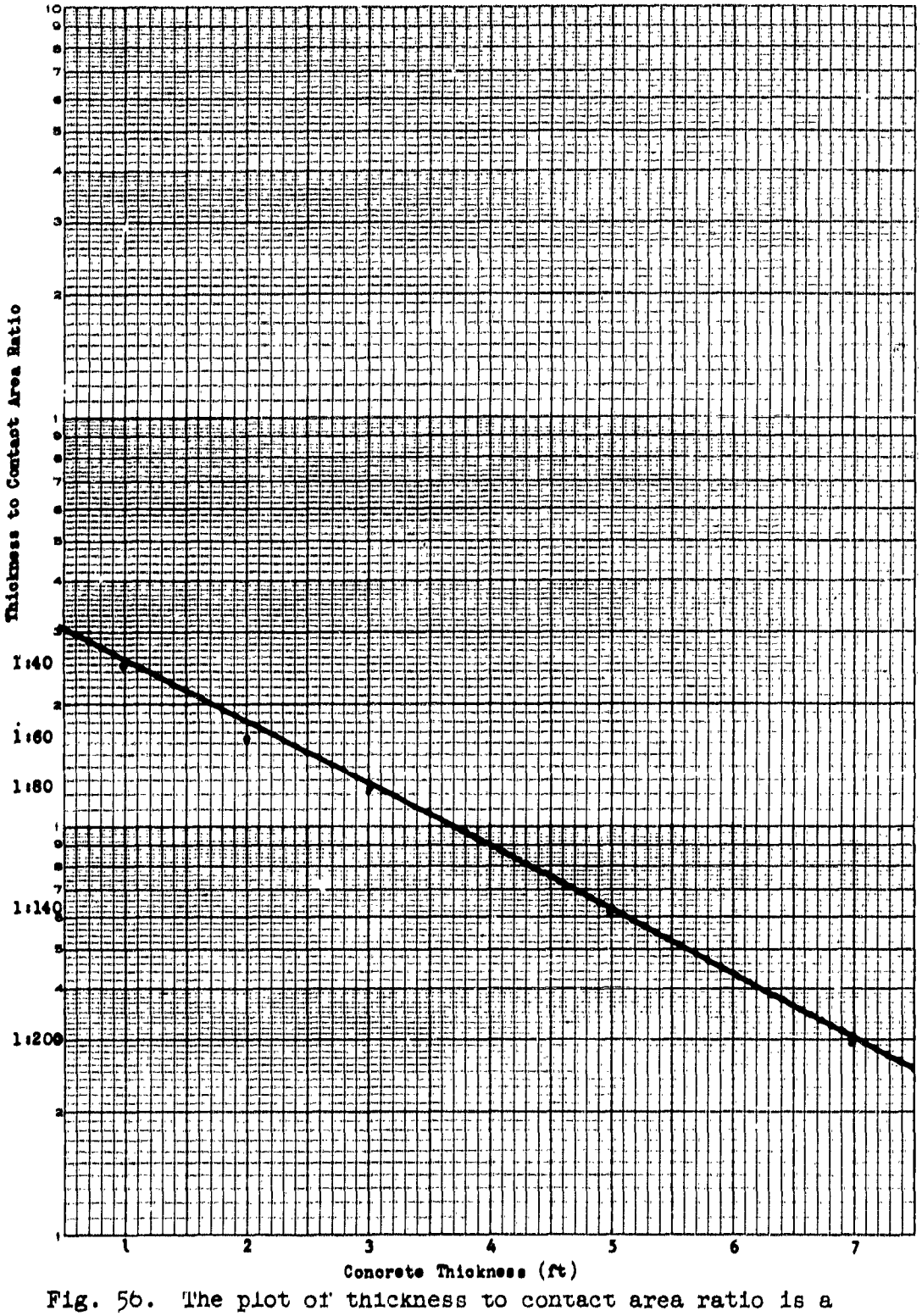

Fig. 56. The plot of thickness to contact area ratio is a straight line on semilog paper, indicating that the curve has a uniform rate of change.

they caused was so extensive as to override possible detrimental end effects.

Table XIII. Summary of Minimum Weight Charges

Concrete Thickness (ft)	Charge Weight (lb)	Optimum Ratio of Thickness to Contact Area
1	2.5	1:40
2	9.1	1:60
3	15.0	1:80
5	85.0	1:140
7	200.0	1:200

f. Extension of Data to 4-, 6-, and 8-Foot-Thick Piers. Data from the 2-, 3-, 5-, and 7-foot piers plotted in a smooth curve with a uniform rate of change of curvature (Figs. 57 and 58). It seems a reasonable assumption that the weight of explosive required for 4-, 6-, and 8-foot piers can be taken directly off the curve. It seems equally logical that the ratios of thickness to contact area can also be taken off the ratios to concrete thickness curve (Fig. 55). In view of the variability always present in explosives experimentation, it should be kept in mind that we cannot be certain of our conclusions on these untested piers until confirmation tests are conducted. Table XIV contains estimates of the minimum amount of explosive required for breaching untested sizes of piers.

Table XIV. Summary of Estimated Minimum Weight Charges

Concrete Thickness (ft)	Charge Weight (lb)	Optimum Ratio of Thickness to Contact Area
4	35	1:100
6	130	1:200
8	480	1:435

g. Procedure for Selecting Recommended Charges for Field Use. Several considerations governed the selection of practical sizes of charges for use by troops in the field. First, the carefully formed experimental charges are impractical since they must be hand made. The standard size block will rarely if ever meet the rigid dimensional requirements which have been established in these tests, and any change in dimensions will reduce effectiveness of the charges; therefore, the recommended charges must allow extra explosive to compensate for this probable deviation. Second, troops

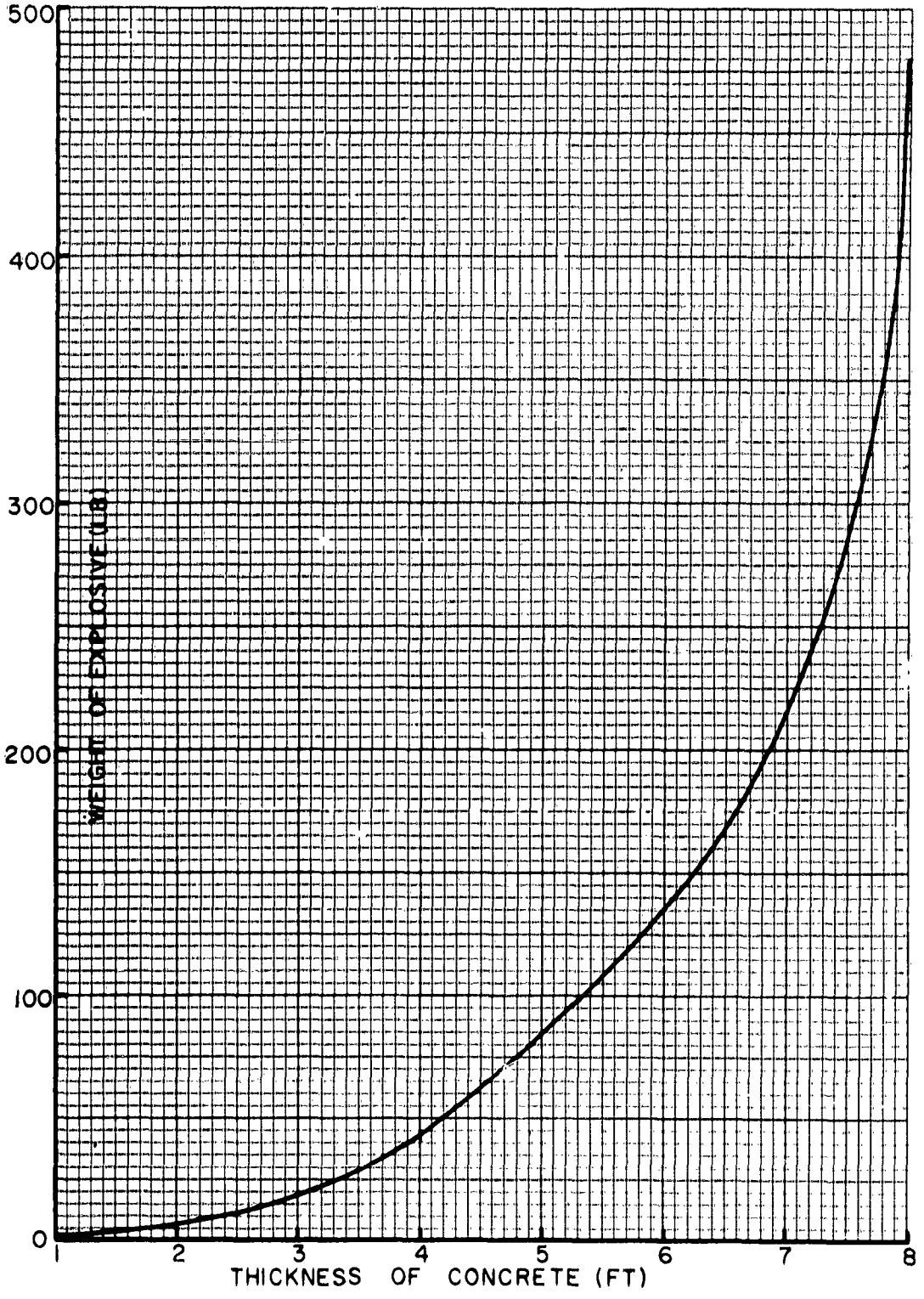

Fig. 57. Weight of explosive for carefully controlled experimental charges on 1- to 8-foot piers. The estimates for 4-, 6-, and 8-foot piers are based on the assumption that the curve has a uniform rate of change.

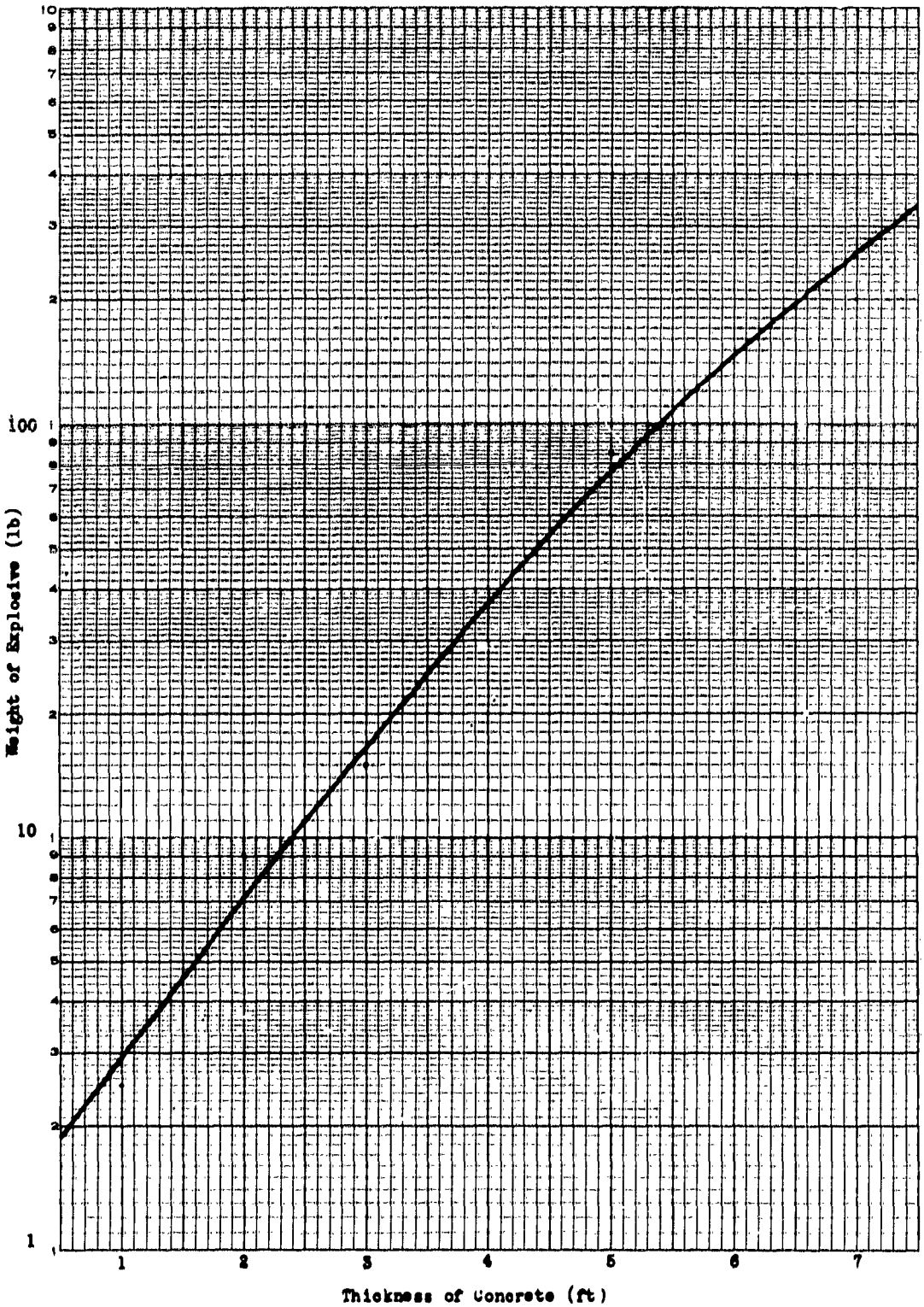

Fig. 58. The line plot of the pounds of explosive--thickness of concrete curve on a rate of change (semilog) graph is almost straight, indicating that its rate of change of curvature was uniform.

cannot be expected to follow the meticulous procedure used by the highly experienced demolition testmen; therefore, a margin of safety must be allowed for errors in technique. Finally, structures may be encountered which are extremely explosive-resistant because of unusually heavy reinforcement or irregular configuration. The final recommended charges should be 100 percent reliable under all conditions within reason.

Dimensions of the standard demolition block are, at present, 2 by 2 by 11 inches. Recommended charges for piers 1 through 4 feet thick will be made up from standard C-4 blocks removed from the packing case or M-37 canvas haversack. When Composition C-4 blocks are placed against 1- through 4-foot concrete piers so that they form a rectangle with a maximum thickness of 2 inches measured from the surface of the concrete to the outer face of the charge, the ratio of thickness to contact area will be near enough to the optimum so that relatively little explosive will have to be added to the minimum experimental charge to achieve a breach.

Removing explosive from the canvas haversack is time consuming; it, therefore, will be recommended that on larger charges (for 5- to 8-foot piers) the explosive be left in the haversack. The canvas detracts from explosive effectiveness, but the M-37 kits can be attached to a pier so easily that saving in time compensates for additional weight of explosive required. M-37 kits were tested on 5- and 7-foot piers; the size of charge to be used can, therefore, be stated with confidence. The recommended charge is one M-37 kit thick (4 inches) which is close enough to the 3- to 3½-inch optimum thickness for breaching charges for the 5- through 8-foot piers so that relatively little explosive will be wasted. Table XV shows the recommended external charges for breaching reinforced concrete bridge piers when the charge is placed approximately the thickness of the pier above ground or water level.

Table XV. Recommended Charges

Concrete Thickness (ft)	Charge Size	Charge Thickness
1	2 Comp. C-4 blocks	One block (2 in.)
2	4 " " "	" " "
3	7 " " "	" " "
4	20 " " "	" " "
5	6 M-37 kits*	One kit (4 in.)
6	8 " "	" " "
7	12 " "	" " "
8	28 " "	" " "

* An M-37 Kit consists of eight C-4 blocks (20 pounds) in a canvas haversack approximately 4 by 8 by 11 inches.

h. Placement of Charges. The importance of careful placement of charges has been implied throughout this report. In the model charge studies on unreinforced slabs, a charge placed at the base of the slab produced a crater which was, on the average, 23 percent smaller than the crater produced by a charge at the center of the slab. A similar decrease in destructiveness can be expected to occur on the opposite (spall) side of the concrete. Water at the base of the pier can be expected to affect the yield of the explosion at least as much as soil. Therefore, time spent planning a method for fastening a charge an effective distance from the water or soil around the base of the pier (a height equal to the thickness of the pier, if practicable) will pay off in increased effectiveness of the charge.

The importance of adhering as closely as possible to the optimum thickness to contact area ratio was demonstrated in the 5- and 7-foot pier tests. Although it is not practicable to custom-make optimum charges for each pier encountered, it is essential to employ the recommended charge thicknesses based on integral numbers of standard blocks or explosive kits. The charge should also be formed on the pier in a shape as near a square as possible without altering the standard blocks and kits.

Explosive should be fastened in close contact with the concrete; any air gap between explosive and concrete will decrease effectiveness of the explosive. Recommendations for charge sizes have been based on the tests conducted with the explosive carefully fastened in close contact with the concrete. No evidence has been developed in these tests which can be used to estimate the detrimental effect of careless charge placement, but the recommended charges cannot be expected to be effective unless reasonably similar techniques are employed.

A single cap placed at the center of the charge proved to be effective for detonating the charges. Other methods of detonation may be somewhat more effective, but it is believed that the simplicity of central priming warrants its continued acceptance for military applications.

Standard bridge piers will require more than one charge. The number of charges may be calculated by the formula contained in FM 5-25: $N = W/2R$ where N = number of charges, W = width of the pier, and R = breaching radius (thickness) of the pier. The distance between charges is, then 2R; each charge must effectively destroy this length of pier. Optimum charges on 2-foot piers destroyed slightly more than 4 feet (2R) of pier. Optimum charges on 3-foot piers destroyed 6 feet of pier although some of the side breakup may be attributed to the shortness of the piers; one charge, however, should still cause more than enough damage to eliminate the

structural value of 6 feet of concrete. The recommended charges on 5- and 7-foot piers are overloaded, so they should easily destroy 10 and 14 feet of pier, respectively, since they will totally demolish piers 8 and 10 feet wide. The untested pier thicknesses, 4, 6 and 8 feet, are also overcharged, so the charge spacing formula should be effective.

i. Untested Aspects of the Concrete Studies. These full-scale tests were limited to consideration of external charges on reinforced concrete. No effective experimentation has been accomplished on the other important aspects of concrete demolition nor have other types of piers such as piers made of rock or masonry been considered. Bridge supports also often consist of heavy steel cylinders filled with and enclosed in concrete and many bridges contain prestressed concrete beams which must be destroyed to effectively eliminate the bridge. A number of other areas of importance to the theory of demolition of concrete structures other than bridges have not been investigated. This report should provide theoretical and experimental data of value as a basis for further work, and it should be possible to extend this data to the other problems with a minimum of additional tests.

IV. CONCLUSIONS

13. Conclusions. It is concluded that:

a. Explosive placed at least the thickness of the pier above the base of a pier is more effective than explosive placed at the base.

b. The relationship of thickness of charge to contact area is critical; a material change from the optimum will significantly decrease destructiveness of the charge.

c. Central initiation of a charge is as effective as corner initiation or two-corner, simultaneous initiation.

d. Plastic placed between explosive and a concrete target (representing the plastic cover of the standard C-4 block) does not significantly alter destructiveness of the explosive.

e On 1-foot-thick walls, mud confinement of the explosive (tamping) makes possible a 30-percent reduction in the weight of explosive required to achieve equivalent results (this conclusion will probably not hold true for thicker walls).

f. A square charge is more effective than a rectangular charge.

g. Optimum practicable charge sizes are as shown in Table XV.

BIBLIOGRAPHY

Anti Concrete Committee Papers (Confidential Report), M of S, England, 6 October 1943.

Atchison, Thomas C., and Wilbur I. Duvall, Rock Breakage by Explosives, U. S. Bureau of Mines, September 1957.

Atchison, Thomas C., and Wilbur I. Duvall, Rock Breakage with Confined Concentrated Charges (U), U. S. Bureau of Mines, June 1959.

Atchison, Thomas C., and William E. Tournay, Comparative Studies of Explosives in Granite (U), U. S. Department of the Interior, 1959.

Atchison, Thomas C., Wilbur I. Duvall, and David E. Fogelson, Strain Energy in Explosion-Generated Strain Pulses (U), U. S. Department of the Interior, 1959.

Borlase, A., Lt. Col., 21A Gp Control Commission Experimental Demolitions, La Panne Siegfried Line (U), 21A Gp Control Commission (British).

Bowden and Yoffee, Initiation and Growth of Explosion in Liquids and Solids, Cambridge University Press, 1952.

Breaching of Sea Wall (First Interim Report) (Secret Report), Combined Operations Headquarters, 1a, Richmond Terrace, Whitehall, S. W. I., February 1944.

Broberg, K. B., "Studies on Scabbing of Solids under Explosive Attack," Journal of Applied Mechanics, Vol 22, pp 317-323.

Cole, R. H., Underwater Explosions, Princeton University Press, 1948.

Cook, M. A., The Science of High Explosives, Reinhold Publishing Corp., New York, 1958.

Courant, R., and H. O. Friedrichs, Supersonic Flow and Shock Waves, Interscience Publishers, Inc., New York, 1948.

Davids, Norman, Alan Jones, and Sudhir Kumar, Studies of Scabbing in Bars and Plates by Plaster Models (U), Pennsylvania State University, 15 July 1958.

Davids, Norman, and Shoi-Yean Hwang, Graphical Analysis of the Formation of Shock Front and Scabbing in Materials, Pennsylvania State University, 15 February 1959.

Davids, Norman, Transient Analysis of Stress-Wave Penetration in Plates (U), Pennsylvania State University, 1 September 1958.

Demolition of Concrete Structures, ERDL Motion Picture Report No. 1897, 1961.

"Demolition Materials," Technical Manual No. 9-1946, Department of Army, November 1955.

Demolition Tests on Model Concrete Bridge Piers (Secret Report), Department of Scientific and Industrial Research, Great Britain, February 1942.

Drummond, W. E., "Comments on Cutting of Metal Plates with High Explosives," Journal of Applied Mechanics, Vol 25, No. 2 (1958), pp 184-188.

Duvall, Wilbur I., and Benjamin Petkof, Spherical Propagation of Explosion-Generated Strain Pulses (U), U. S. Department of the Interior, 1959.

"Explosives and Demolitions," Field Manual No. 9-1946, Department of Army, May 1959.

Foreign Military Weapons and Equipment (Confidential Report), 10 July 1958.

Foreign Weapons Effects Reports - Model Studies of the Reinforced Concrete Structures Used in the Monte Bello Atomic Bomb Trial (Confidential Report), Atomic Energy Commission, 25 May 1958.

German Experimental Work on the Attack of Reinforced Concrete by Explosives and Projectiles - Part I (Confidential Report), British Intelligence Objectives Sub-Committee, September 1945.

Hoel, Alfred G., Jr., 1st Lt., Demolition of Structures, Engineer Board.

Inspection of the Möhne and Eder Dams - Part II (Confidential Report), British Intelligence Objectives Sub-Committee, September 1945.

Johansson, C. H., Plastic Deformation and the Formation of Cracks by Detonating Charges, IVA (1955):1, pp 16-25.

Kolsky, H., Armament Research and Development Establishment (U), Basic Research and Weapon Systems Analysis Division, April 1959.

Kolsky, H., Stress Waves in Solids, Clarendon Press, Oxford, 1953.

Kretsinger, D. G., Contact Explosions on Concrete (Confidential Report), National Research Council, 30 June 1944.

Kumar, Sudhier, Scabbing and Pulse Propagation in Materials (U), Pennsylvania State University, 1 August 1958.

Mining by Block Caving and Rock Fragmentation by Blasting, Colorado School of Mines Quarterly, Vol 51, No. 3.

Moses, S. A., and G. B. Huber, Fundamental Studies of Explosive Charges Vol I: Steel Cutting Charges (U), Stanford Research Institute, Menlo Park, California, 15 April 1957.

Moses, S. A., and G. B. Huber, Fundamental Studies of Explosive Charges Vol II: Concrete Breaching and Wood Cutting Charges (U), Stanford Research Institute, Menlo Park, California, 12 June 1957.

Moses, S. A., Experiments with Massive Boulders (Confidential Report), Stanford Research Institute, Menlo Park, California, September 1953.

Moses, S.A., Fundamental Study of the Destruction of Beach and Underwater Obstacles by Explosives (Confidential Report), Stanford Research Institute, Menlo Park, California, for Department of Navy, Bureau of Ordnance, 15 August 1957.

O'Brien, T. P., and Pepita Pirrie, Investigation of the Effect of Blast Loading on the Damage Sustained by 1/10 Scale Reinforced Concrete Panels (Confidential Report), Atomic Weapons Research Establishment, England, January 1957.

Rinehard, J. S., and J. Pearson, "Metals under Propulsive Loads," American Society of Metals, Cleveland, Ohio, 1954.

Symposium on Rock Mechanics, "Part IV - Rock Fragmentation by Blasting," The Quarterly of the Colorado School of Mines, Vol 51, No. 3, July 1956.

Taylor, J., Detonation in Condensed Explosives, Clarendon Press, Oxford, 1953.

Timoshenko, S., Strength of the Materials, Part II, Advanced Theory and Problems, D. Van Norstrand Co., Inc., New York, 1956.

APPENDICES

APPENDIX A

AUTHORITY

Item No. 3054
CETC Mgt. No. 311

R & D PROJECT CARD	TYPE OF REPORT: New	REPORT CONTROL SYMBOL: CSCRD-1(R1)
1. PROJECT TITLE: ENGINEERING STUDIES & INVESTIGATIONS, DEMOLITIONS	2. SECURITY OF PROJECT: Uncl	3. PROJECT NO: 8F07-10-002
	4. INDEX NUMBER: 8F07-10-002-01	5. REPORT DATE: 4 Jan 60
6. BASIC FIELD OR SUBJECT: Mines & Obstacles	7. SUB FIELD OR SUBJECT SUB GROUP: Fortifications, Obstacles & Demolitions	7A. TECH. OBJ.: LC-13
8. COGNIZANT AGENCY: Corps of Engineers	12. CONTRACTOR AND/OR LABORATORY: US Army Engr. Res. & Dev. Labs, Fort Belvoir, Va.	CONTRACT/W. O. NO.:
9. DIRECTING AGENCY: Res. & Dev. Div., OCE		
10. REQUESTING AGENCY: Office, Chief of Engineers		
11. PARTICIPATION AND/OR COORDINATION	13. RELATED PROJECTS	17. EST. COMPLETION DATES: RES. Cont; DEV.; TEST Cont; OP. EVAL.
	14. DATE APPROVED: 4 January 1960 by OCE	18. FY. / FISCAL ESTIMATES: 60 5M; 61 5M; 62 20M
	15. PRIORITY: 2; 16. MAJOR CATEGORY: 6.32	
19. REPLACED PROJECT CARD AND PROJECT STATUS		Est Rate P/A 20M

20. REQUIREMENT AND/OR JUSTIFICATION

There is a requirement for conducting studies and investigations in connection with this field which cannot be scheduled under other tasks in this area. The principal activities to be performed will pertain to keeping abreast of the state of the art and to providing consultant services to user agencies and higher authority.

21. BRIEF OF PROJECT AND OBJECTIVE

a. Brief.

(1) Objective:

(a) Conduct necessary investigations to keep abreast of the state of the art and, prior to the establishment of a requirement for the initiation of a project or task, to develop data for the user, at his request, which will determine necessity for, or the feasibility of, specific research and development of equipment, techniques, or materials in the field of demolitions.

22. OASD (R & D)	SN.	CN.	C.	X.	I.	C.

DD FORM 1 APR 58 613
REPLACES DD FORM 613, 1 JAN 58.

PAGE 1 OF 2 PAGES

R&D PROJECT CARD
CONTINUATION SHEET

Item No. 3054
CETC Mtg. No. 311

1. PROJECT TITLE	2. SECURITY OF PROJECT	3. PROJECT NO.
ENGINEERING STUDIES & INVESTIGATIONS, DEMOLITIONS	Uncl	8F07-10-002
	4. 8F07-10-002-01	5. REPORT DATE 4 Jan 60

(b) Conduct studies and investigations required for determination of technical data concerning existing equipment, techniques, or materials in support of research and development in the field of demolitions.

(c) Prepare and submit comments, recommendations and special reports in connection with the above activities as may be appropriate, or as specifically requested by higher authority.

APPENDIX B

STATISTICAL ANALYSIS OF EXPERIMENTATION ON BREACHING OF CONCRETE WALLS

by 17 July 1958

Richard E. Deighton
Statistical Services Branch
Data Processing and Statistical Services Branch

Four complete factorial experiments were conducted on the breaching of concrete walls. These experiments were then analyzed by the statistical tool known as analysis of variance. The analysis of variance indicates whether or not the factors tested contribute significantly to the experiment. The significance of the interactions of factors was tested as well as the significance of the factors. Whenever a factor or interaction was found to be significant, Student's "T" test for determining the significance in differences of means was used to determine the optimum combination of the levels of the factors to use.

The first experiment was a complete factorial experiment with three factors. Each factor combination was repeated once. Only 4-inch concrete walls were used. The factors with their levels were as follows:

Factor	Level
Thickness of explosive	1/4 inch 3/8 inch 1/2 inch 5/8 inch 3/4 inch
Height of explosive above ground	On ground 24 inches above ground
Plastic between target and explosive	No plastic Plastic 0.006 inch thick

The analysis of variance indicated that both the thickness of the explosive and the height above ground are highly significant. The plastic was not found to be significant.

The "T" test was then conducted on the five levels of thickness and the 1/4-inch charges were found to be the best. Since only two

levels of the height above ground were tested, a "T" test was not required for this factor. The experimental results show that a height of 24 inches should be used. Since the plastic was not significant, one may use either no plastic or plastic 0.006 inch thick.

The second experiment involved testing the thickness of explosive and plastic on 6-inch walls. The same five levels of thickness and the same two levels of plastic were tested. As before, all combinations of all factors were tested and each combination was repeated once.

The analysis of variance indicated that none of the factors or their interactions were significant. Consequently, no further analysis or interpretation could be performed. The reason for these results may be that the experimental error was too large to permit proper interpretation. Large experimental error is sometimes caused by unknown and/or untested factors.

The third experiment involved testing four levels of the ratio of the explosive thickness to the cross section area, three levels of priming, and two levels of tamping. A complete factorial experiment, repeated once, was performed. The factors and their levels for this test were as follows:

Factor	Level
Ratio of explosive thickness to cross section area	1:126 1:57 1:32 1:20
Priming	Single, in center Single, in corner Double, opposite corners
Tamping	Untamped Tamped

Three separate analyses of variance tests were conducted. The ratio factor and the priming were first analyzed for the craters formed by the untamped charges. An analysis of variance was next performed on the craters for both tamped and untamped charges. Finally, the analysis of variance was applied to the spalls formed by the tamped charges. The only conclusive statement that can be drawn from any of these analyses is that tamping is a significant factor. The tamped charges yield the better results. Unexplained experimental variation may account for lack of significance in the other results.

The fourth and final experiment dealt with testing four levels of the explosive thickness to the cross section area ratio and two levels of the explosive length to explosive width ratio. A complete factorial experiment was performed. The experiment was repeated twice instead of only once as the others were. The reason for this was to reduce the experimental error by selecting the two most similar out of the three observations for every factor combination. These two factors and their levels were as follows:

Factor	Level
Ratio of explosive thickness to cross section area	1:25 1:50 1:75 1:125
Ratio of explosive length to explosive width	1:1 1:3

The statistical analysis for this experiment consisted of both an analysis of variance and a "T" test. The analysis of variance indicated that both ratios are significant as well as their interaction. A "T" test on the first ratio indicated that the level of 1:25 should be used. For the second ratio, the analysis of variance indicated the level 1:1. Since the interaction of the two factors is significant, a "T" test should be applied for the combinations of the levels of the two factors. However, this would involve computing variances based on samples of only size two which would be absurd. Therefore, the mean for every factor combination was computed. On inspection, the above results agreed with the previous decision for selecting levels of the two ratios.

In conclusion, a few facts should be pointed out. Experimental error is a serious problem and reasons for large experimental errors should be investigated. The method of selecting the two most similar out of the three observations per factor combination has an intuitive appeal but is without theoretical foundation. Other problems exist in the application of the "T" test. The mathematical models for the analysis of variance and for the "T" test are slightly different. Therefore, is the "T" test applicable to an analysis of variance problem? If not, what are some better tools for determining optimum levels of significant factors from an analysis of variance problem? Another problem involving the "T" test is to determine how to apply the "T" test when an analysis of variance indicates that interactions of factors are significant.

APPENDIX C

PROCEDURE FOR DETERMINING COMPRESSIVE STRENGTH OF CONCRETE

The Schmidt concrete test hammer Model N2 was used to estimate the compressive strength of the concrete test structures at Camp A. P. Hill. Construction personnel had made test cylinders from each batch of concrete, but the cylinders cured faster than the massive concrete structures and indicated a strength considerably under the estimated strength of the structures.

Five points were marked on the front and rear faces of each pier; Schmidt hammer readings were then made at each point. These readings were averaged, and the average of all ten points on each pier was used as the best estimate of the compressive strength of the pier.

The average compressive strengths of concrete in 2-, 3-, 5-, and 7-foot-thick test structures estimated from Schmidt hammer readings taken at five points on the front and five points on the rear of each structure are shown in Table XVI.

Table XVI. Average Compressive Strengths

Wall Number	Strength of Piers (psi)			
	2-Ft	3-Ft	5-Ft	7-Ft
1	5,850	5,200	6,050	5,850
2	6,550	5,250	5,900	5,750
3	6,850	5,450	6,000	5,150
4	7,000	5,200	5,600	5,300
5	5,750	5,250	5,350	5,400
6	6,100	5,300	5,300	5,450
7	6,250	5,300	5,200	5,300
8	5,500	5,400	5,150	5,350
9	6,400	5,800	5,600	6,100
10	5,800	5,750	5,000	5,650

The concrete cylinders taken during construction of the piers were employed to evaluate the effectiveness of the Schmidt hammer for testing concrete. The following report from the Materials Branch, USAERDL, provides details of the evaluation procedure.

NONDESTRUCTIVE DETERMINATION OF COMPRESSIVE STRENGTH OF CONCRETE

by

George D. Farmer, Jr.
Metals and Materials Conservation Section
Materials Branch, USAERDL

1. This work was conducted to determine:

a. An estimate of the compressive strength of concrete test cylinders by nondestructive tests utilizing the Schmidt concrete test hammer Model N2.

b. The compressive strength of the same concrete test cylinders by destructive test in accordance with ASTM Method C39-49.

c. The relation, if any, between data obtained by the two methods.

2. We emphasize at the outset that the Schmidt concrete test hammer does not measure compressive strength. It measures rebound, which is a function of the resilience of the hammer and the material struck by the hammer. The problem is to determine if a relation exists between data obtained by the two tests which will justify using the hammer for estimating probable compressive strength of concrete.

3. The sample unreinforced concrete cylinders were capped. They were tested nondestructively in accordance with operating instructions "Concrete Test Hammer Model N2" which were supplied with the Schmidt hammer. The destructive test procedure used was ASTM C39-49 "Method of Test for Compressive Strength of Molded Concrete Cylinders." The following literature references were obtained for background information:

a. "Test Hammer Provides New Method of Evaluating Hardened Concrete," by Gordon W. Greene, including discussion, Journal of The American Concrete Institute V. 51, p. 249.

b. "Use of the Swiss Hammer for Estimating the Compressive Strength of Hardened Concrete," by W. E. Grieb, Div. of Physical Research, Bureau of Public Roads; Public Roads Vol. 30, No. 2, June 1958.

c. "Investigation of Schmidt Concrete Test Hammer," Report No. 6-267, June 1958; U. S. Army Engineer Waterways Experiment Station, Vicksburg, Miss.

The Schmidt hammer method of estimating compressive strength of concrete requires that the angle of the hammer relative to the horizon be used in converting hammer readings to pounds per square inch compressive strength. The angle reading is said to be -90 degrees when the instrument is pointed downward perpendicular to the ground and 0 degrees when parallel to the ground. A conversion chart for the conversion of Schmidt hammer readings to pounds per square inch compressive strength of concrete cylinders is attached to the side of the instrument.

4. An analysis of the problem of correlating Schmidt hammer readings with data obtained from standard concrete test cylinders evaluated in accordance with ASTM C39-49 reveals a number of inherent noncontrollable variables in both the ASTM and Schmidt hammer test methods. The presently accepted ASTM method of determining compressive strength of concrete cylinders has a standard deviation of 150 to 250 psi depending on the age of the concrete.* The size of the increments or divisions of the Schmidt hammer indicator is such that one division is equal to approximately 500 psi, which necessitates interpolation with a possible variance of plus or minus 250 psi but probably more in the order of plus or minus 75 psi. This variance inherent in reading the Schmidt hammer scale can be reduced by a large number of determinations. The author believes that the structural rigidity of the concrete being tested with the Schmidt hammer influences the data obtained. The results are reported in Table XVII. The data obtained by using the Schmidt hammer at -90 degrees was obtained on unrestrained standard size concrete test cylinders. When the data was obtained at 0 degrees the concrete cylinders were restrained with a compressive force of approximately 300 psi applied on the top and bottom of the cylinders. The scatter in individual Schmidt hammer determinations was less when obtained on concrete cylinders that were tested under restraint.

The data determined on concrete cylinders under restraint and the corresponding data from ASTM Method C39-40 is plotted in Fig. 59. It is believed that the data is too scattered to be used to draw a single correlation curve; thus, a correlation band is superimposed over the reference curve (the theoretical curve of perfect correlation) about which correlated data should arrange itself.

The standard deviation of the ASTM data is $\pm$ 700 psi. The standard deviation of the means of 10 observations each of Schmidt hammer data is $\pm$ 450 psi. The standard deviation of the difference is $\pm$ 680 psi. From the last statement it may be expected that 68 percent of the Schmidt hammer data taken on a rigid unreinforced concrete structure will be within $\pm$ 680 psi of the compressive strength of the concrete, as measured by the ASTM method.

---

* Ref. par. 3a hereof.

Table XVII. Compressive Strength of 51 Concrete Test Cylinders

Sample No.	Cylinder Designation	ASTM Method* C39-40 Breaking Strength (psi)	Schmidt Hammer Method** Estimated Breaking Strength (psi)		
			-90°		0°
			Cylinder Side	Cylinder Tops	Cylinder Side
1	A1B	5,210	4,370	-	-
2	A3B	5,030	4,575	4,750	4,500
3	A3T	4,720	4,390	-	4,380
4	A4B	5,200	4,880	5,260	4,910
5	A5B	4,400	3,450	-	-
6	A5T	4,190	4,370	-	-
7	A8B	4,450	3,950	-	4,330
8	A9T	3,950	3,800	-	3,680
9	A10T	3,320	4,160	4,220	3,880
10	B1T	4,050	4,030	4,360	2,700
11	B2B	3,410	3,880	3,700	4,230
12	B3B	2,990	3,340	-	-
13	B3T	3,370	3,700	-	3,500
14	B4T	3,910	4,440	-	-
15	B5T	3,120	3,520	-	-
16	B6T	3,950	4,420	4,320	4,120
17	B10M	5,280	4,430	4,130	4,530
18	B10T	2,700	3,200	-	-
19	C1T	4,570	3,710	-	4,430
20	C2B	3,960	4,530	-	-
21	C2T	3,500	4,320	-	-
22	C3T	4,360	4,500	-	-
23	C4T	3,310	3,940	-	4,630
24	C5B	5,200	4,200	4,750	3,880
25	C5T	4,030	3,700	-	-
26	C6T	3,470	4,500	4,830	3,990
27	C7B	3,870	3,900	-	-
28	C7T	2,820	4,000	3,530	4,430
29	C8B	2,610	3,920	-	-
30	C8T	3,030	3,300	3,260	3,800
31	C9B	4,060	5,100	4,880	4,060
32	C10B	2,590	3,200	-	-
33	C10T	2,930	3,600	-	-
34	D1T	4,340	3,800	4,360	4,530
35	D2B	3,530	3,850	-	4,320
36	D2M	2,950	4,530	3,500	3,620
37	D3B	4,320	3,800	3,580	3,880
38	D4B	4,210	3,850	-	-
39	D5M	3,810	3,630	4,000	3,740
40	D5T	2,740	3,500	-	-
41	D6B	3,740	3,970	4,630	3,820

Table XVII (cont'd)

Sample No.	Cylinder Designation	ASTM Method* C39-40 Breaking Strength (psi)	Schmidt Hammer Method** Estimated Breaking Strength (psi)		
			-90°		0°
			Cylinder Side	Cylinder Tops	Cylinder Side
42	D6M	3,050	3,580	3,100	3,660
43	D6T	2,620	3,350	-	-
44	D7	4,130	4,340	4,500	4,530
45	D8B	4,730	3,300	3,730	3,620
46	D8T	3,450	3,570	-	-
47	D5B	3,480	3,550	-	-
48	W	3,840	2,800	3,600	3,150
49	X	3,610	2,900	3,680	3,000
50	Y	4,150	3,970	4,480	3,760
51	Z	2,980	3,000	-	-

* Data is a single determination.
** Data is average of 10 determinations.

5. It is concluded that:

a. The compressive strength estimated nondestructively by the Schmidt hammer of the different concrete cylinders had a range of 3,000 psi to 4,910 psi for restrained samples.

b. The compressive strength determined by ASTM Method C39-49 of the different concrete cylinders had a range of 2,590 psi to 5,280 psi.

c. There is a relationship of limited accuracy, -680 psi to +680 psi, between the compressive strength determinations in accordance with ASTM Method C39-49 and the means of 10 observations each by the Schmidt hammer method, as shown by Fig. 59.

6. The following recommendations apply to unreinforced concrete. It is recommended that:

a. The Schmidt hammer determinations be made on rigid concrete structures.

b. A standard deviation of $\pm$ 680 psi be used in interpreting Schmidt hammer data developed from means of 10 observations on each sample.

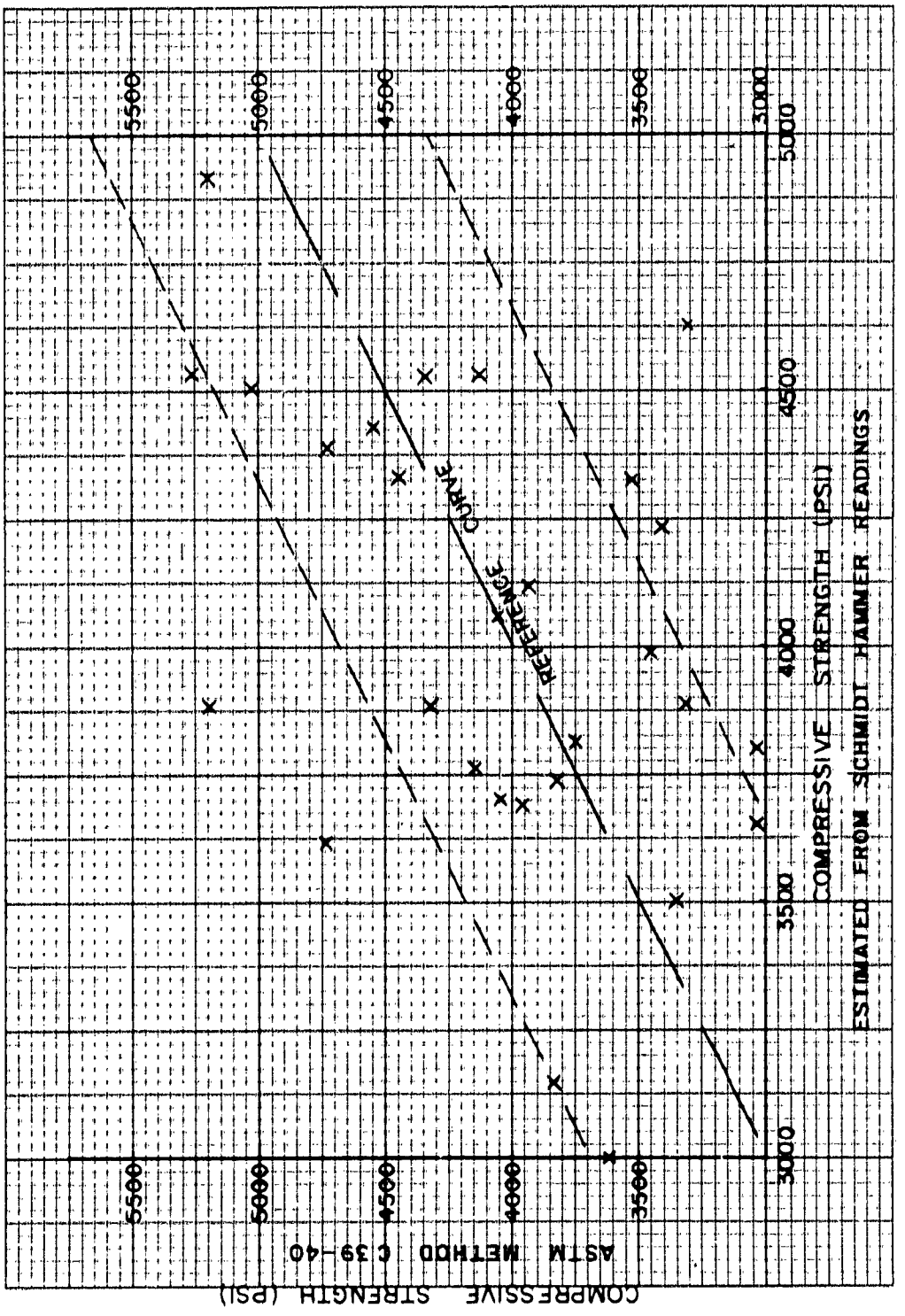

Fig. 59. Compressive strength, ASTM method versus Schmidt hammer method.

APPENDIX D

EXPLOSIVE SHOCK PROPAGATION IN CONCRETE

by

John Cogan and Robert K. Stevens

I. Introduction

In the summer of 1959, the Demolitions Section of the U. S. Army Engineer Research and Development Laboratories, Fort Belvoir, Virginia, conducted tests on the hasty demolition of concrete structures. The investigations were designed to determine the least weight of explosive required to destroy concrete bridge piers or similar concrete structures. It was known from previous experiments[6] that the charge is most effective when placed at least the thickness of the structure above ground or water level; that the charge is simplest to construct when square in shape; and that the ratio of thickness to contact area of the explosive has a definite effect on the destructive efficiency of the explosive.

Results of tests not only showed that the thickness to area ratio was an influential parameter of explosive effectiveness but also indicated strongly that more than one stress wave was introduced into the concrete pier.

This paper describes the analytic procedure which was followed in arriving at the conclusion that multiple explosive shock pulses are responsible for the various spall patterns in large concrete structures when they are demolished. This conclusion was reached as a result of studies of high-speed camera pictures of the explosive process and examination of the break-up patterns of the piers. We have considered the theoretical findings of a number of the workers in the field and compared them with our experimental results.

II. Description of Explosive Charges and Concrete Test Structures

Test piers were constructed of concrete with steel reinforcing. There were four rows with ten piers in each row. The first row had piers 2 feet thick, 6 feet wide, and 9 feet high; the second row, 3 feet thick, 6 feet wide, and 9 feet high; the third row, 5 feet thick, 10 feet wide, and 11 feet high; and the fourth row, 7 feet thick, 11 feet wide, and 13 feet high.

---

6. Previous experiments were conducted by the Demolitions Section, USAERDL, at Point Pleasant, West Virginia, in the summer of 1958.

In the 2-foot- and 3-foot-thick piers, 3 feet were underground while in the 5- and 7-foot piers, the structures stood entirely above the ground.

In order to approximate a continuous wall, earth was piled between the piers (Fig. 60) and at each end of the rows. This procedure was not altogether successful, because many of the larger walls exhibited side fracture.

F4194

Fig. 60. Three-foot piers showing the earth fill piled between the piers.

III. Break-up Patterns of the Piers

The concrete piers exhibited four general characteristics after undergoing explosive attack: (1) Cratering, (2) spalling, (3) top fracture, and (4) side failure. The craters were generally smaller than the spalls except in the cases where the material did not completely pull away from the rear face as in the 3-foot walls. The outline of the crater and spall shapes are generalized in Fig. 61, the form taken being consistent throughout the tests.

The crushed zone appeared on the explosive side of the wall in an area lining the blown-out region (Fig. 62). The material here was fractured to a state near pulverization. Top fracture and end failure were not as consistent as the spalling and cratering. In the 2- and 3-foot piers, the tops were either blown off or broken into large chunks (Fig. 63), whereas the 5- and 7-foot piers were

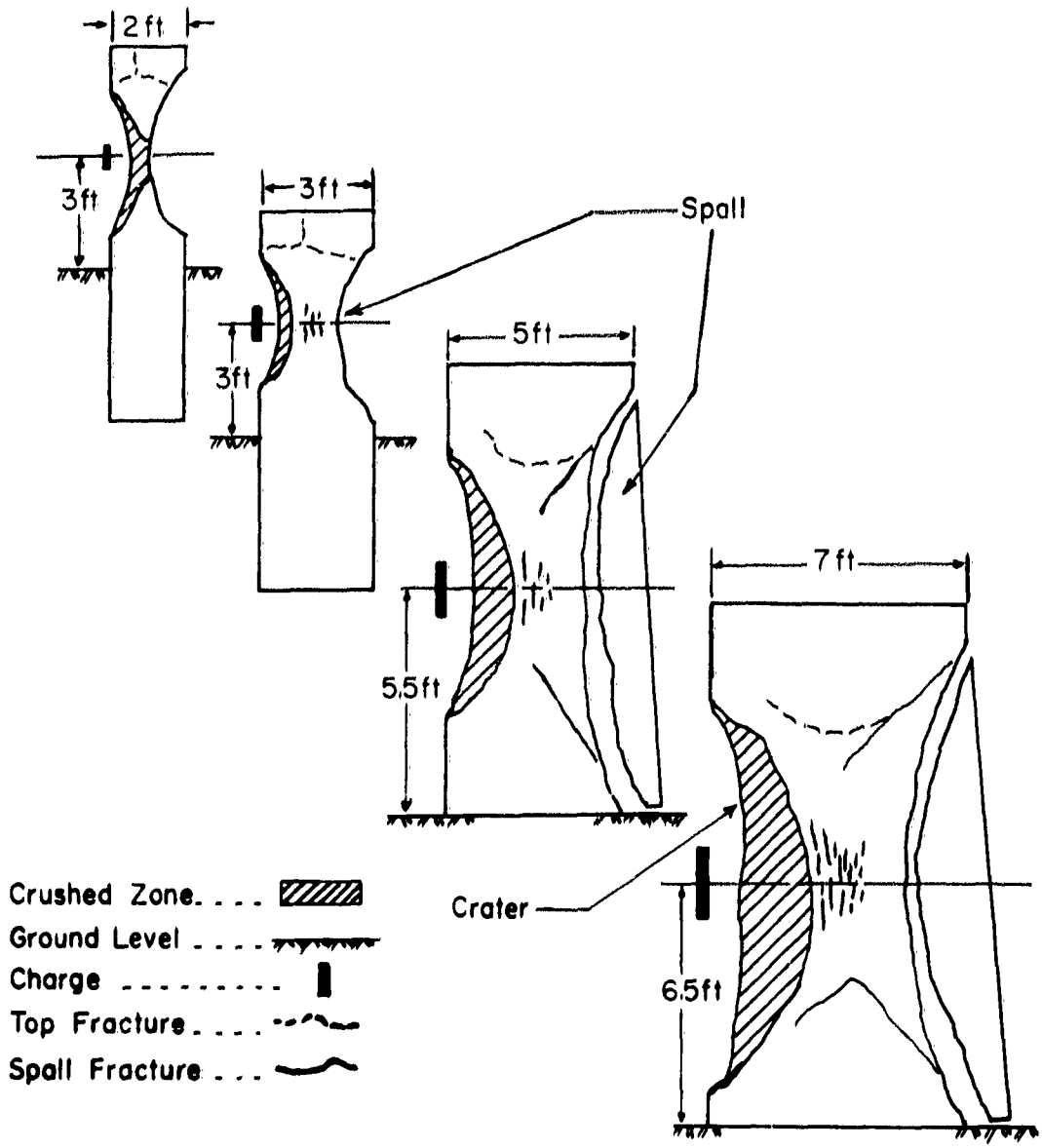

Fig. 61. Cross-sectional drawings of main failure characteristics of the piers showing spalls, craters, charge position, and ground level (cross-hatched lines).

Fig. 62. Explosive side of a 2-foot pier. F4145

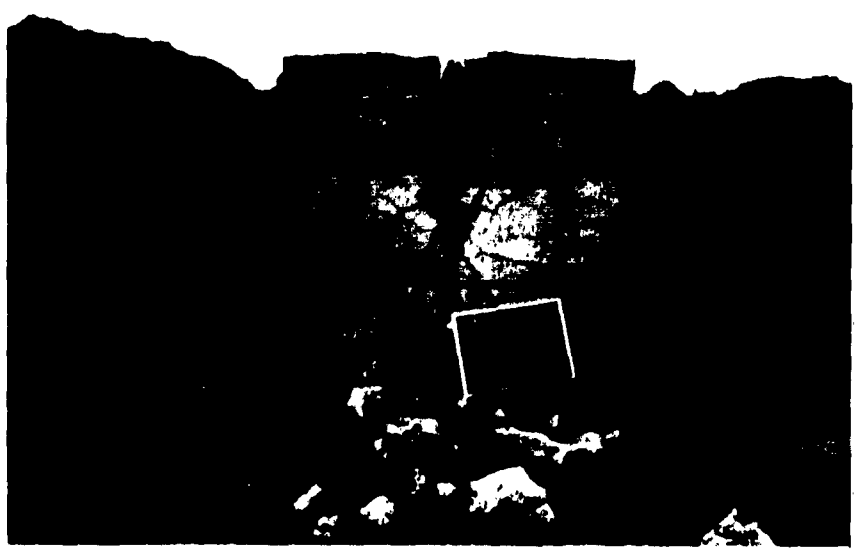

F4161

Fig. 63. Face of 3-foot pier opposite the explosion.

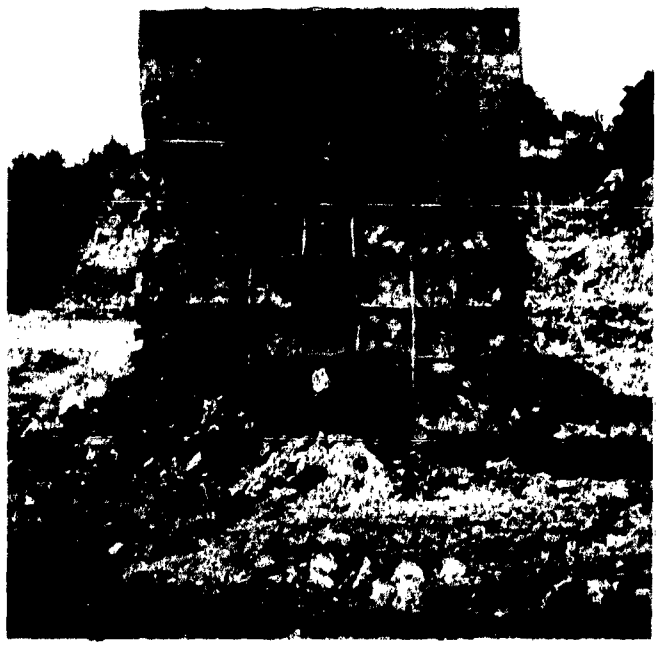

F5575

Fig. 64. Crater face of a 5-foot pier. The top of the pier is only slightly cracked.

F6059

Fig. 65. The end of a 7-foot pier.

F4173

Fig. 66. Side opposite the explosive on a 3-foot pier. Measurement of the cracks, crevices, and fracture holes proved impracticable.

F6082

Fig. 67. Another example of difficult conditions for volume measurements of spalls.

merely cracked to a limited extent (Fig. 64). On the other hand, end failure took an opposite trend; the ends of the 2- and 3-foot piers cracked, whereas the ends of the 5- and 7-foot piers ruptured (Fig. 65).

IV. Collection of Experimental Data

An attempt was made to correlate the measurements taken of the crater and spall volumes for the charges used on respective piers. Unfortunately, no correlation could be made because of the extent of fracture (Figs. 66 and 67). Accurate measurements were impossible. In the 5-foot-thick piers, the successive spalls often did not even break away from the rear face.

Two methods of photography were used in an attempt to capture the sequence of events during the explosive process: A Fastax camera run at 3,000 to 6,000 frames per second aimed at the side of the pier opposite the explosion, and a Courtney-Pratt lenticular camera run at 100,000 frames per second aimed at the explosive face of the pier. Fastax films taken of most of the piers showed a definite similarity in all the breakup patterns of walls of the same thickness and a general similarity between the walls of different thickness. A mass of small chunks of concrete grouped in the shape of an almost smooth parabola of revolution spalled off 2-foot piers (Fig. 68).

Fig. 68. A frame from a Fastax film showing mushroom spall moving out from the face of the wall opposite the explosion.

The 3-foot piers spalled in a more erratic pattern. A few fairly large pieces were thrown out from the center while the rest of the concrete showed a tendency to hang in position. In the 5-foot piers, a few chunks of larger dimensions than those of the 3-foot piers blew off, the rest of the spall traveling out in one

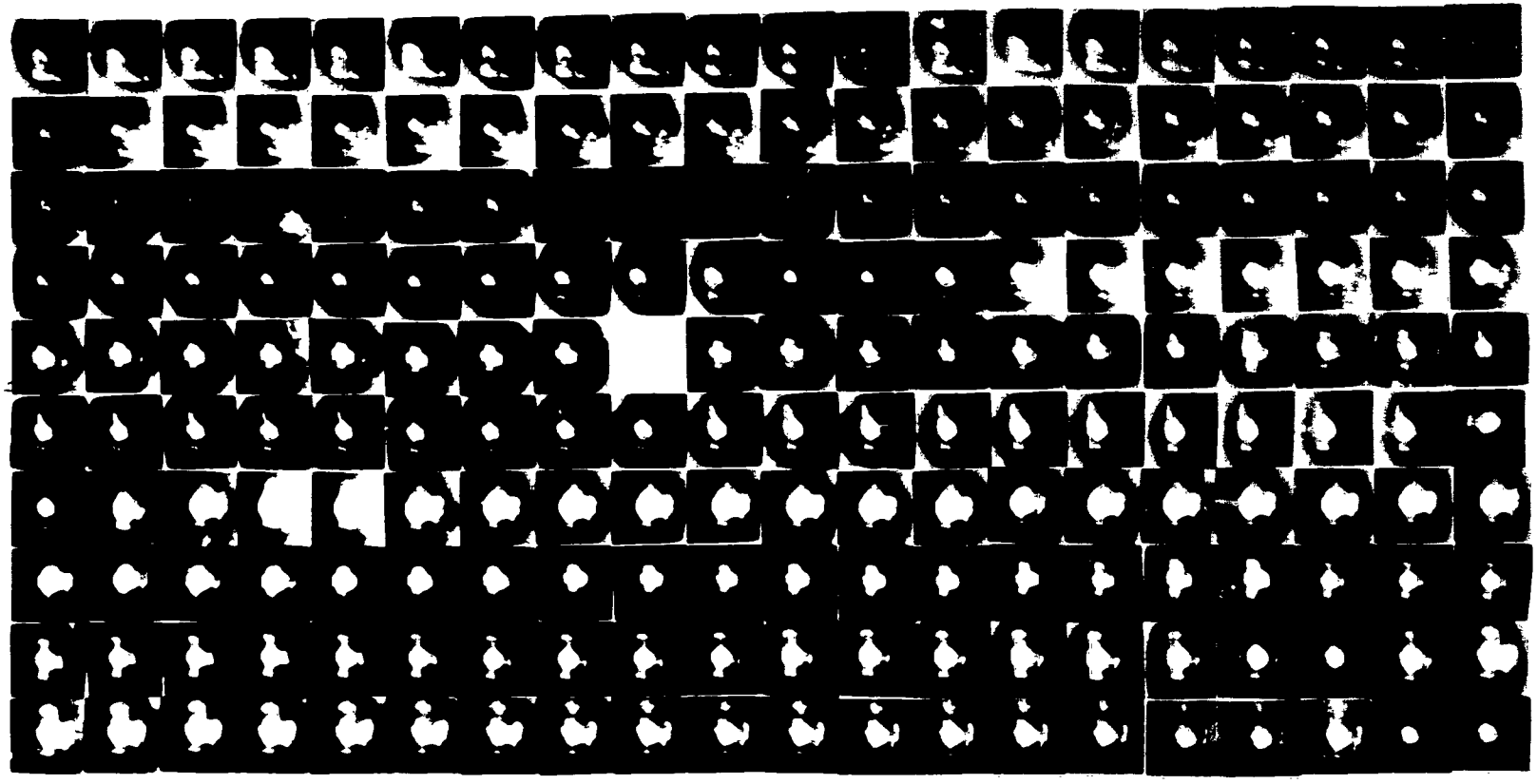

G7682

Fig. 69. A sequence of frames showing detonation of a flat, square charge on a concrete pier as recorded by the Courtney-Pratt lenticular camera at 100,000 frames per second.

large slab. As in the 3-foot piers, this slab sometimes completely spalled off and sometimes only partially broke away. An even larger slab spalled on the 7-foot pier. Here again, chunks flew off the center of the rear face. As the pier thickness increased, the pattern of spalling showed a change from an extensive breakup of spalled material to a more nearly slab-like separation. There was also a tendency for the number of spall layers broken away to increase as the wall thickness increased. The larger piers showed signs of multiple spalling while the thinner piers exhibited single spalls.

The lenticular camera photographs taken of three of the detonations on 5-foot piers showed a pulsation of the detonation. A small spot of light of high intensity appeared which quickly built up in size to reach a peak in about 100 microseconds. Then, in the space of one frame (10 microseconds), the spot was obliterated by a flash. The flash cleared, losing intensity and forming, roughly, the pattern of a cross (Fig. 69). The cross decayed with the light, steadily losing its strength until, after 550 microseconds, a second flash appeared superimposed on the cross. This flash built up in a cross similar to the first one but covered a larger area. This flashing and decaying action continued cyclically. We cannot be sure how many flashes occurred because of the limit of 200 effective frames running at 100,000 frames per second. A time period of 2,000 microseconds was covered; however, in this period as many as four pulses could be identified (Fig. 70).

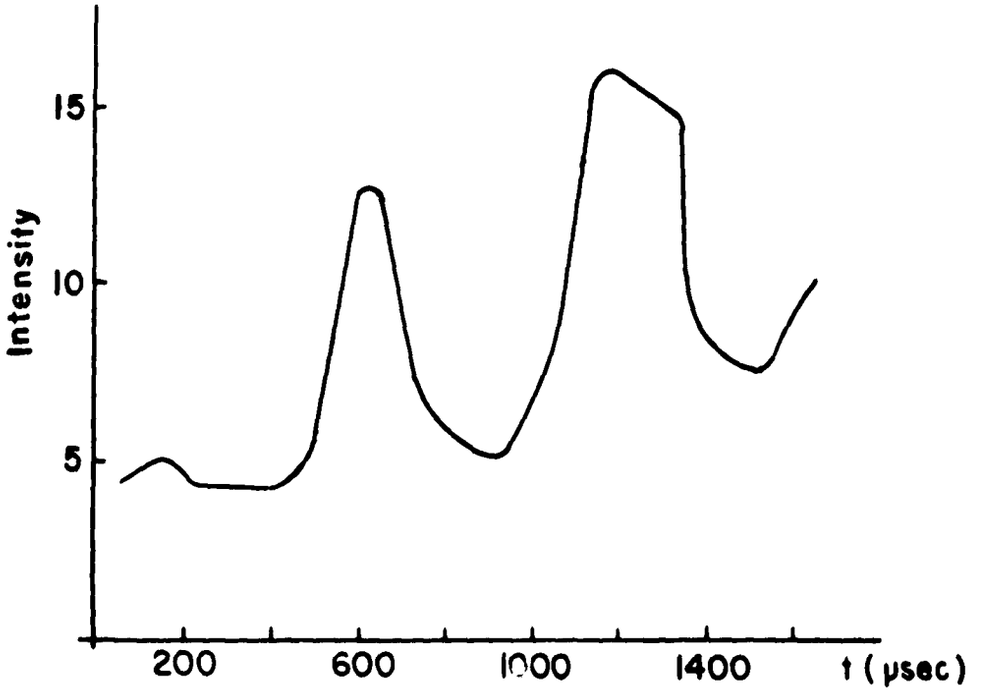

Fig. 70. Comparison of fireball size versus time.

V. Summary of Literature Study of Shock Wave Propagation

The detonation of explosive is a complex, physiochemical process in which the properties of energy release, wave speed, and peak pressure are difficult to calculate. In an explosive shaped in slabs, the problem of finding these values is even more difficult, especially since very little experimentation has been done on this geometric shape. Therefore, two assumptions must be made about the reaction of the explosive: first, that the reaction reaches equilibrium; and second, that the peak pressures for the detonation waves in the different shapes and weight of charges are approximately the same. The detonation fronts will then travel at equal velocity and with equal pressure. The variations in wave shape will depend on the decay of the pressure behind the detonation front as it acts on the wall face.

When a longitudinal wave in a medium encounters another medium, part of the wave rebounds from the interface and part of it is transferred through it. The equation for the reflected stress (for normal incidence) is:

$$A_2 = A_1 \frac{(\rho_2 c_2 - \rho_1 c_1)}{(\rho_2 c_2 + \rho_1 c_1)} \qquad (1)$$

The equation for the transferred stress is:

$$A_3 = A_1 \frac{2\rho_1 c_1}{\rho_2 c_2 + \rho_1 c_1} \qquad (2)$$

A_1 = incident stress

A_2 = reflected stress

A_3 = transferred stress

ρ = density of medium

c = velocity of wave in medium

ρc is a parameter known as the characteristic acoustical impedance, and it is values of this that determine the type and the strength of the resulting waves. For example, if in equation (1) $\rho_2 c_2$ is less than $\rho_1 c_1$, the resulting amplitude is negative, that is, a rarefaction wave. If the opposite is true, the reflected wave is a compressive wave. Also, the greater the difference is between $\rho_1 c_1$ and $\rho_2 c_2$, the greater is the pressure amplitude.

The angle at which the wave approaches the interface is also of importance. The wave that rebounds from a surface of discontinuity reflects at an angle equal to the angle of incidence (Fig. 71).

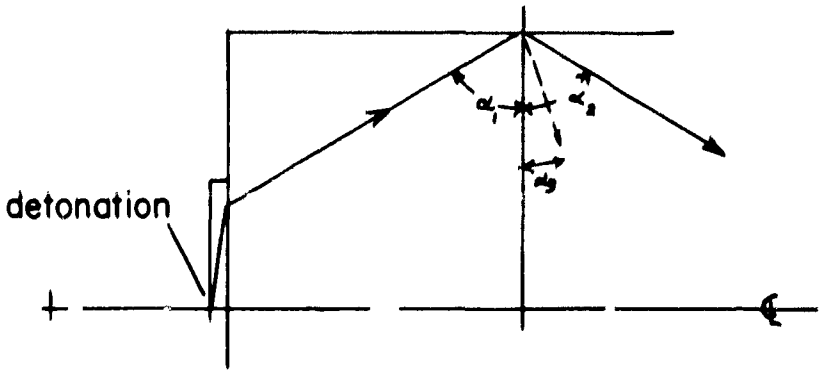

Fig. 71. A stress wave reflecting from a free boundary showing development of both shear and rarefaction waves.

The angle at which the transferred wave enters the new medium, however, depends on the sine of the angle of approach and the wave velocities in the respective media.

$$\frac{\sin \varphi_1}{C_1} = \frac{\sin \varphi_2}{C_1}$$

This relationship holds up to values of φ that approach 90°. In the transfer of the wave across the interface, residual stresses are set up in the new medium so that a transverse (shear) wave develops. The characteristics of these waves are shown in graph form in Fig. 72.

Between 40° and 80°, much of the wave is transferred as a shear wave, thus taking considerable energy away from the longitudinal pulse. These shear waves travel at a lower speed than the compressive or rarefaction ones so that any effect they have on the wall occurs behind the initial front.[7]

7. For a more complete discussion of this section see Kolski, H., Stress Waves in Solids (Oxford, The Clarendon Press, 1953) pp. 24-38.

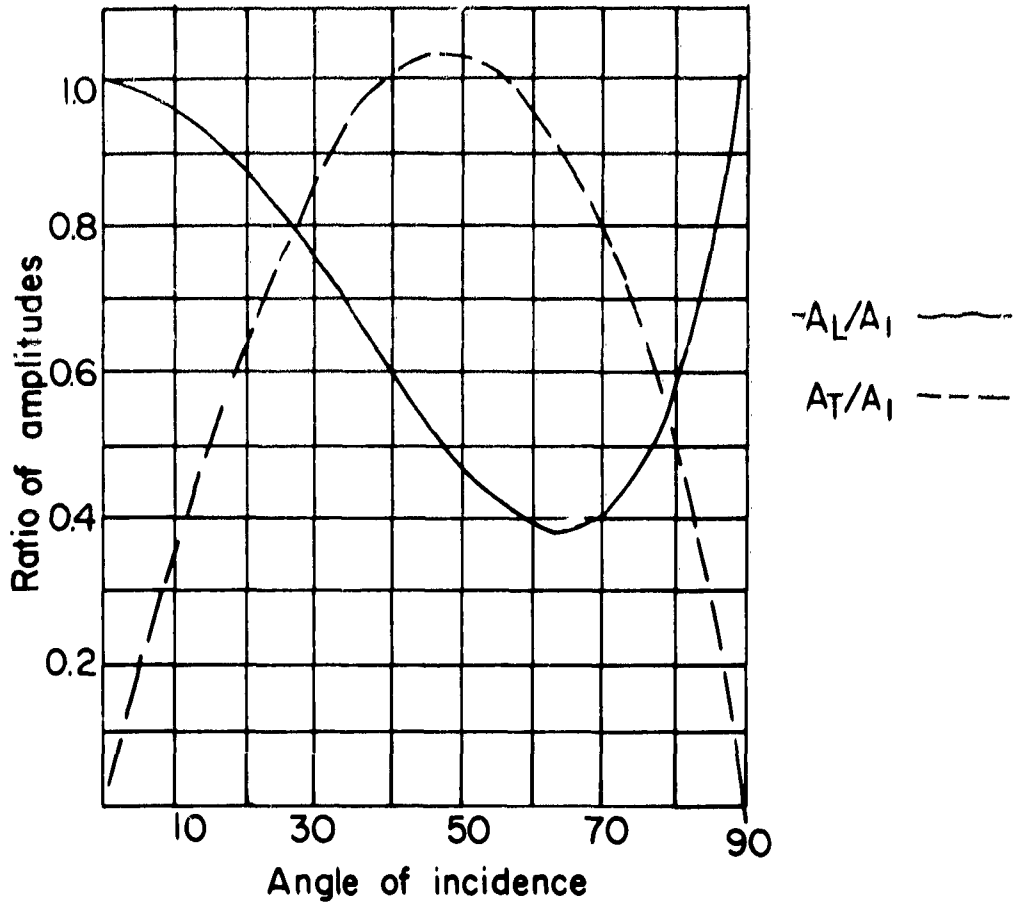

Fig. 72. Characteristics of a longitudinal stress wave rebounding from a free surface. A is the incident compressive wave; A_L, the reflecting compressive wave; and A_T, the reflecting tensile wave.

VI. Stress Wave Theory Compared to Experimental Results

The action of a single stress wave in the pier will be considered first, followed by a discussion of multiple waves. In this description, the possibility of multiple spalling due to the effects from one wave will also be considered.

As a stress wave moves through a solid, the wave loses energy as a result of internal friction from the motion of the particles that make up the solid.[8] As the high-pressure front moves through the material, molecules that make up the solid rub against each

8. Ibid., pp. 99-128.

other, contracting and expanding and in some cases changing from one crystalline phase to another. From experimental observation, another adverse effect on wave strength which is probably connected with internal friction is the transfer of pressure head energy to the wave tail.[9] The high initial peak pressure of a stress wave traveling through a solid seems to diminish rapidly, and, at the same time, the wavelength increases.

The cratering on the explosive face of the pier is caused by the crushing of the material in the immediate vicinity of the charge. The compressive strength of the concrete was measured to be between 4,000 and 5,000 psi for a static load.[10] The dynamic values would not be more than 2 or 3 times as high.[11] The pressure produced by the explosive is well above the dynamic compressive strength of the concrete.

As the wave reaches the rear face, a rarefaction is created. The wave transferred into the air is almost negligible and most of the energy is retained in the pier. The tensile wave takes time to build up to a peak value, however, because it is initially canceled out by the tail of the compressive wave (Fig. 73). As the

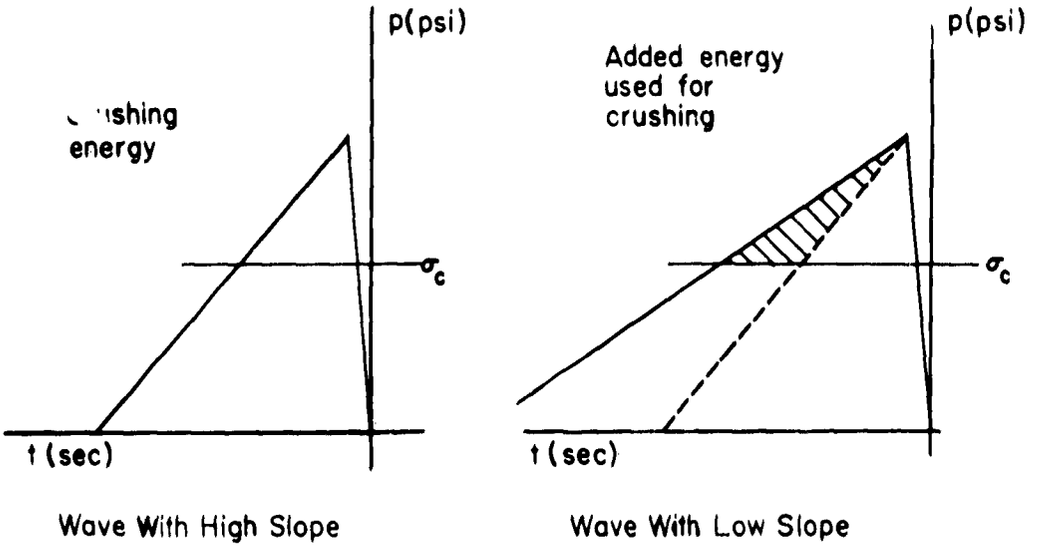

Fig. 73. An idealized crushing action. The area above the line of σ_c is the total energy available for crushing. The wave with the lesser slope has more crushing ability.

9. J. S. Rinehart, J. Applied Physics, Vol. 22, 1951, p. 1178.
10. Compressive strength readings were obtained with a Schmidt hammer, a device that measures the rebound of a spring loaded steel plunger from a concrete face.
11. Rinehart, op. cit., pp. 550-560 and 1229-1233.

rarefaction wave builds up, it surpasses the tensile strength of the material which is in the order of 500 to 600 psi. The wave is trying to reach a peak pressure value that is of the magnitude of the dynamic compressive stress, but before it can the material fails in tension and a slab of concrete spalls off. If the decay of the wave is not too great as it travels through the medium, it is also possible for more than one slab to scab off. The diagram (Fig. 74) shows a case in which three slabs spall off.

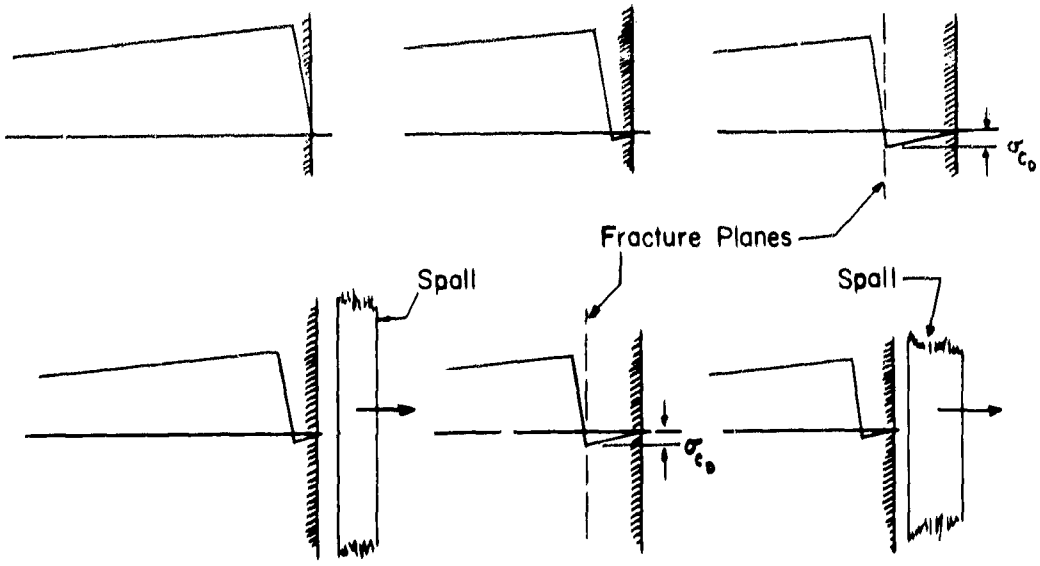

Fig. 74. Action of a rarefaction wave. σ_{c_d} represents the dynamic tensile strength of the material. The rarefaction builds up until it reaches the tensile strength of the concrete and spalls off a layer at this point.

In the 2- and 3-foot piers, it appeared that only one spall scabbed off, but this is difficult to ascertain. The 5- and 7-foot piers, however, exhibited multiple spalling in which two or three spalls were formed.

Spalling also occurred on the tops of the 2- and 3-foot piers. Material was fractured and thrown upward in large chunks. This effect did not occur in the 5- and 7-foot piers, probably because the charges were placed relatively lower (below the center of gravity of the piers) than on the 2- and 3-foot piers.

The shape of the wave front as it progresses through the pier could also have affected the top spall. The wave travels through the concrete as an expanding spherical surface and, if its radius is large, the angle of incidence with the top of the wall will be high. If the angle is between 40 and 80 degrees, a large transverse

pulse will be reflected, thus taking energy away from the wave of rarefaction so that the ability to spall is lessened (Fig. 72).

Another effect that occurs on the walls is the formation of a diagonal plane of failure. Diagonal fracture occurs because of the meeting of the rarefactions from the rear face and the top face.[12] The two waves reinforce each other and, if their sum is higher than the tensile strength of the concrete, failure occurs. As the two waves progress, the point of intersection describes a straight line from the corner point into the pier at a diagonal angle. This type of fracture did not occur at all in the 2- and 3-foot piers, probably because of the energy taken away by top failure. However, in the 5- and 7-foot piers there was evidence of diagonal fracture; but in most cases it was not very well defined (Figs. 62 and 65).

The stress pattern thus far discussed has been simplified to a great extent. The initial configuration is not too complex, but after rarefactions begin to occur from the top, end, and rear faces, the stress pattern becomes much more involved. With shear waves, compression waves, rarefaction waves, and failures of compression and tension all interacting, the picture becomes obcure. To add to the confusion, the pulsating effect observed in the lenticular camera pictures suggest that more than one pulse entered the pier from the explosion.

The 2-foot and 3-foot piers did not show any evidence of multiple pulses in their spall patterns but 5-foot and 7-foot piers did. Figure 75 shows the actions of multiple spalling due to one strong

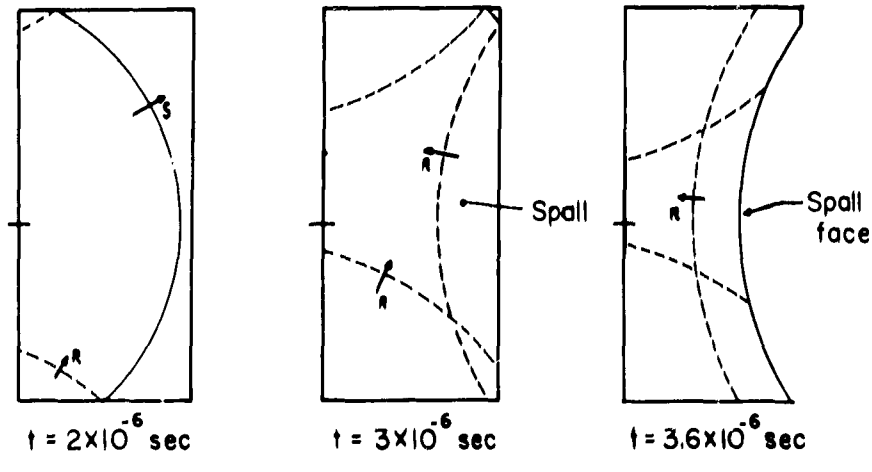

Fig. 75. Wave front as it progresses into pier and reflects from rear face.

12. Kolski, op. cit.

stress wave. Figure 76 shows the actions for two waves in which the distance separating the pulses is larger than twice the initial spall width. The third diagram, Fig. 77, shows the two wave phenomena again, but with the separation being less than twice the spall width. If the material spalls before the second wave can reach the new surface, this second wave must rarefact from the new interface. As the second rarefaction builds up, the wave front takes a larger curvature so that the second spall will be deeper in the wall center than the first (Fig. 76), and it will cause the final state as shown in the figure. If the second wave closely follows the first wave, then some of this wave will be caught in the spall and much of its energy will be lost.

For both of the wave configurations, the rarefaction waves will be weak at their perimeters. The angle of incidence at these points is larger than at the center so that more of the energy of the wave is transformed into a transverse stress wave, subtracting from the longitudinal one. If a third shock pulse occurred, the center section would again be reinforced but the stress pattern in the perimeter regions would become even more involved. This could possibly explain the haphazard breakup patterns on the ends and top of the large piers.

It may be that the thickness to contact area ratio of the explosive influences the distances between pulses. The separation that seemingly would do the most damage is one in which the second wave meets the new interface immediately after the spall has occurred. The time lapse between the first and second pulse observed when an 85-pound charge with a ratio of 1:140 was fired on a 5-foot wall was 500 microseconds. Assuming the rarefaction wave travels at 2.500 feet per second in concrete, the waves were 1.25 feet apart. The first spall thickness was 1.5 feet so that in this case some of the first wave would have been caught in the spall and the point of maximum effect was missed. The time lapse for an 85-pound charge with a ratio of 1:180 was 370 microseconds, so that the separation distance was 0.92 foot. Hence, more of the wave was trapped in the spall and the ability to produce multiple spall was lessened. This charge was not as effective as the one with a thickness to contact area ratio of 1:140, so there is some evidence of validity of the theory.

IX. Conclusions

The analysis described in this paper brought to light the hypothesis that explosive damage to large structures may be strongly influenced by a multiple pulse propagated by the explosive itself. This hypothesis has interesting potential, both for explaining many observed explosive phenomena and for use as a device for guiding

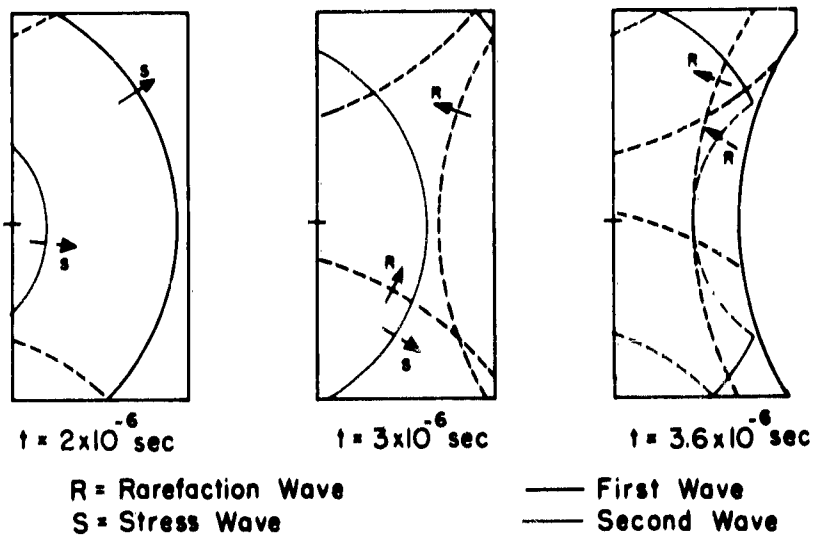

Fig. 76. Diagram of two wave fronts as they progress in pier and rarefact. The distance between the waves is more than twice the spall width.

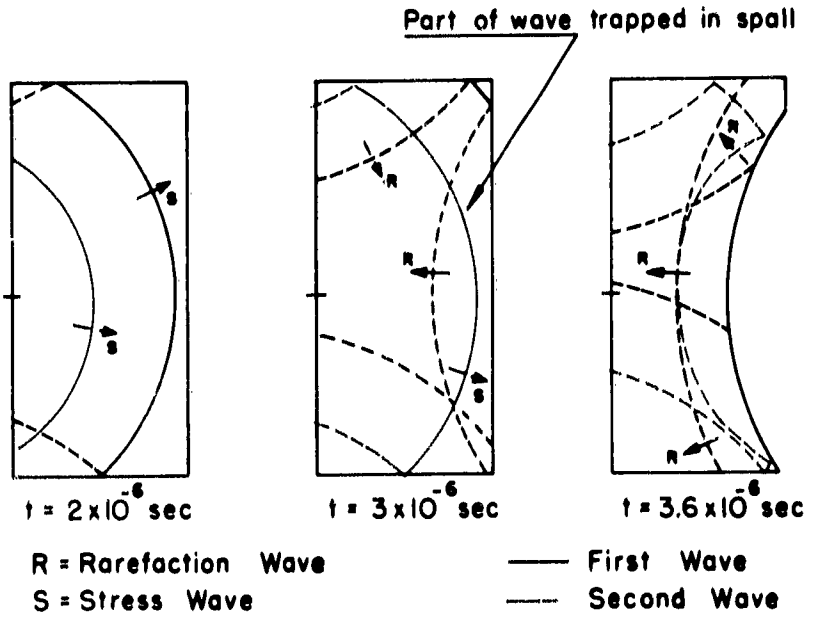

Fig. 77. Two stress waves in a pier with the separation distance equal to less than twice the spall width.

future research activities designed to increase explosive effectiveness. Much of the available energy of explosives is lost in current demolition procedures. It may be that multiple pulses can be controlled in such a way that they can be made to reinforce and cancel each other as required for a particular mission and thus greatly increase the effectiveness of explosive while reducing the amount of undesirable damage.

The hypothesis may be summarized by stating that it is believed that, as a result of shock wave reactions from the air surrounding the explosive, multiple explosive pulses, perhaps 500 microseconds apart, are produced in the target. When these pulses reach a free surface on the opposite side of the target, they produce tensile pulses traveling back into the target which spall material out of the target when they build up to a strength greater than the tensile strength of the target material. Successive pulses produce tensile pulses from the free surfaces which were created by the spall from the previous pulse.

The evidence which has been collected in favor of the multiple pulse hypothesis has been limited to data obtained as a by-product of tests designed to develop improved bridge pier demolition techniques. The hypothesis must, therefore, be considered tentative and should be verified by extensive research.

Category 13 - Mine Warfare and Demolitions

DISTRIBUTION FOR USAERDL REPORT 1663-TR

TITLE Hasty Demolition of Concrete Structures

DATE OF REPORT 13 Jan 61 PROJECT 8F07-10-002-01 CLASSIFICATION Uncl.

ADDRESSEE	REPORT	ABSTRACT
Department of Defense		
Technical Library Office, Asst Secretary of Defense Washington 25, D. C.	2	1
ASTIA, Documents Service Center Arlington Hall Station Arlington, Va	10	-
Department of the Army		
Command & General Staff College Fort Leavenworth, Kansas	1	-
Commandant, Army War College Carlisle Barracks, Pa. Attn: Library	1	-
Chemical Corps		
U. S. Army Chemical Warfare Laboratories Technical Library Army Chemical Center, Maryland	1	1
Corps of Engineers		
Research and Development Division Office, Chief of Engineers Department of the Army Washington 25, D. C. Attn: ENGNF	4	-
Chief of Engineers Department of the Army Washington 25, D. C. Attn: ENGRD	1	-
Chief of Engineers Washington 25, D. C. ENGTL (for release to OTS)	2	-